Targeted carbon conservation at national scales with high-resolution monitoring

Gregory P. Asner[a,1], David E. Knapp[a], Roberta E. Martin[a], Raul Tupayachi[a], Christopher B. Anderson[a], Joseph Mascaro[a], Felipe Sinca[a], K. Dana Chadwick[a], Mark Higgins[a], William Farfan[b], William Llactayo[c], and Miles R. Silman[b]

[a]Department of Global Ecology, Carnegie Institution for Science, Stanford, CA 94305; [b]Department of Biology, Wake Forest University, Winston-Salem, NC 27106; and [c]Dirección General de Ordenamiento Territorial, Ministerio del Ambiente, San Isidro, Lima 27, Perú

Contributed by Gregory P. Asner, October 13, 2014 (sent for review September 17, 2014; reviewed by William Boyd, Anthony Brunello, and Daniel C. Nepstad)

Terrestrial carbon conservation can provide critical environmental, social, and climate benefits. Yet, the geographically complex mosaic of threats to, and opportunities for, conserving carbon in landscapes remain largely unresolved at national scales. Using a new high-resolution carbon mapping approach applied to Perú, a megadiverse country undergoing rapid land use change, we found that at least 0.8 Pg of aboveground carbon stocks are at imminent risk of emission from land use activities. Map-based information on the natural controls over carbon density, as well as current ecosystem threats and protections, revealed three biogeographically explicit strategies that fully offset forthcoming land-use emissions. High-resolution carbon mapping affords targeted interventions to reduce greenhouse gas emissions in rapidly developing tropical nations.

carbon sequestration | forest degradation | deforestation | light detection and ranging | REDD+

Terrestrial carbon sequestration is internationally championed as a strategy for mitigating climate change. Carbon emissions from developing tropical countries are dominated by deforestation and forest degradation, which together contribute approximately 10% of the world's total emissions each year (1). This has driven an effort, known as REDD+, to reduce carbon emissions from deforestation and forest degradation, and to enhance carbon stocks through forest management (2). The geography of terrestrial carbon remains poorly known, however, leading to large uncertainties when developing estimates of carbon losses and gains over time (3). In turn, carbon stock uncertainties contribute to discounted monetary valuation, which decreases investment opportunities and thus diminishes the power of carbon-based conservation to combat climate change (4, 5). This problem has contributed to the low number and slow adoption of REDD+ programs. Consequently, carbon conservation is limited to volunteer markets or demonstration activities that are unlikely to compete financially with other land uses that generate large carbon emissions, such as oil palm plantations and surface mining (6, 7).

Transforming terrestrial carbon management into a cost-effective climate change mitigation strategy requires accurate and geographically detailed monitoring to facilitate action among multiple stakeholders, ranging from individual landowners to subnational jurisdictional agencies and national governments. The world's most common unit of land tenure, ownership, regulatory policy, and status reporting is the hectare (~2.5 acres) (8). Accurate and verifiable information on carbon stocks is needed at this high spatial resolution. Neither field plot networks nor global satellite mapping approaches have delivered spatially contiguous information on carbon stocks at a 1-ha resolution. Working at this resolution also will advance targeted conservation and management interventions designed to increase carbon stocks and protect biological diversity.

In the context of terrestrial carbon monitoring for policy and management, often insufficient emphasis is placed on the environmental conditions that determine the natural distribution of carbon stocks throughout ecosystems. Understanding the factors controlling carbon distribution is essential to targeting specific landscapes with interventions that achieve maximal returns on investments. These factors include climate, topography, geology, hydrology, and their interactions, which together set fundamental limits on the amount of carbon that may be stored on any given parcel of land. Current maps of carbon stocks based on field inventory or coarse-resolution satellite techniques do not accurately capture the natural spatial variability that ultimately underpins land use decisions at the 1-ha scale (1, 9–12).

A case study of the importance of understanding the drivers of carbon stock variation for climate change mitigation and conservation involves the megadiverse South American country of Perú. Like many rising economies, Perú is undergoing rapid land use change, driven by multisectorial interests that are altering carbon stocks throughout its ecosystems. The country harbors enormous environmental and biological gradients, ranging from the absolute desert of the Atacama on the Pacific coast to hyperpluvial forests at the base of the Andes and from arid high-elevation grasslands and large tropical ice caps to hot Amazonian lowlands, all of which strongly affect carbon storage and its interaction with human disturbances.

Perú's combination of large size, high diversity, and rapidly shifting array of human activities places the country at a crossroads between large-scale ecological loss and sustainable development. Nonetheless, despite the numerous threats to carbon storage from expanding land use throughout Perú, a portfolio of mitigation

Significance

Land use is a principal driver of carbon emissions, either directly through land change processes such as deforestation or indirectly via transportation and industries supporting natural resource use. To minimize the effects of land use on the climate system, natural ecosystems are needed to offset gross emissions through carbon sequestration. Managing this critically important service must be achieved tactically if it is to be cost-effective. We have developed a high-resolution carbon mapping approach that can identify biogeographically explicit targets for carbon storage enhancement among all landholders within a country. Applying our approach to Perú reveals carbon threats and protections, as well as major opportunities for using ecosystems to sequester carbon. Our approach is scalable to any tropical forest country.

Author contributions: G.P.A. designed research; G.P.A., D.E.K., R.E.M., R.T., C.B.A., J.M., F.S., K.D.C., M.H., W.F., W.L., and M.R.S. performed research; G.P.A., D.E.K., R.E.M., and J.M. contributed new reagents/analytic tools; G.P.A., D.E.K., R.E.M., R.T., and C.B.A. analyzed data; and G.P.A. and M.R.S. wrote the paper.

Reviewers: W.B., University of Colorado; A.B., Green Technology Group/California EPA; and D.C.N., Earth Innovation Institute.

The authors declare no conflict of interest.

Freely available online through the PNAS open access option.

[1]To whom correspondence should be addressed. Email: gpa@carnegiescience.edu.

This article contains supporting information online at www.pnas.org/lookup/suppl/doi:10.1073/pnas.1419550111/-/DCSupplemental.

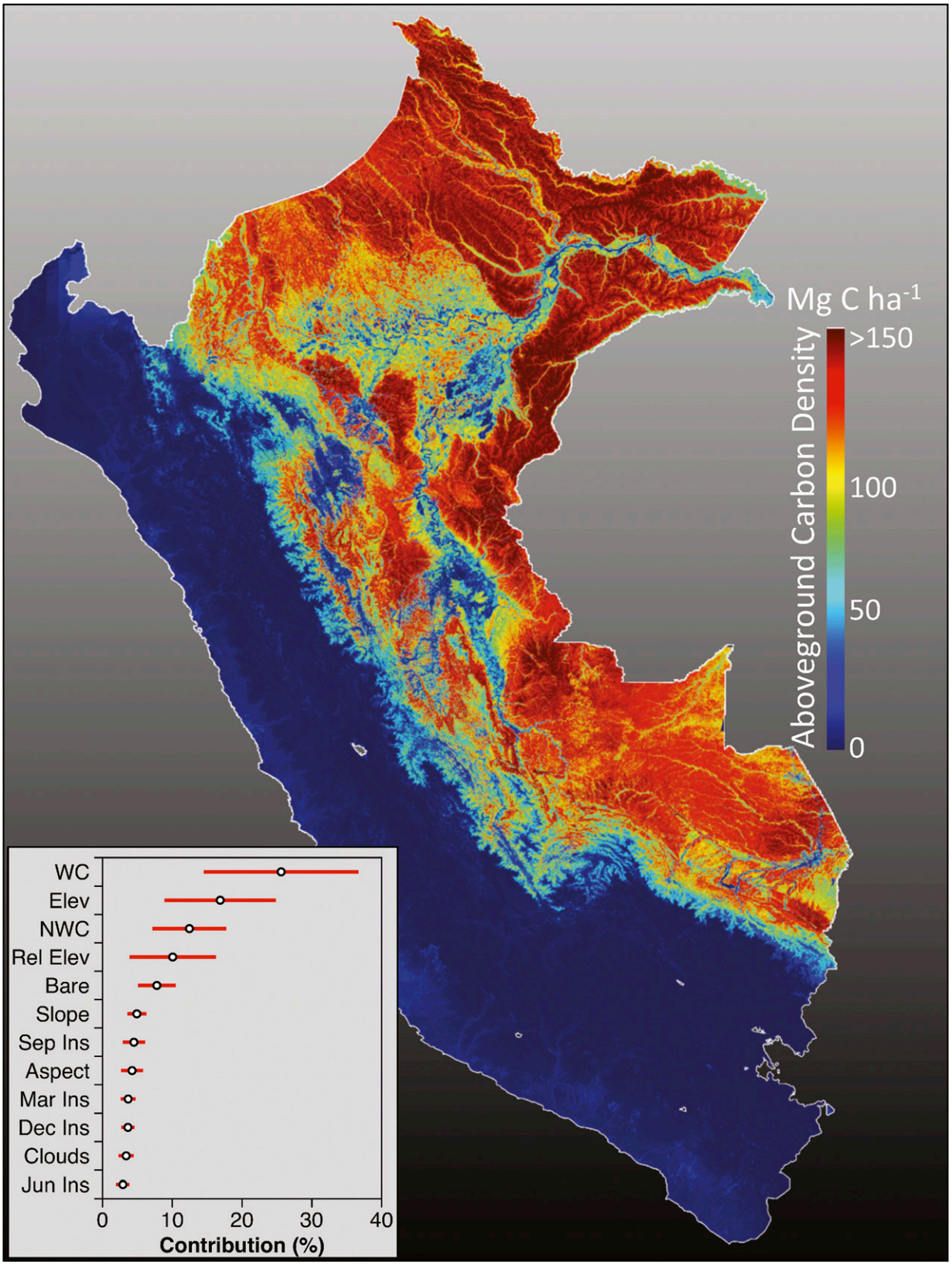

Fig. 1. The geography of aboveground carbon density (ACD) throughout Perú, derived at a 1-ha resolution with uncertainty reported for each hectare (*SI Appendix*, Fig. S9). (*Inset*) Graph reporting the relative importance of environmental factors predicting ACD (*SI Appendix*). These factors include the fractional cover of woody plants (WC), elevation, nonwoody plant cover (NWC), relative elevation above nearest water body (Rel Elev), bare substrate cover, topographic slope and aspect, solar insolation at four points of the year (e.g., Jan Ins), and cloud cover.

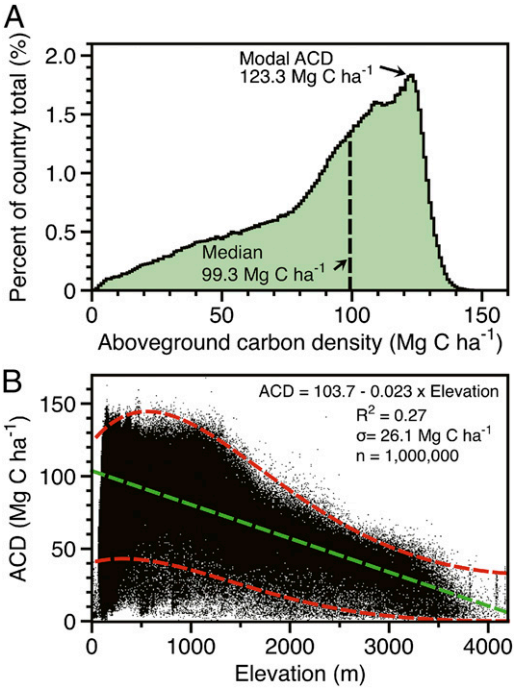

Fig. 2. (*A*) Distribution of aboveground carbon density (ACD) throughout Perú. (*B*) Decreasing ACD with increasing elevation in 1 million randomly selected hectares in intact forest. Green and red lines indicate mean and 2 SDs, respectively.

strategies can be developed to reduce or counterbalance carbon emissions from these sources; however, practical limitations require that these strategies be specific to geographic location, ecological context, and land tenure status throughout the country.

To generate a geography of carbon at the scales required for targeted conservation interventions, we integrated countrywide ecosystem sampling using airborne light detection and ranging (LiDAR) with high-resolution satellite imaging, a distributed field plot calibration and validation network, and a geospatial scaling technique to map the aboveground carbon density (ACD) of Perú at a 1-ha resolution (*SI Appendix*, Figs. S1–S7). After validating the new ACD map, we assessed natural and human controls on carbon stocks to identify opportunities for new interventions as well as limitations to potential REDD+ activities. Here we report ACD in units of Mg C ha^{-1} (Mg, metric tons) and total stock in Pg (billion metric tons).

Results and Discussion

High-Resolution Carbon Map. The high-resolution map of Perú reveals a wide range of ACD values, from <1 Mg C ha^{-1} in dry desert systems on the western, leeward side of the Andes to >150 Mg C ha^{-1} in the northeastern lowland Amazonian forests (Fig. 1). The country's total estimated aboveground carbon stock is 6.922 Pg, with a country-scale uncertainty of <1%. ACD variability in the Amazonian lowlands is driven by highly localized variations in river and stream incisions, soil fertility gradients associated with diverse geologic substrates, and hydrological conditions (*SI Appendix*). On the Pacific coast leeward of the Andes, carbon stocks are naturally suppressed by the ultra-dry climate, with localized peaks in highly managed plantations.

Field-based validation indicates high precision and accuracy of the nationally mapped ACD (*SI Appendix*, Fig. S8). Spatially explicit analyses reveal an ACD uncertainty on any given hectare of ≤20% in lowland Amazonian forests (*SI Appendix*, Fig. S9). On the dry western slopes of the Andes, uncertainty increases beyond 50% owing to the extremely sparse nature of the vegetation; however, large uncertainties in these low-carbon ecosystems result in absolute errors of only 1–4 Mg C ha^{-1}. Spatial averaging of mapped carbon stocks leads to greatly diminished overall uncertainty for a large region such as Perú (13).

Environmental Controls. Analysis of the high-resolution carbon map against satellite-derived environmental data identified the percentage cover of woody vegetation per hectare as the most important factor determining ACD throughout Perú (Fig. 1, *Inset*). Accounting for 26 ± 9% of the ACD variation, woody canopy cover is foremost a function of precipitation (14), which decreases along a steep gradient from the wet Amazon to the dry Pacific side of the Andes. In closed-canopy forests, decreases in woody canopy cover are tightly coupled to deforestation (15). Elevation also has a large overarching effect (18 ± 6%) on ACD (*SI Appendix*, Fig. S10). The next three most significant factors, including the fractional cover of nonwoody plants and bare substrate as well as relative elevation above nearest water body, accounted for an additional 32% of the ACD variation throughout the country. Within forest ecosystems, nonwoody canopy and bare substrate cover are well-known metrics of deforestation and degradation via logging and fire that removes woody plants (16–22). Relative elevation above the nearest water is highly indicative of a water deficit in deserts and grasslands or of a water surplus (which can cause anoxia) in rainforests, both of which reduce vegetation carbon storage. Together, these five factors account for approximately 75% of the variation in carbon densities throughout the country, and they integrate the effects of both natural and human-mediated processes.

To isolate the natural controls on large carbon stocks, we analyzed 1 million ha of randomly selected intact closed-canopy forest that exhibited a highly skewed ACD distribution ($\gamma = -0.831$; Fig. 2*A*). The median and modal values were 99.3 and 123.3 Mg C ha^{-1}, respectively. Departures from these values indicate conditions that mostly reduce, and in fewer cases enhance, forest carbon densities. Critically, average forest ACD decreased by 2.3 Mg C per 100 m of elevation gain (Fig. 2*B*), driven by a natural decrease in the growth-to-mortality ratio in colder montane climates (23, 24). Elevation is a key control on maximum carbon densities, yet variation at all elevations reflects additional controls, such as geology and hydrological conditions (25). These sources of variability diminish as the treeline is approached [3,720–4,260 m above sea level (ASL)], where temperature limitations are maximal.

Carbon Threats. Using a high-resolution carbon accounting approach, we quantified threats to carbon stocks by activities in current land use concessions. To date, more than 19.6 million ha of lowland Amazonian forests have been assigned to concessions for fossil fuel oil extraction and logging (Fig. 3*A*). These concessions currently hold high carbon densities, averaging 93–105 Mg C ha^{-1}, and a massive total aboveground carbon stock of 1.92 Pg (Table 1). Carbon losses from these concessions will vary based on the intensity of oil or timber extraction; however, recent studies suggest that road building and forest access generate at least a 30% decrease in carbon stock per hectare, but with high spatial variance (17, 25, 26). Applying this percentage loss to these concessions, ∼0.58 Pg C is at imminent risk for emission from oil and logging in the high-carbon density Amazonian lowlands. In the submontane and montane regions of the country, oil exploration threatens an additional 0.28 Pg of carbon aboveground, or 0.08 Pg C at the 30% loss threshold. We note that ∼19% of the fuel oil and logging concessions overlap geographically with protected or indigenous lands (Fig. 3), likely resulting in additional threats to the future carbon stocks of these large forest tracts.

Beyond these threats, ongoing carbon losses via deforestation for animal and crop agriculture or for urban and suburban development have resulted in low ACD levels (5 ± 5 Mg C ha^{-1}) in

and around Perú's Amazonian cities (*SI Appendix*, Fig. S11). Based on Peruvian government deforestation statistics (27), roughly 1.4 million ha of forest (or 0.14 Pg C at 100 Mg C ha^{-1}) have been lost via agriculture and infrastructural development since 2000. If these rates continue, we estimate a future loss of 0.14 Pg C in the next decade (Table 1). Additional emerging threats to Perú's lowland carbon stocks include artisanal gold mining and oil palm plantations (*SI Appendix*, Fig. S12) (7, 28). Comparing current gold mining and oil palm plantation carbon stocks with intact forest carbon densities within 10 km of them, we find that these activities remove 70–95% of the aboveground carbon stock, leaving just 15–34 Mg C ha^{-1}, down from ~96 Mg C ha^{-1} (Table 1). Because the future of Peruvian gold mining and oil palm plantations is unknown, owing to the lack of land use allocation policy (e.g., concessions) and subsequent law enforcement challenges (29, 30), the threat posed by these activities to future carbon emissions cannot be better quantified.

In sum, we find that more than 2.34 Pg C in land use concessions or in the active path of infrastructural and agricultural development equates to at least 0.80 Pg of aboveground carbon at risk for emission to the atmosphere. This does not include carbon emissions associated with uncontrolled gold mining or unknown oil palm plantation development. Also not included are belowground carbon losses, which will add an additional 25–50% (31) to the total carbon threatened by land use change in Perú.

Carbon Protections. We identified current land allocations that serve to protect carbon stocks in Perú. Protected areas, such as national parks and reserves, represent one of the most robust potential sources of carbon conservation. A total of 1.82 Pg C is currently stored aboveground in 174 government-administered protected areas covering 21.7 million ha (Fig. 3, Table 1, and *SI Appendix*, Table S1). ACD averages 83.6 Mg C ha^{-1} in these protected areas, with enormous variation (SD, ±40.9 Mg C ha^{-1}) resulting from variable environmental conditions and encroaching human activity. In addition, we found that nearly 870,000 ha of government-administered Brazil nut and rubber concessions in southern Perú contain 0.11 Pg C aboveground in high-biomass forests averaging 90.6–110.3 Mg C ha^{-1}.

We analyzed carbon stocks among 1,350 nongovernment landholders whose tenure is predicated on some form of nature conservation. These include ecotourism, wildlife management and conservation concessions, and rubber, Brazil nut, and reforestation concessions (*SI Appendix*, Table S1). Individual land areas in these concessions range from 1 to 224,618 ha, and yet they store surprisingly consistent ACDs, averaging 100.9 ± 14.8 Mg C ha^{-1}. However, owing to their limited extent of just 1.7 million ha in total, these lands currently protect only 0.17 Pg C aboveground. In

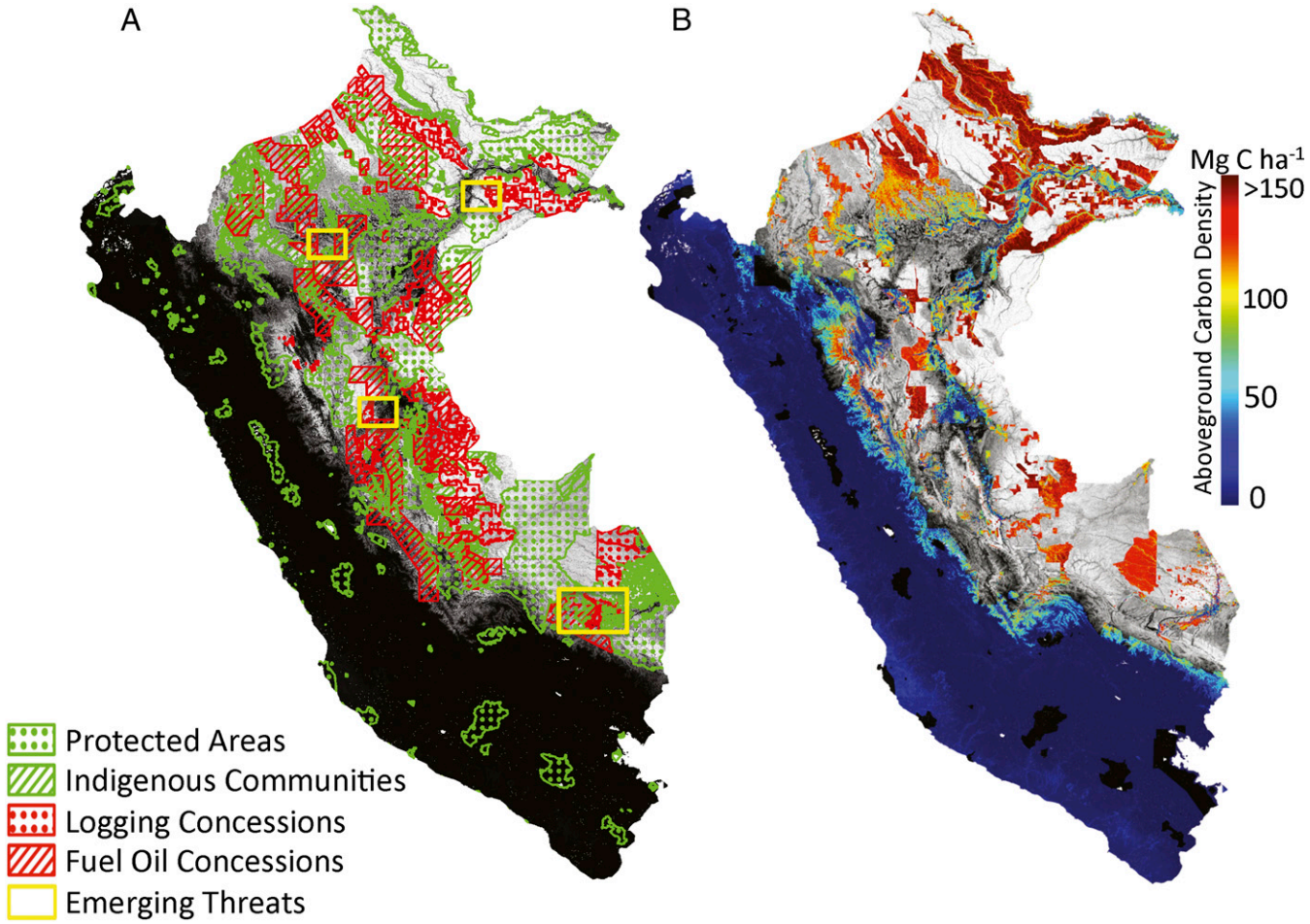

Fig. 3. The distribution of major carbon storage threats, protections, and opportunities throughout Perú. (*A*) Threats in logging and fuel oil concessions vs. current protections in government and nongovernment administered protected areas, indigenous communities, and extractive reserves. Yellow boxes highlight emerging threats of oil palm plantations and informal gold mining (*SI Appendix*, Fig. S12). (*B*) Geographic distribution and carbon densities of lands outside of known threat and protective areas.

Table 1. Carbon conservation threats, protections, and opportunities throughout Perú

Type	ACD, Mg C ha^{-1} Mean	SD	Area, ha	Total AG carbon stock, Pg
Threats				
Selective logging*	104.9	22.1	6,417,552	0.68
Oil concessions (<500 m ASL)[†]	93.1	32.3	13,226,773	1.24
Oil concessions (500-2,000 m)[†]	76.4	30.8	2,959,029	0.24
Oil concessions (>2,000 m)[†]	42.9	20.3	76,231	0.04
Infrastructure, animal and crop farming	5.0	5.8	1,400,000[‡]	0.14[§]
Total threats			22,679,585	2.34
Emerging threats				
Artisanal gold mining[¶]	34.5	29.6	37,831	0.01
Oil palm plantations[#]	15.4	10.9	9,684	0.001
Protections*				
Government-protected areas	83.6	40.9	21,728,378	1.82
Nongovernment-protected areas	100.9	14.8	1,743,277	0.17
Indigenous communities	93.1	27.2	9,051,407	0.84
Brazil nut concessions	110.3	16.8	869,312	0.10
Rubber concessions	90.6	19.1	16,158	0.01
Total protections			33,408,532	2.94
Opportunities				
Lowland Amazonia (<500 m ASL)	86.3	39.4	22,639,377	1.95
Sub-montane vegetation (500–2,000 m)	39.2	36.9	7,680,728	0.30
High Andean vegetation (>2,000 m)	7.4	4.8	19,353,554	0.14
Total opportunities			49,673,659	2.39

Calculations are based on land use concession and other maps shown in Fig. 3 and *SI Appendix*, Fig. S12. AG, aboveground; ASL, above sea level.
*Peruvian Ministry of the Environment (geoservidor.minam.gob.pe/geoservidor/repositorio.aspx).
[†]PetroPeru (www.perupetro.com.pe/wps/wcm/connect/480a8b89-0353-4879-a850-523ec62c3024/Lotes+de+Contrato+%28Mayo+2014%29.zip?MOD=AJPERES).
[‡]Decadal deforestation rate reported by the Peruvian Ministry of the Environment and dominated by urban-suburban development, animal ranching, and crop agriculture.
[§]Estimated losses over the next 10 years at the current rate of deforestation.
[¶]Based on Asner et al. (7); ACD mapped in active and abandoned gold mining areas.
[#]For a few large plantations mapped in this study (*SI Appendix*, Fig. S12); small plantations not included.

contrast, indigenous community lands contain similar ACD levels (93.1 ± 27.2 Mg C ha^{-1}) but cover ∼9 million ha, thereby protecting more than 0.84 Pg C (Table 1).

The degree to which indigenous lands should be considered as protective of carbon stocks remains unclear, given the plethora of land use and land encroachment issues and the deficiency of knowledge regarding native land uses (30). Nonetheless, evidence gathered from Brazil's indigenous territories strongly suggests that these lands are far more carbon-protective compared with neighboring forms of land use (32). Combining all current forms of protective land uses, we estimate that a total of 2.94 Pg C are currently stored aboveground on 33.4 million ha throughout Perú.

Carbon Opportunities. Spatially explicit tracking of current carbon threats and protections reveals new opportunities for carbon conservation, which vary widely based on underlying environmental conditions that naturally limit or promote carbon storage. First, there is a major opportunity to avoid carbon emissions by establishing additional forest protections in biogeographically distinct regions of Perú (Fig. 3*B*). Much of the opportunity rests in the lowland Amazonian region of Loreto, where very high carbon densities were found. Additional major lowland targets exist in the central and southern lowlands of Ucayali and Madre de Dios. A total of 1.95 Pg C are available aboveground in the Amazonian lowlands for use in emission avoidance (Table 1). In addition, a large amount of fragmented land near lowland urban and rural centers already contains highly degraded carbon densities. Comparing degraded areas with neighboring lowland forests with high ACD levels of 86.3 ± 39.4 Mg C ha^{-1}, we contend that lowland degraded areas offer large carbon gains if assigned to restoration projects.

A second opportunity exists in the submontane region between lowland Amazonia and the Andean highlands (500-2,000 m ASL), where we mapped 0.30 Pg C available for protection (Fig. 3*B* and Table 1). These lands contain a highly variable average ACD of 39.2 ± 36.7 Mg C ha^{-1} on 7.7 million ha, with carbon densities decreasing with increasing elevation. Once in the high Andes above 2,000 m ASL, potential carbon conservation gains diminish as ACD levels drop to 7.4 ± 4.8 Mg C ha^{-1}. Together, submontane and montane lands offer 0.44 Pg C aboveground and perhaps 50% more belowground for new protection.

Beyond the establishment of these new carbon protections, the current portfolio of government-protected areas spans a wide range of enforcement levels, with some areas strictly guarded against land use and others unmanaged or unenforced altogether (33) (*SI Appendix*, Table S1). Government-protected areas represent just 26% of the total aboveground carbon stock of Perú, and more than 85% of the aboveground carbon stored in these protected areas is found in just 10 parks and reserves, of which only 4 are afforded the status of full protection. As a result, the majority of Perú's government-protected areas remain accessible to land use. Transitioning partially protected areas to full protection would ensure that carbon is conserved to help counterbalance at least 0.8 Pg of aboveground carbon at risk for emission from land use concessions. Moreover, our analyses reveal that an average of 95.1 Mg C is sequestered in aboveground vegetation for every hectare of Amazonian forest placed under full protection, with up to 50% more invested belowground (*SI Appendix*, Fig. S13).

Targeted Carbon Conservation. The key to using ecosystems to help achieve national emissions reduction goals rests in devising interventions that target sufficient areas of biogeographically

appropriate land. High-resolution mapping reveals the key abiotic factors, including elevation and climate, that generate a natural carbon template on which policies and management can work to maximize carbon storage. Our analysis reveals that 2.94 Pg of aboveground carbon is currently stored on land allocated for protective activities throughout Perú, compared with more than 2.34 Pg threatened by land use change. Carbon densities are distributed similarly throughout the country in protected and threatened areas (Fig. 4*A*), and these two areas show nearly the same carbon storage response to increasing elevation (Fig. 4*B*). By integrating this information spatially, we identified opportunities to secure an additional 2.39 Pg of aboveground carbon.

To secure additional aboveground carbon on such a large scale, it is critically important to decrease forest disturbance in land use concessions. Our forecast of 0.8 Pg of aboveground carbon emissions is driven largely by oil and timber extraction plans, but emissions can be reduced by restricting road access to oil concession areas and via reduced-impact logging (34, 35). Studies show that reduced-impact logging greatly reduces collateral canopy damage and leaves more forest cover (34, 36, 37), which is a principal determinant of carbon stocks throughout Perú (Fig. 1). The concept of reduced-impact oil exploration remains largely untested (38), suggesting the need for close monitoring of these concessions. The cobenefits of reduced disturbance include more secure hydrological functioning and biodiversity.

Any practical effort to achieve a net neutral carbon balance depends not only on reducing gross emissions, but also on promoting carbon uptake at a gross rate that balances losses. For example, field studies suggest that western Amazonian forests sequester an average of 0.45 Mg C ha^{-1} y^{-1} aboveground (39). Thus, to offset our estimated 0.8 Pg of aboveground carbon in imminent danger of release via land use, ~18 million hectares of additional forest protection will be required for active carbon sequestration over the next 100 y. Currently, the unprotected forests of the lowland Amazon and submontane Andes are the most viable candidates for this additional forest protection, offering ~30 million ha of new protection (Table 1). Moreover, a geographically distributed portfolio of new areas across widely varying environmental conditions will be needed to increase resilience to losses incurred from unplanned land use encroachment and climate change (40). Drought poses a particular threat to carbon stocks (39, 41), and, given the regional specificity of past mega-droughts (42), maintaining a diverse national portfolio of forest carbon protections will be critically important in the coming decades.

Tactical Carbon Management at Scale. Land use can be traced to most human sources of greenhouse gases. Emissions occur directly through land change processes, such as deforestation, or indirectly via transportation networks and industries supporting natural resource extraction, energy and food production, and other essential societal needs (43). To minimize the effects of emissions on the climate, natural ecosystems are needed to store as much carbon as possible and to offset gross emissions through sequestration, even in the face of a changing climate system. Managing this critically important resource must be achieved tactically if it is to be cost-effective. This will allow for successful regulatory, market-based, and volunteer actions at multiple geographic scales, using specific land parcels distributed among currently threatened, protected, and still-unallocated ecosystems.

Here we have shown that high-resolution carbon mapping can uniquely identify biogeographically explicit targets for carbon storage enhancement at a national scale. Field-based inventory plot networks are not designed to deliver this type of spatially explicit information, hectare by hectare, at scales ranging from local to subnational to national levels; however, doing so will promote the involvement and participation of stakeholders whose efforts range in scale from small landholdings (1 ha) to large government-administered regions of millions of hectares. The approach that we have developed and implemented can be rapidly updated at low cost, significantly reducing the lag times of years to decades incurred when using field plot inventory approaches alone. Our project cost was approximately 1 US cent ($0.01) per hectare when applied over the entire country of Perú. The common misunderstanding that airborne LiDAR is overly expensive is an artifact of the past use of airborne LiDARs over too small of a geographic extent and without quantitative methods for scaling the LiDAR data up to full geographic coverages at regional to national levels. The integrated use of massive airborne LiDAR sampling and wall-to-wall high-resolution satellite information overcomes the cost-to-coverage barrier. As a result, this high-resolution, rapid assessment methodology can be replicated and applied anywhere in the world (44).

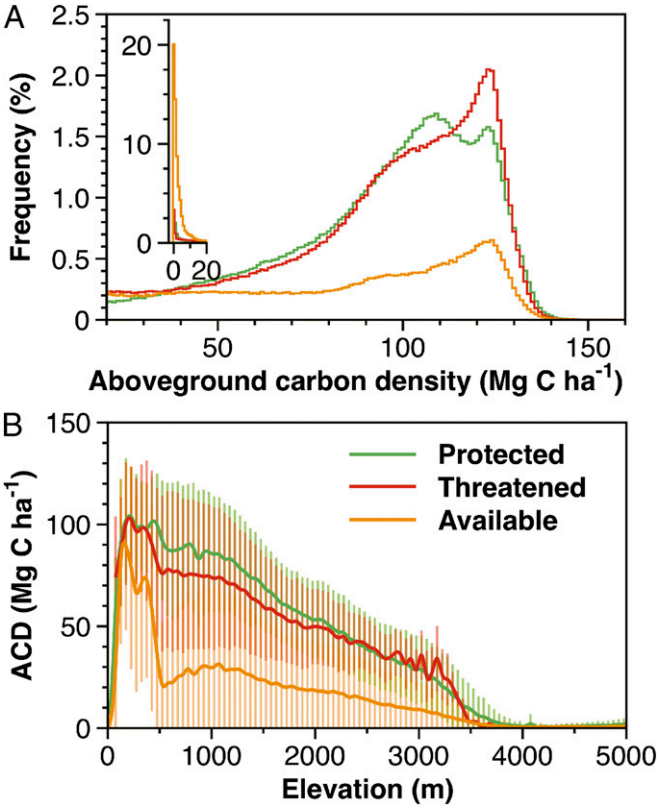

Fig. 4. (*A*) Percentage distribution of threatened, protected, and available aboveground carbon density throughout Perú. (*B*) Changes in aboveground carbon density (ACD) with elevation change in threatened, protected, and available categories. Vertical bars indicate 2 SDs.

Despite the demonstrable gains in geographic coverage, reduced cost, and increased accuracy of carbon mapping presented here, we recognize the importance of additional considerations when developing tactical carbon conservation approaches at the national level. These include the marginal cost of land, biodiversity value, ownership issues (including indigenous rights), and other factors. Nonetheless, we contend that high-resolution mapping, with known accuracies at a 1-ha resolution, provides a tangible medium with which stakeholders can engage one another. In effect, the map facilitates a dialogue based on something real: the amount of carbon stored on each hectare of land under the ownership, control, and/or interest of all potential parties.

Finally our map-based analysis serves as only one (albeit major) input into a larger set of calculations of baseline carbon stocks and emissions in the context of international and subnational REDD+ investments. In the case of Perú, a business-as-usual emissions baseline is needed, and our carbon map and the

historical analysis component of our study can be readily used to develop a high-resolution, geographically explicit emissions baseline. This already has been done retrospectively, on an annual basis dating back to 1999, at a subnational scale for the Madre de Dios region (25). Expanding this to the national level is straightforward using deforestation data already generated by the Peruvian Ministry of the Environment (27). More work is needed to bring these component inputs together in an operational framework, however. All nations will need to implement such an approach to manage their contributions to climate change.

Methods

The study covers the 128.5 million-ha country of Perú. The vast majority of the aboveground carbon is found in humid forests stretching from the Andean treeline to the lowland Amazonian forests as far as the Ecuadorian, Colombian, Brazilian, and Bolivian borders. A much smaller amount of dry tropical forest exists primarily in the northern portion of the country, and those areas were fully incorporated into the study. The study also included less well-understood regions, including alpine tundra and high-altitude grasslands, as well as woodlands and shrublands in the inter-Andean corridor.

Our mapping approach is based on the original high-resolution method presented by Asner (45), with a series of improvements developed through testing and analysis in a wide variety of countries and ecosystems (25, 46–49). The approach combines readily available satellite and geographic information system datasets at 1-ha or finer resolution with airborne LiDAR and field plot calibration data in a modeling framework to develop maps of ACD with spatially explicit uncertainty estimates (*SI Appendix*).

ACKNOWLEDGMENTS. This study was made possible by an interinstitutional working agreement between the Carnegie Institution Department of Global Ecology and the Dirección General de Ordenamiento Territorial, Peruvian Ministry of the Environment. We thank the Peruvian Air Force, collaborating organizations, and the members of the Carnegie Airborne Observatory team for important contributions to this study. Special thanks go to G. Powell, J. Clark, and G. Paez-Acosta for logistical assistance, and to the three reviewers for their critique of the manuscript. This study was funded by the John D. and Catherine T. MacArthur Foundation. The Carnegie Airborne Observatory is supported by the Avatar Alliance Foundation, Grantham Foundation for the Protection of the Environment, John D. and Catherine T. MacArthur Foundation, Gordon and Betty Moore Foundation, W. M. Keck Foundation, Margaret A. Cargill Foundation, Mary Anne Nyburg Baker and G. Leonard Baker Jr., and William R. Hearst III.

1. Baccini A, et al. (2012) Estimated carbon dioxide emissions from tropical deforestation improved by carbon-density maps. *Nat Clim Change* 2:182–185.
2. Angelsen A (2008) *Moving Ahead with REDD: Issues, Options and Implications* (Center for International Forestry Research, Bogor, Indonesia), p 156.
3. Pelletier J, Ramankutty N, Potvin C (2011) Diagnosing the uncertainty and detectability of emission reductions for REDD+ under current capabilities: An example for Panama. *Environ Res Lett* 6(2):024005.
4. REDD Offset Working Group (2013) *California, Acre and Chiapas: Partnering to Reduce Emissions from Tropical Deforestation*, ed Johnson E (Green Technology Leadership Group, Sacramento, CA), p 69.
5. Newell RG, Stavins RN (2000) Climate change and forest sinks: Factors affecting the costs of carbon sequestration. *J Environ Econ Manage* 40(3):211–235.
6. Carlson KM, et al. (2012) Committed carbon emissions, deforestation, and community land conversion from oil palm plantation expansion in West Kalimantan, Indonesia. *Proc Natl Acad Sci USA* 109(19):7559–7564.
7. Asner GP, Llactayo W, Tupayachi R, Luna E Re (2013) Elevated rates of gold mining in the Amazon revealed through high-resolution monitoring. *Proc Natl Acad Sci USA* 110(46):18454–18459.
8. International Bureau of Weights and Measures (2006) *The International System of Units* (Organisation Intergouvernementale de la Convention du Metre, Paris, France), p 186.
9. Malhi Y, et al. (2006) The regional variation of aboveground live biomass in old-growth Amazonian forests. *Glob Change Biol* 12(7):1107–1138.
10. Mitchard ETA, et al. (2014) Markedly divergent estimates of Amazon forest carbon density from ground plots and satellites. *Glob Ecol Biogeogr* 23(8):935–946.
11. Lefsky MA, et al. (2005) Estimates of forest canopy height and aboveground biomass using ICESat. *Geophys Res Lett* 32:L22S02.
12. Saatchi SS, et al. (2011) Benchmark map of forest carbon stocks in tropical regions across three continents. *Proc Natl Acad Sci USA* 108(24):9899–9904.
13. Mitchard ET, et al. (2013) Uncertainty in the spatial distribution of tropical forest biomass: A comparison of pan-tropical maps. *Carbon Balance Manag* 8(1):10.
14. Asner GP, Elmore AJ, Flint Hughes R, Warner AS, Vitousek PM (2005) Ecosystem structure along bioclimatic gradients in Hawai'i from imaging spectroscopy. *Remote Sens Environ* 96(3-4):497–508.
15. Asner GP, Rudel TK, Aide TM, Defries R, Emerson R (2009) A contemporary assessment of change in humid tropical forests. *Conserv Biol* 23(6):1386–1395.
16. Asner GP, Keller M, Pereira R, Zweede JC, Silva JNM (2004) Canopy damage and recovery after selective logging in Amazonia: Field and satellite studies. *Ecol Appl* 14(Suppl 4):S280–S298.
17. Asner GP, et al. (2005) Selective logging in the Brazilian Amazon. *Science* 310(5747):480–482.
18. Broadbent EN, et al. (2008) Forest fragmentation and edge effects from deforestation and selective logging in the Brazilian Amazon. *Biol Conserv* 141:1745–1757.
19. Koltunov A, Ustin SL, Asner GP, Fung I (2009) Selective logging changes forest phenology in the Brazilian Amazon: Evidence from MODIS image time series analysis. *Remote Sens Environ* 113(11):2431–2440.
20. Bryan JE, et al. (2013) Extreme differences in forest degradation in Borneo: Comparing practices in Sarawak, Sabah, and Brunei. *PLoS ONE* 8(7):e69679.
21. Souza C, Firestone L, Silva LM, Roberts D (2003) Mapping forest degradation in the Eastern Amazon from SPOT 4 through spectral mixture models. *Remote Sens Environ* 87(4):494–506.
22. Souza C, Roberts DA, Cochrane MA (2005) Combining spectral and spatial information to map canopy damages from selective logging and forest fires. *Remote Sens Environ* 98:329–343.
23. Girardin CAJ, et al. (2010) Net primary productivity allocation and cycling of carbon along a tropical forest elevational transect in the Peruvian Andes. *Glob Change Biol* 16(12):3176–3192.
24. Asner GP, et al. (2014) Landscape-scale changes in forest structure and functional traits along an Andes-to-Amazon elevation gradient. *Biogeosciences* 11:843–856.
25. Asner GP, et al. (2010) High-resolution forest carbon stocks and emissions in the Amazon. *Proc Natl Acad Sci USA* 107(38):16738–16742.
26. Viña A, Echavarria FR, Rundquist DC (2004) Satellite change detection analysis of deforestation rates and patterns along the Colombia–Ecuador border. *Ambio* 33(3):118–125.
27. MINAM (2012) *Memoria Técnica de la Cuantificación de los Cambios de la Cobertura de Bosque y Deforestación en el Ambito de la Amazonía Peruana (Periodo 2009-2010-2011)* (Peruvian Ministry of the Environment, Lima, Peru), p 62.
28. Gutiérrez-Vélez VH, DeFries R (2013) Annual multi-resolution detection of land cover conversion to oil palm in the Peruvian Amazon. *Remote Sens Environ* 129(0):154–167.
29. Victor HG-V, et al. (2011) High-yield oil palm expansion spares land at the expense of forests in the Peruvian Amazon. *Environ Res Lett* 6(4):044029.
30. Oliveira PJC, et al. (2007) Land-use allocation protects the Peruvian Amazon. *Science* 317(5842):1233–1236.
31. Berenguer E, et al. (2014) A large-scale field assessment of carbon stocks in human-modified tropical forests. *Glob Change Biol*, 10.1111/gcb.12627.
32. Nepstad D, et al. (2006) Inhibition of Amazon deforestation and fire by parks and indigenous lands. *Conserv Biol* 20(1):65–73.
33. Naughton-Treves L, et al. (2006) Expanding protected area and incorporating human resource use: a study of 15 forest parks in Ecuador and Peru. *Sustain Sci Pract Policy* 2(2): 32–44.
34. Keller M, Palace M, Asner GP, Pereira R, Silva JNM (2004) Coarse woody debris in undisturbed and logged forests in the eastern Brazilian Amazon. *Glob Change Biol* 10(5):784–795.
35. Huang M, Asner GP (2010) Long-term carbon loss and recovery following selective logging in Amazon forests. *Global Biogeochem Cycles* 24(3):GB3028.
36. Healey JR, Price C, Tay J (2000) The cost of carbon retention by reduced- impact logging. *Forest Ecol Manag* 139(1-3):237–255.
37. Holmes TP, et al. (2002) Financial and ecological indicators of reduced-impact logging performance in the eastern Amazon. *Forest Ecol Manag* 163:93–110.
38. Finer M, Jenkins CN, Pimm SL, Keane B, Ross C (2008) Oil and gas projects in the Western Amazon: Threats to wilderness, biodiversity, and indigenous peoples. *PLoS ONE* 3(8):e2932.
39. Phillips OL, et al. (2009) Drought sensitivity of the Amazon rainforest. *Science* 323(5919): 1344–1347.
40. Asner GP, Loarie SR, Heyder U (2010) Combined effects of climate and land use change on the future of humid tropical forests. *Conserv Lett* 3:395–403.
41. Cox PM, et al. (2004) Amazonian forest dieback under climate-carbon cycle projections for the 21st century. *Theor Appl Climatol* 78(1):137–156.
42. Lewis SL, Brando PM, Phillips OL, van der Heijden GMF, Nepstad D (2011) The 2010 Amazon drought. *Science* 331(6017):554.
43. Foley JA, et al. (2005) Global consequences of land use. *Science* 309(5734):570–574.
44. Mascaro J, Asner GP, Davies S, Dehgan A, Saatchi S (2014) These are the days of lasers in the jungle. *Carbon Balance Manag* 9(1):7.
45. Asner GP (2009) Tropical forest carbon assessment: Integrating satellite and airborne mapping approaches. *Environ Res Lett* 3:034009.
46. Asner GP, et al. (2011) High-resolution carbon mapping on the million-hectare island of Hawaii. *Front Ecol Environ* 9(8):434–439.
47. Asner GP, et al. (2012) Human and environmental controls over aboveground carbon storage in Madagascar. *Carbon Balance Manag* 7(1):2.
48. Asner GP, et al. (2012) High-resolution mapping of forest carbon stocks in the Colombian Amazon. *Biogeosciences* 9(7):2683–2696.
49. Asner GP, et al. (2013) High-fidelity national carbon mapping for resource management and REDD+. *Carbon Balance Manag* 8(1):7.

SUPPORTING INFORMATION

Targeted Carbon Conservation at National Scales with High-Resolution Monitoring

Gregory P. Asner[1], David E. Knapp[1], Roberta E. Martin[1], Raul Tupayachi[1], Christopher B. Anderson[1], Joseph Mascaro[1], Felipe Sinca[1], K. Dana Chadwick[1], Mark Higgins[1], William Farfan[2], William Llactayo[3], Miles R. Silman[2]

[1]Department of Global Ecology, Carnegie Institution for Science, Stanford, CA USA (gpa@carnegiescience.edu, dknapp@carnegiescience.edu, rmartin@carnegiescience.edu, r2t.dge@gmail.com, cbanders@carnegiescience.edu, jmascaro@stanford.edu)

[2]Department of Biology, Wake Forest University, Winston-Salem, NC USA (wfarfan@gmail.com, silmanmr@wfu.edu)

[3]Dirección General de Ordenamiento Territorial, Ministerio del Ambiente, San Isidro, Lima, Perú (wllactayo@minam.gob.pe)

* Author for correspondence: gpa@carnegiescience.edu; Tel: 650.3251521; Fax 650.462.5968

This file includes:

Methods

Our mapping approach is summarized in **Fig. S1**. The core technology is airborne Light Detection and Ranging (LiDAR), which yields highly detailed measurements of forest canopy height and vertical canopy profile that predictably scale with variation in aboveground carbon stocks. Recent studies of a wide range of vegetation types worldwide demonstrate that airborne LiDAR can be used to estimate ACD at one-hectare resolution with a precision and accuracy matching estimates based on field measurements alone (1). When properly calibrated, airborne LiDAR-based and field plot-based estimates of forest carbon stocks approach just 10% absolute disagreement at one-hectare spatial resolution, across a wide range of vegetation types including tropical forests (2, 3). This offset of around 10% is lower than the typical errors incurred in field plot-based estimates of tropical forest carbon stocks at one-hectare resolution (4). This suggests that airborne LiDAR can be used to extend field-plot networks to far larger spatial scales. Critically, airborne LiDAR-estimated stocks of aboveground carbon can be generated over hundreds of thousands of hectares per day -- a task that cannot be accomplished with field plots.

A second key component of the approach to derive high-resolution carbon maps relies on machine learning algorithms to scale airborne LiDAR samples up to full regional or country-wide coverage maps. For decades, stratification and sampling of forests based on *a priori* environmental information, such as elevation or forest type, has served as the method to extrapolate carbon stock estimates from field inventory plots (5). However, stratification-based methods can yield artificial boundaries in the resulting carbon maps, particularly when applied across highly diverse environmental

conditions (6). In response to this problem, Baccini et al. (7) employed a Random Forest Machine Learning (RFML) algorithm to model the relationship between LiDAR-based forest carbon samples and a portfolio of spatially extensive satellite data sets. RFML fits multiple environmental datasets (predictors) to estimates of vegetation structure or biomass (response), as described later. In doing so, a direct scaling of LiDAR samples to full-coverage maps can be derived without artificial boundaries between ecosystems that often occur using traditional stratification approaches. Recently, Mascaro et al. (8) showed that scaling LiDAR-based carbon samples up to a regional level was 60% more accurate with RFML compared to traditional stratification approaches. In addition, Baccini and Asner (9) demonstrated that RFML methods can be quickly and cost-effectively updated with new carbon data over time, allowing for dynamic long-term monitoring. Another attractive characteristic of RFML is its ability to provide quantitative information on the environmental variables most predictive of current carbon distributions (8, 10).

LiDAR Flight Planning

We used airborne LiDAR to massively sample plant canopy structure throughout Perú. The final map of aboveground carbon density (ACD) relied on an airborne LiDAR sampling approach that supplies data to the RFML upscaling methodology (described below). This required a focus of many aircraft flights on forested ecosystems, but it also included extensive portions of grassland, shrubland, savanna, and open woodland ecosystems. We approached this challenge by over-sampling the land surface using a preliminary national stratification of the country as a flight-planning guide. The

stratification was based on geologic substrate, soils, topography and large known shifts in community composition, and was described in detail in (11).

LiDAR Data Acquisition

The LiDAR data were collected using the Carnegie Airborne Observatory-2 Airborne Taxonomic Mapping System (AToMS; 12), which is carried onboard a twin turbopropeller Dornier 228 aircraft. The AToMS LiDAR is a dual laser, scanning waveform system capable of firing at 500,000 laser shots per second. To cover the maximum area per flight hour, the aircraft was operated at speeds of up to 150 knots at an altitude averaging 2000 m above ground level. The LiDAR settings were configured to achieve an average on-the-ground laser spot spacing of 4 shots m^{-2}, peaking at 8 shots m^{-2} in areas of flightline overlap.

Airborne LiDAR sampling was carried out using 100 x 100 km grid cells overlaid on the stratification map. For this study, we sought to sample at least 2% (200 km^2) of each grid cell, with the additional goal of sampling at least 2% of the weighted contribution each stratification class to each grid cell. Past work has shown that 1% coverage per vegetation type yields robust and stable statistical distributions for landscapes of about 500 ha or larger (6). A total of 6,761,624 ha of LiDAR data were collected throughout the country in an extensive sampling pattern shown in **Fig. S2a**. The LiDAR sampling density achieved by stratification class averaged 6.47% or 655.8 km^2 per grid cell (**Fig. S2b**). Some grid cells to the far edges of the mapping area were sampled less, with the lowest coverage amounting to 179.2 km^2 (1.8%) of a grid cell along the border with Colombia.

LiDAR-based Canopy Height

Mean top-of-canopy height (TCH) was calculated for each hectare of LiDAR coverage (n = 6,761,624). To create this data layer, laser range measurements from the LiDAR were combined with embedded high resolution Global Positioning System-Inertial Measurement Unit (GPS-IMU) data to determine the 3-D locations of laser returns, producing a 'cloud' of LiDAR data. The resulting LiDAR data cloud consisted of a very large number of precisely georeferenced point elevation measurements (n = ~278 trillion), where elevation is relative to a reference ellipsoid (WGS 1984).

These LiDAR data points were processed to identify which laser pulses penetrated the canopy volume and reached the ground surface, from which a high-resolution digital terrain model (DTM) was developed. This was achieved using a 10 m x 10 m filter kernel throughout the LiDAR coverage, and the lowest elevation in each kernel was deemed a possible ground detection. These filtered points were then evaluated by fitting a horizontal plane through each point. If the closest unclassified point was < 5.5^{o} and < 1.5 m higher in elevation, the pre-filtered point was finalized as a ground-classified surface point. This process was repeated until all potential ground points within the LiDAR coverage were evaluated. A digital surface model (DSM), which is essentially the top-most surface (e.g., canopies, buildings, exposed ground), was also generated based on interpolations of all first-return points at 1.0 m spatial resolution. By combining the DTM and DSM in a tightly matched pair of data layers, the vertical difference between them yielded a high-accuracy model of top-of-canopy height (TCH) at 1.1 m spatial resolution throughout the 6,761,624 ha LiDAR sampling coverage.

Previous validation studies of this CAO LiDAR TCH estimation approach has demonstrated it to be highly accurate in a wide range of forests including extremely densely foliated, tall tropical forests exceeding 60 m in height and leaf area index (LAI) levels (13, 14). The 1.1-m TCH data were then averaged to one-hectare resolution, which further decreases uncertainty in derived mean top-of-canopy canopy height (15).

Upscaling LiDAR to a Full Map Coverage

Scaling up a large volume of LiDAR TCH data to full map coverage can be accomplished with a variety of techniques, one of which is applying LiDAR-derived statistics of canopy height to an environmental stratification map. Often stratification maps are based on *a priori* knowledge of vegetation type and/or abiotic factors such as soils, elevation, and climate. This "paint by numbers" stratified sampling approach is often used with plot-based forest inventory data to assign field-based estimates to different stratification classes (16-18). Stratification has also been used with airborne LiDAR in nearly the same type of approach (6).

The problem with stratification is that it is overly dependent upon *a priori* knowledge of the factors that may or may not drive variation in the ecological metric of interest -- aboveground carbon density in this case. In an environmentally complicated region like Perú, with ecosystems ranging from cold highland deserts to humid submontane assemblages to vast lowland forests on varying geologies, we likely cannot stratify well enough to develop confidence in bridging the scale gap from LiDAR or field plots to full geographic coverages. Moreover, because extremely large geographies contain exceedingly remote habitats and highly variable cloud densities, neither LiDAR

datasets nor field inventory plots can be placed throughout them in a random or systematically-aligned design (19). This renders typical spatial methods for scaling, such as averaging or kriging (20), prone to very large errors. As a result, maps based on stratification or simple spatial extrapolation are unreliable, and they cannot be used to properly generate spatially-explicit maps of uncertainty, which is paramount to understanding the stocks, gains and losses of carbon from a large, heterogeneous region such as the Peruvian Andes or the Amazon basin.

To meet this challenge, machine learning algorithms have been developed and applied to spatially-discontinuous datasets, like field plots and LiDAR sampling, in order to develop spatially-explicit estimates of vegetation properties based on spatially-contiguous environmental variables such as topography, geologic substrate and long-term climate maps. In this context, the Random Forest Machine Learning (RFML) algorithm (21), has been used in global tropical forest carbon mapping (7), as well as in national, sub-national, and down-scaled global carbon mapping (9, 10). RFML fits multiple decision trees to input data (e.g. spatially-coincident environmental datasets) using a random subset of the input variables for each tree constructed for a given response variable (e.g., LiDAR TCH samples). The modal value of the calculated decision trees is used to create an "ensemble" tree that is used for prediction (e.g. spatially-contiguous TCH). RFML is non-parametric, insensitive to data skew, and robust to a high number of variable inputs (22). Recently, a comprehensive comparison of RFML to the traditional stratification-based approach for upscaling LiDAR samples has demonstrated the RFML approach in a 16 million ha portion of lowland Amazonia (8). However, that study also suggested that spatial context plays a major role in

determining how well RFML can scale from local samples to full coverage, particularly with respect to strong gradients in environmental factors. In the case of the Andes-to-Amazon, or Perú as a whole, the region contains enormous variation in most abiotic factors including elevation, slope, aspect, geologic substrate and soils, floristics, and climate. Thus, RFML cannot perform well unless it has a mechanism to accommodate numerous and rapid spatial changes in environmental conditions.

To address this issue, we developed a new version of RFML based on a moving tile technique that ingests the airborne LiDAR data in local models (**Fig. S3**). These tiles are then mosaicked together to form large, contiguous, national-scale mapping products. Specifically, we created hundreds of RFML models by dividing the LiDAR and environmental data into a system of geographic tiles, each covering 200 x 200 km per tile. In addition, we ran the models on these tiles with an overlap of 50 km on each side, for a total coverage of 300 x 300 km per tile. In each tile, up to 60,000 1-ha LiDAR measurements of average TCH were randomly selected from all possible LiDAR 1-ha TCH values in the tile. The remaining unselected LiDAR data were used later for validation of the RFML modeling approach, described later.

The environmental variables used in each of the tiled RFML models were taken from co-aligned predictor spatial datasets (**Fig. S4**). These include the fractional cover of photosynthetic vegetation (PV), non-photosynthetic vegetation (NPV), and bare substrate (Bare) derived from a national-scale mapping of Perú using the CLASlite approach with a mosaic of Landsat satellite imagery (23). Each fractional cover map quantitatively indicates the percentage cover in every 30-m Landsat pixel, and as a result, the maps of PV, NPV and Bare substrate are highly sensitive to spatial variation

in canopy gap fraction, openness and roughness, as described in previous studies (24, 25). The fractional cover maps were computed from a mosaic of cloud-free imagery using the compositing method presented in Asner et al. (10), with an additional cross-image brightness normalization (26). Previous studies have demonstrated that fractional PV and NPV are highly correlated with woody and non-woody cover, respectively, in nearly all ecosystems (27-32).

An additional set of environmental variables was derived from NASA Shuttle Radar Topography Mission (SRTM) at 90 m resolution: elevation, slope and aspect (**Fig. S4**). A relative elevation model (REM) was also developed by calculating the height of the ground above nearest water body (33), thus providing a spatial proxy for vegetation-related water resources. We included multiple potential incoming solar insolation models using SRTM elevation data in the SAGA GIS Potential Insolation module (34). These insolation layers (units of $kWhm^{-2}$) were created by modeling total insolation (direct and diffuse) for the days of the equinoxes and solstices (21st of Mar, Jun, Sept, and Dec). Additionally, we included long-term (2000-2010) cloudiness data derived from the NASA Moderate Resolution Imaging Spectroradiometer (MODIS). Cloudiness is based on the number of times a MODIS pixel was identified as being affected by clouds in the Quality Assurance (QA) flags of the 8-day reflectance product (35). The QA flags used in the compilation included the following: Pixel Adjacent to Cloud, Internal Cloud Algorithm, Cirrus Detected, Cloud Shadow and MOD35 Cloud. The number of flags that were set to "on" for each pixel were added and averaged to yield a percent cloudiness per pixel. All environmental predictor maps were resampled to one-

hectare resolution, co-aligned, and combined into a stack of predictor variables covering the entire country of Perú.

The predictor maps and the LiDAR one-hectare TCH samples were run through the tile-based RFML models to create regression trees (**Fig. S1, S3**). Because the process was carried out on individual 300 x 300 km tiles, some discontinuities along the edges of each tile were observed. A mosaicking methodology was therefore developed to adjust the data in the overlap area of each tile in the mosaic. To accomplish this goal, a central tile was used as the start of the national-scale mosaic, and adjacent overlapping tiles were added one by one along the edges of the central tile. Each new tile added to the mosaic was adjusted as a weighted average of each pixel based on its proximity to the edge of the tile. For example, a one-hectare pixel on the very edge of a 300 x 300 km tile would be weighted more with the value of the overlapping pixel of its neighbor tile. Similarly, a pixel close to the center of its tile, but still in the overlap area, would be weighted more with the tile center to which it is closest.

To further increase the robustness of this tile-based RFML approach, we ran ten iterations for each tile, with each iteration randomly selecting a different set of up to 60,000 one-hectare LiDAR TCH observations. Additionally, in each tile RFML run, we successively shifted the extent of the tile by 10% (20 km) in the East-West and North-South directions. Each of these ten iterations formed a separate mosaic of the mapped (upscaled) TCH throughout Perú. The ten individual, national-scale mosaics were then averaged to produce a single national-scale map of TCH at one-hectare resolution, with a corresponding standard deviation map generated from the ten individual RFML modeling runs. The standard deviation map is an indicator of how uncertain predicted

TCH is in each hectare of Perú based on using different sets of direct LiDAR TCH observations throughout the tiling system.

We left out 10.5% (536,874 ha) of the LiDAR data from the RFML models, randomly distributed throughout the entire LiDAR coverage. We used these data to validate the upscaled TCH map, which indicated a $R^2 = 0.78$ and a root mean squared error (RMSE) of 3.50 m (**Fig. S5a**). In addition, we analyzed our relative error in mapped TCH as a percentage RMSE against LiDAR-measured canopy height (**Fig. S5b**). This indicated large relative errors of more than 60% on short (low biomass) vegetation of less than 5 m height, and decreasing relative error of less than 20% on higher biomass vegetation of 15 m or taller. For the purposes of ecological analysis or carbon accounting, these errors are quite low, and are heightened only in smaller canopies that often represent very low-biomass shrublands or rapidly regrowing successional vegetation associated with agricultural systems that are not large aboveground carbon stores. In contrast, our errors are demonstrably low for tall forest ecosystems where the overwhelming majority of aboveground carbon is stored.

Calibrating Mapped TCH to ACD

Aboveground carbon density (ACD) was estimated from the mapped TCH data following the approach of plot-aggregate allometric scaling (1, 2). They determined that a highly precise and accurate link between TCH and field estimates of ACD can be made by applying regional plot-aggregated estimates of vegetation wood density and diameter-to-height relationships. To develop this TCH-to-ACD calibration for Andean and Amazonian forests, and other vegetation types throughout the region, a permanent

inventory plot network was established in three latitudinal belts covering northern, central and southern Perú. The network includes 272 plots comprised of 262 0.3-ha plots, and an additional ten 1.0-ha plots as shown in **Fig. S6**. The plot network is arranged in a nested design of 5-30 individual plots in 13 regionally distributed clusters to capture landscape-scale heterogeneity in carbon stocks across geological, soil, topographic and floristic compositional conditions. The plots include major forest types in lowland Amazonia including white sand, clay terrace, alluvial floodplain, swamp, *Mauritia* palm and bamboo-dominated ecosystems. Additionally, the plot network incorporates an extensive sampling of submontane and montane dry to wet forests, woodlands and shrublands up to treeline at multiple altitudes and latitudes. Finally, the plot network includes coverage of both primary and secondary forests, selectively logged forests, Brazil-nut concession forests, and highly degraded to deforested lands.

We estimated ACD in each field plot using allometric models. We first accounted for dead trees and non-tree growth forms, such as palms, bamboo, and lianas, by using growth-form-specific allometric models (6). For palms and dead trees we used models incorporating height measured using laser range finders. For all other individuals, we used a new, generalized allometric model from Chave et al. (36), which in addition to diameter, requires inputs of wood density and height. We identified 98.7% of living stems to genus, and obtained a genera-specific wood density estimate from a global wood density database for 96.4% of living stems. We accounted for height variation using a combination of direct measurements (with either laser range finders or clinometers) and diameter-based estimation. We measured the height of the three

largest-diameter trees in each plot (e.g., those with the greatest importance to carbon estimation) as well as seven or more additional trees in each plot spanning a range of diameters. These tree height data were used in two ways: (a) measured trees retained their measured heights for input into the Chave et al. (36) allometric model, and (b) more than 10,400 tree measurements were used for the creation of a diameter-to-height model that was used to estimate the height of all other trees. We multiplied all dry biomass estimates by 0.48 to calculate ACD.

We used maximum likelihood analysis to fit a power-law model between field-estimated ACD and TCH. The fit was performed on the un-transformed TCH and ACD values using a non-arithmetic error term to account for heteroskedasticity; this method is analogous to fitting a linear model to the log-transformed TCH and ACD data, but avoids the need for back-transformation (37). In addition, a recently identified change in wood density with elevation was incorporated into the TCH-to-ACD calibration using plots along an Andean-Amazon elevation gradient (38), thereby establishing the regression slope of a linear relationship between wood density and elevation. This slope was found to be 0.00005 mg cm^{-3} m^{-1} of elevation gain above 400 m elevation. The adjustment was applied to plots of elevations above 400 m:

$$WD_{adj} = WD_{orig} + ((ELEV_{site} - 400) * 0.00005) \quad \text{(i)}$$

Incorporating this adjustment for the elevation-dependence of wood density, the average increase in ACD at 1-ha resolution was 5.0 Mg ha^{-1} or 5.24%. The resulting relationship between TCH and ACD is shown in **Fig. S7**, with an RMSE = 27.4 Mg C ha^{-1} and an $R^2 = 0.82$. We view this accuracy and precision as excellent given the extreme breadth of vegetation structural, floristic and land-use variation incorporated in our

permanent plot network. The final calibration equation relating top-of-canopy height (TCH) to aboveground carbon density (ACD) for Andean and Amazonian forests is:

$$ACD = 0.8245 \times TCH^{1.573} \quad (2)$$

This equation was applied to the Perú-wide TCH map generated from the Random Forest modeling.

Validation of Mapped Carbon Densities

To validate the accuracy of our final carbon map, we held back field-based ACD estimates from 43 Carnegie plots spread throughout the permanent plot network coverage (**Fig. S8**). In addition, we used the eight published RAINFOR plots in lowland Amazonia (39) and six published sub-montane and montane plots (40). These field plot-based estimates of ACD were regressed against one-hectare mapped estimates from the fully upscaled (RFML modeled) results in Fig. 1 of the main text.

References

1. Asner GP, *et al.* (2012) A universal airborne LiDAR approach for tropical forest carbon mapping. *Oecologia* 168(4):1147-1160.
2. Asner GP & Mascaro J (2014) Mapping tropical forest carbon: Calibrating plot estimates to a simple LiDAR metric. *Remote Sensing of Environment* 140(0):614-624.
3. Zolkos SG, Goetz SJ, & Dubayah R (2013) A meta-analysis of terrestrial aboveground biomass estimation using lidar remote sensing. *Remote Sensing of Environment* 128:289-298.
4. Rejou-Mechain M, *et al.* (2014) Local spatial structure of forest biomass and its consequences for remote sensing of carbon stocks. *Biogeosciences Discuss.* 11(4):5711-5742.
5. Danae M & Mollicone D (2010) Options for sampling and stratification for national forest inventories to implement REDD+ under the UNFCCC. *Carbon Balance and Management* 5:1-9.
6. Asner GP, *et al.* (2010) High-resolution forest carbon stocks and emissions in the Amazon. *Proceedings of the National Academy of Sciences* 107:16738-16742.
7. Baccini A, *et al.* (2012) Estimated carbon dioxide emissions from tropical deforestation improved by carbon-density maps. *Nature Clim. Change* doi:10.1038/nclimate1354.
8. Mascaro J, *et al.* (2014) A tale of two "forests": Random Forest machine learning aids tropical forest carbon mapping. *PLoS ONE* 9(1):e85993.
9. Baccini A & Asner GP (2013) Improving pantropical forest carbon maps with airborne LiDAR sampling. *Carbon Management* 4(6):591-600.
10. Asner G, *et al.* (2013) High-fidelity national carbon mapping for resource management and REDD+. *Carbon Balance and Management* 8(1):7.
11. Asner GP, *et al.* (2014) *The High-Resolution Carbon Geography of Peru* (Minuteman Press, Berkeley, CA USA) p 69.
12. Asner GP, *et al.* (2012) Carnegie Airborne Observatory-2: Increasing science data dimensionality via high-fidelity multi-sensor fusion. *Remote Sensing of Environment* 124(0):454-465.
13. Asner GP, Hughes RF, Varga TA, Knapp DE, & Kennedy-Bowdoin T (2009) Environmental and biotic controls over aboveground biomass throughout a tropical rain forest. *Ecosystems* 12:261-278.
14. Taylor PG, *et al.* (in press) Landscape-scale controls on aboveground forest carbon stocks on the Osa Peninsula, Costa Rica.
15. Mascaro J, Detto M, Asner GP, & Muller-Landau HC (2011) Evaluating uncertainty in mapping forest carbon with airborne LiDAR. *Remote Sensing of Environment* 115(12):3770-3774.
16. Brown S, Gillespie AJR, & Lugo AE (1989) Biomass estimation methods for tropical forests with application to forest inventory. *Forest Science* 35:881-902.
17. Lowell K (1996) Discrete polygons or a continuous surface: which is the appropriate way to model forests cartographically? *Spatial Accuracy Assessment in Natural Resources and Environmental Sciences: 2nd International Symposium*, eds Mowrer HT, Czaplewski RL, & Hamre RH (U.S. Department of Agriculture,

Forest Service, Rocky Mountain Forest and Range Experiment Station, Fort Collins, Colorado), pp 235-242.
18. USDA Forest Service (2008) Forest Inventory and Analysis Program. (USDA, Arlington, VA).
19. McRoberts RE, Næsset E, & Gobakken T (2013) Inference for lidar-assisted estimation of forest growing stock volume. *Remote Sensing of Environment* 128:268-275.
20. Mitchard ETA*, et al.* (2014) Markedly divergent estimates of Amazon forest carbon density from ground plots and satellites. *Global Ecology and Biogeography*:n/a-n/a.
21. Breiman L (2001) Random forests. *Machine Learning* 45:5-32.
22. Evans JS, Murphy MA, Holden ZA, & Cushman SA (2011) Modeling species distribution and change using random forest. *Predictive species and habitat modeling in landscape ecology: concepts and applications*, eds Drew CA, Wiersma YF, & Huettmann F (Springer Science, New York, NY), pp 139-159.
23. Asner GP, Knapp DE, Balaji A, & Paez-Acosta G (2009) Automated mapping of tropical deforestation and forest degradation: CLASlite. *Journal of Applied Remote Sensing* 3:033543.
24. Bryan JE*, et al.* (2013) Extreme differences in forest degradation in Borneo: comparing practices in Sarawak, Sabah, and Brunei. *PLoS ONE* 8(7):e69679.
25. Carlson KM*, et al.* (2012) Committed carbon emissions, deforestation, and community land conversion from oil palm plantation expansion in West Kalimantan, Indonesia. *Proceedings of the National Academy of Sciences* 109(19):7559-7564.
26. Higgins MA*, et al.* (2012) Use of Landsat and SRTM Data to Detect Broad-Scale Biodiversity Patterns in Northwestern Amazonia. *Remote Sensing* 4(8):2401-2418.
27. Asner GP, Elmore AJ, Flint Hughes R, Warner AS, & Vitousek PM (2005) Ecosystem structure along bioclimatic gradients in Hawai'i from imaging spectroscopy. *Remote Sensing of Environment* 96(3–4):497-508.
28. Asner GP & Heidebrecht KB (2002) Spectral unmixing of vegetation, soil and dry carbon cover in arid regions: comparing multispectral and hyperspectral observations. *International Journal of Remote Sensing* 23(19):3939-3958.
29. Lobell DB, Asner GP, Law BE, & Treuhaft RN (2001) Subpixel canopy cover estimation of coniferous forests in Oregon using SWIR imaging spectrometry. *Journal of Geophysical Research-Atmospheres* 106(D6):5151-5160.
30. Roberts DA*, et al.* (2004) Spectral and structural measures of northwest forest vegetation at leaf to landscape scales. *Ecosystems* 7(5):545-562.
31. Souza C, Firestone L, Silva LM, & Roberts D (2003) Mapping forest degradation in the Eastern Amazon from SPOT 4 through spectral mixture models. *Remote Sensing of Environment* 87(4):494-506.
32. Asner GP, Knapp DE, Cooper AN, Bustamante MMC, & Olander LP (2005) Ecosystem structure throughout the Brazilian Amazon from Landsat observations and automated spectral unmixing. *Earth Interactions* 9:1-31.
33. Asner G*, et al.* (2012) Human and environmental controls over aboveground carbon storage in Madagascar. *Carbon Balance and Management* 7(1):2.

34. Cimmery V (2010) User Guide for SAGA (version 2.0.5) (SourceForge).
35. LPDAAC (2011) MOD09A1. ed Center NLPDAA (USGS Earth Resources Observation and Science (EROS), Sioux Falls, SD USA).
36. Chave J*, et al.* (2014) Improved allometric models to estimate the aboveground biomass of tropical trees. *Global Change Biology*:n/a-n/a.
37. Mascaro J, Litton CM, Hughes FR, Uowolo A, & Schnitzer SA (2011) Minimizing bias in biomass allometry: model selection and log-transformation of data. *Biotropica* 43(6):649-653.
38. Malhi Y*, et al.* (2010) Introduction: Elevation gradients in the tropics: laboratories for ecosystem ecology and global change research. *Global Change Biology* 16(12):3171-3175.
39. Peacock J, Baker TR, Lewis SL, Lopez-Gonzalez G, & Phillips OL (2007) The RAINFOR database: monitoring forest biomass and dynamics. *Journal of Vegetation Science* 18(4):535-542.
40. Girardin CAJ*, et al.* (2013) Comparison of biomass and structure in various elevation gradients in the Andes. *Plant Ecology and Diversity* 6(3):100-110.

Figure Legends

Fig. S1. Overview of the methodology used to map vegetation carbon stocks throughout the country of Perú: (A) A pre-stratification step combines geological, soil, community floristic composition, elevation, and forest cover maps to forecast the potential range of environmental conditions to be encountered during airborne surveys. (B) The country is gridded into 200 x 200 km sampling cells, and airborne Light Detection and Ranging (LiDAR) is used to massively sample each grid cell. Over-sampling is achieved by ensuring that large areas are covered for each potential set of environmental conditions estimated during pre-stratification. (C) A diverse array of satellite data is produced to provide continuous geographic information on vegetation cover, topographic variables, and climate. (D) The satellite and LiDAR data are processed through a geostatistical modeling approach, and combined with calibrations of LiDAR to field-estimated carbon stocks, to map aboveground carbon stocks at one-hectare resolution, along with spatially explicit uncertainty maps.

Fig. S2. (A) Airborne Light Detection and Ranging (LiDAR) from the Carnegie Airborne Observatory is used to sample the region shown in red lines. Total LiDAR observation coverage for this study was 6.7 million hectares. (B) Percentage coverage of each 200 x 200 km sampling grid cell. Previous studies indicate that over-sampling occurs at 1% LiDAR coverage, thus we consider this a "massive" sampling of the region.

Fig. S3. New geostatistical modeling approach based on the Random Forest Machine Learning (RFML) algorithm. The country of Perú is gridded into 300 x 300 km cells. In each cell, a diverse set of compiled satellite predictor maps (Fig. S4) are precisely co-aligned with airborne LiDAR samples. Up to 60,000 hectares of LiDAR data are randomly selected within a grid, and the RFML method is used to develop a prediction of LiDAR-based top-of-canopy height (TCH). This procedure is repeated ten times for each grid cell, with random selection of the input LiDAR data. An independent subset of LiDAR data are held back from the analysis of each grid cell to provide validation of the modeling results. This provides an estimate of the uncertainty in each grid cell.

Fig. S4. Geospatial datasets used in the Random Forest Machine Learning (RFML) algorithm to develop relationships between airborne LiDAR samples of top-of-canopy height (TCH; first image panel) and satellite-derived, continuous fields of fractional canopy cover (PV, NPV, Bare), topographic variables (elevation, slope, aspect, relative elevation above water body), average insolation at four points in the year, and cloudiness.

Fig. S5. (A) Validation of top-of-canopy height (TCH) modeled at the national scale using the Random Forest Machine Learning (RFML) approach and direct measurements of TCH from airborne LiDAR. (B) Decline in uncertainty of RFML-based TCH estimates with increasing TCH. This result is critically important since the majority of aboveground carbon stock is associated with vegetation heights of 15 meters or more.

Fig. S6. Regional distribution and density of Carnegie permanent field calibration-validation plot network in Perú. Circle locations indicate the centroid of each cluster of inventory plots; Circle colors indicate general forest type and condition; Elevation map indicates the partitioning of plots in lowland (blue-green), submontane (yellow) and montane (red) conditions.

Fig. S7. Calibration of airborne LiDAR-based measurements of top-of-canopy height (TCH) against field-based estimates of aboveground carbon density (ACD) in lowland, submontane and montane vegetation throughout Perú.

Fig. S8. Validation of nationally mapped estimates of aboveground carbon density (ACD) versus field plot inventory estimates of ACD for sites across Northern, Central and Southern Perú.

Fig. S9. Estimated percentage uncertainty of aboveground carbon density at one-hectare resolution for the country of Perú. See Fig. 1 of main text for the mean estimates of ACD associated with these uncertainty estimates.

Fig. S10. Zoom images of aboveground carbon density (ACD) to highlight natural sources of extreme variation, such as (A) Amazon river floodplain dynamics; (B) Prevalence of bamboo in Southern Peruvian Amazon forests; and (C) Dissipation of carbon stocks toward treeline in the Andes.

Fig. S11. Zoom images of aboveground carbon density (ACD) to highlight human-dominated sources of variation, such as (A) Deforestation and forest degradation around the city of Puerto Maldonado in Madre de Dios; (B) Deforestation along the Iquitos-Nauta road in Loreto; and (C) Massive areas of deforestation and land conversion outside of the city of Pucallpa in Ucayali.

Fig. S12. Zoom images from the high-resolution aboveground carbon map of Perú highlighting regions shown in yellow boxes of Fig. 3 (main text). These include areas threatened by oil palm plantations and gold mining in the central and northern Peruvian Amazon, as well as areas of protection in Brazil nut and rubber tree extractive reserves in southern Perú.

Fig. S13. Relationship between the size of protected areas in Perú and their total carbon stored above ground.

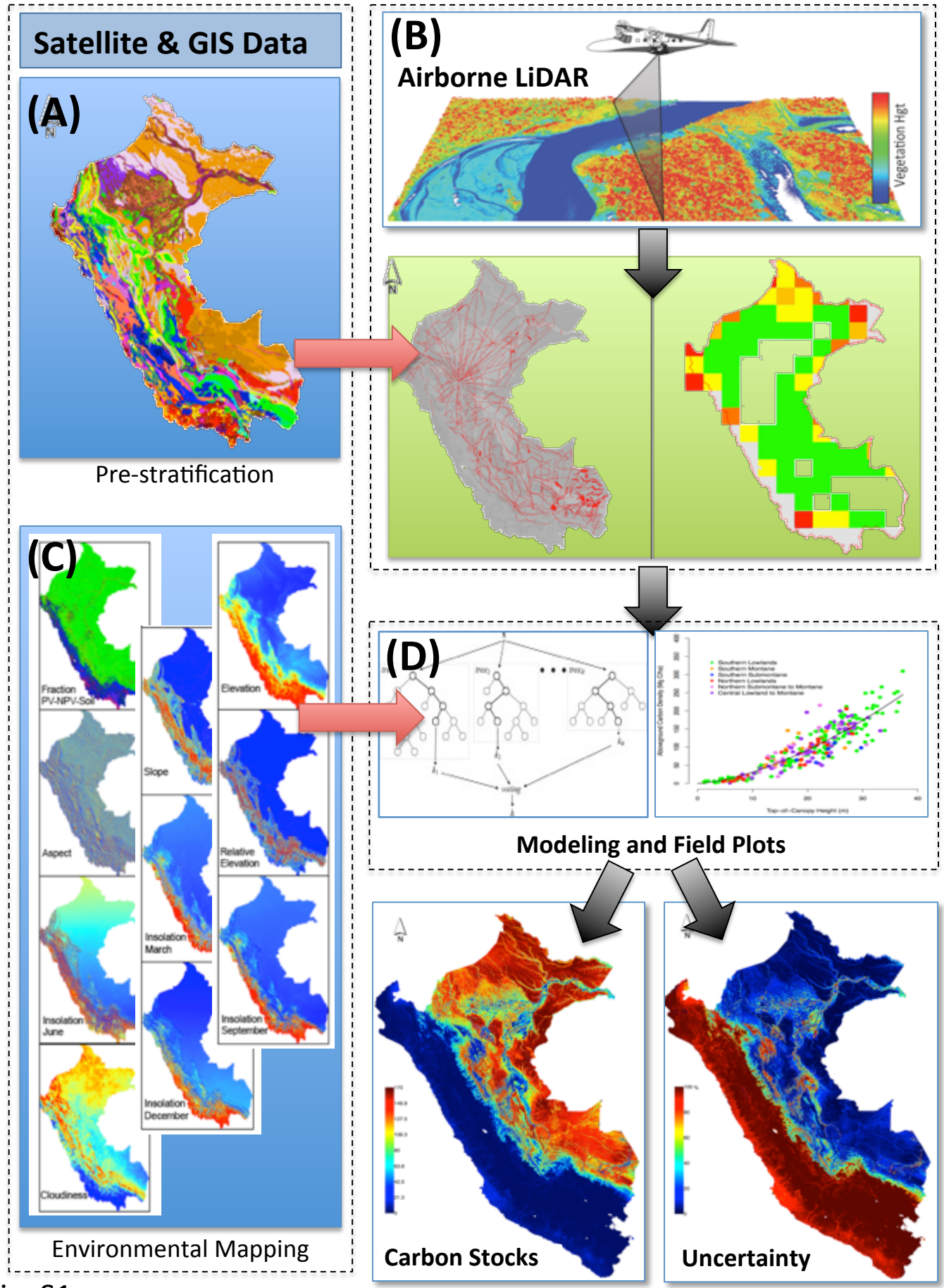
Satellite & GIS Data
(A)
Pre-stratification
(B)
Airborne LiDAR
Vegetation Hgt
(C)
Fraction PV-NPV-Soil
Elevation
Slope
Aspect
Relative Elevation
Insolation March
Insolation June
Insolation September
Insolation December
Cloudiness
Environmental Mapping
(D)
Modeling and Field Plots
Carbon Stocks
Uncertainty

Fig. S1

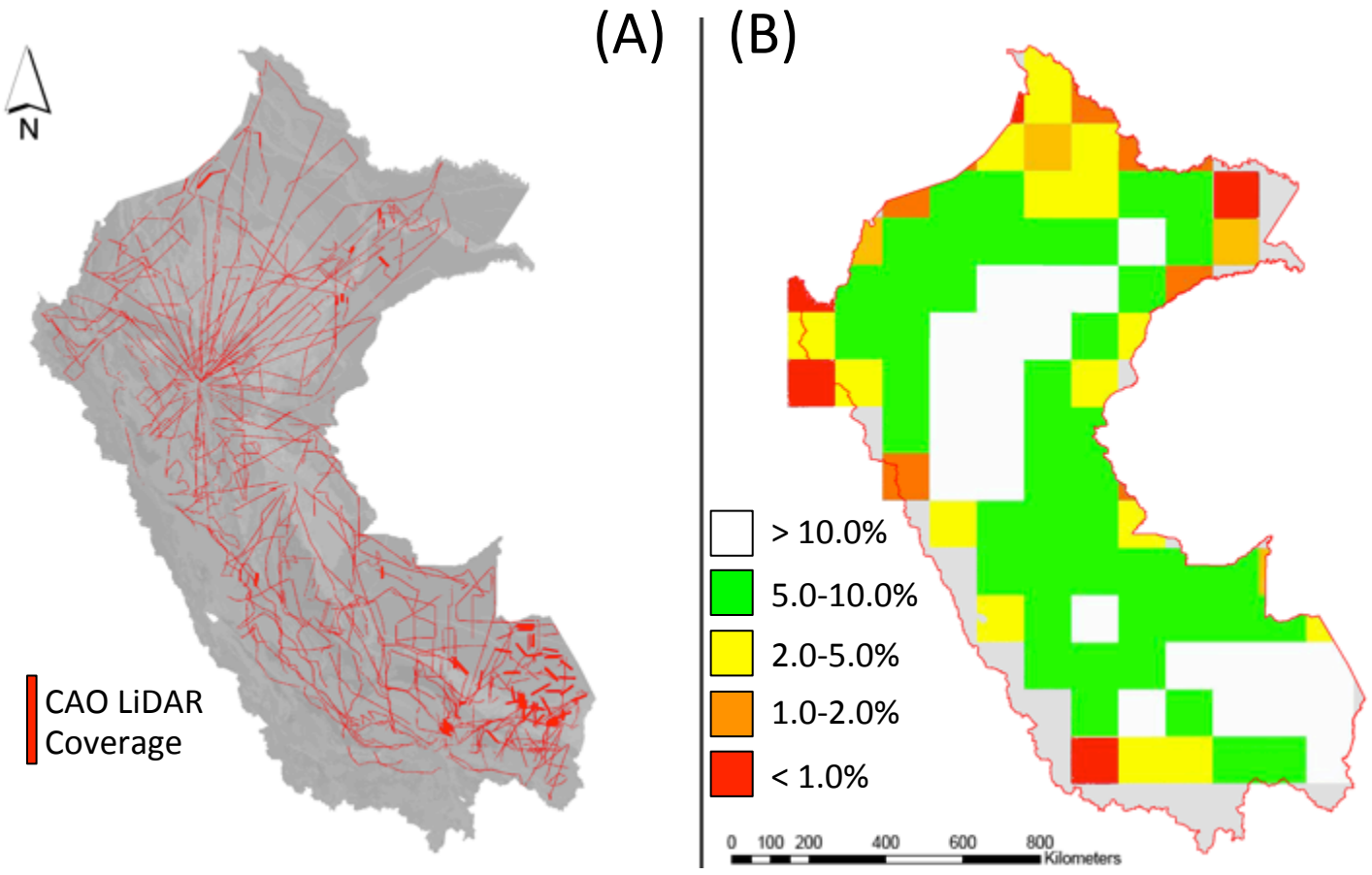
(A)
(B)
N
CAO LiDAR
Coverage
> 10.0%
5.0-10.0%
2.0-5.0%
1.0-2.0%
< 1.0%
0 100 200 400 600 800
Kilometers

Fig. S2

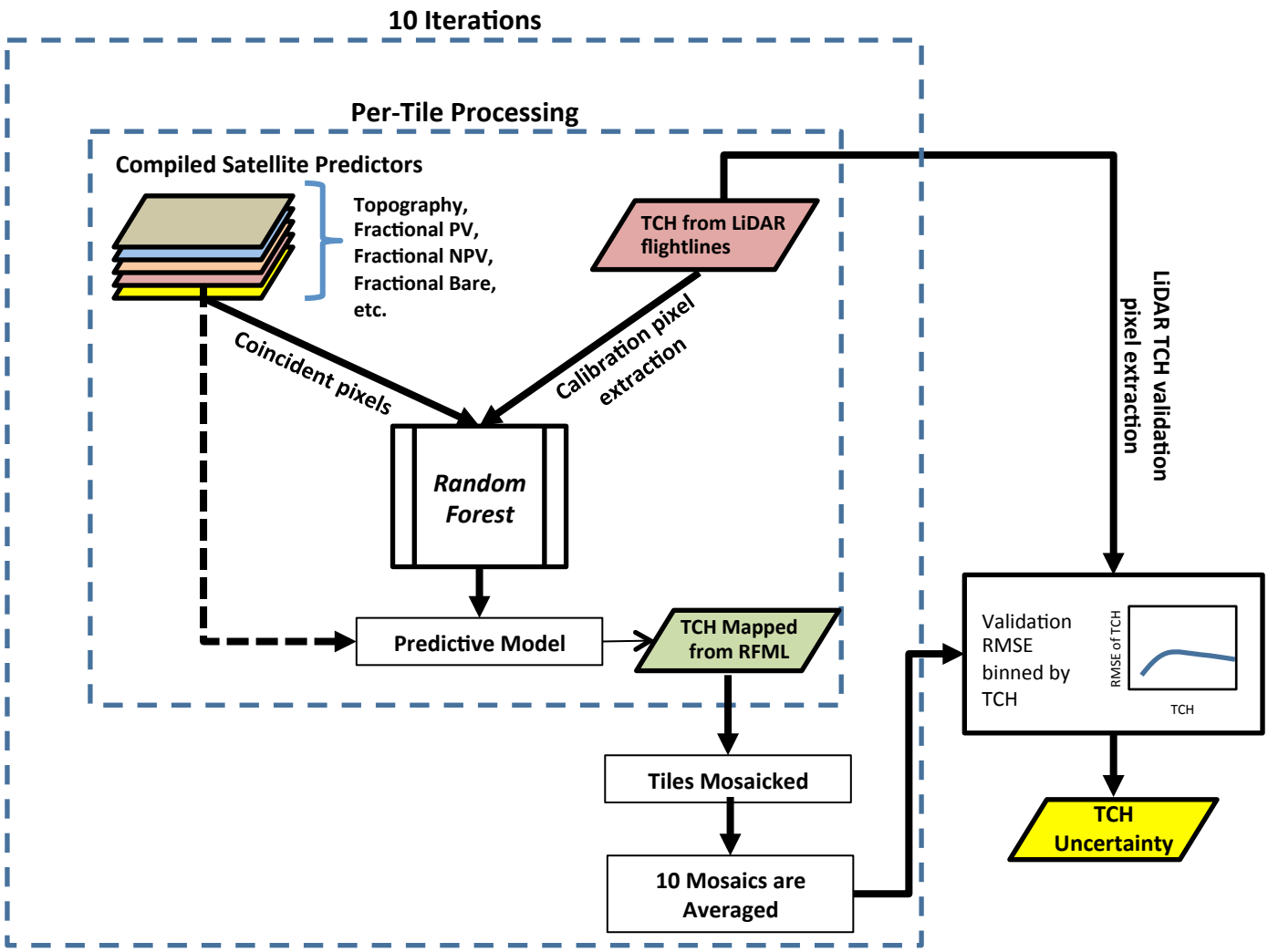
10 Iterations
Per-Tile Processing
Compiled Satellite Predictors
Topography,
Fractional PV,
Fractional NPV,
Fractional Bare,
etc.
TCH from LiDAR flightlines
LiDAR TCH validation pixel extraction
Coincident pixels
Calibration pixel extraction
Random Forest
Predictive Model
TCH Mapped from RFML
Validation RMSE binned by TCH
RMSE of TCH
TCH
Tiles Mosaicked
TCH Uncertainty
10 Mosaics are Averaged

Fig. S3

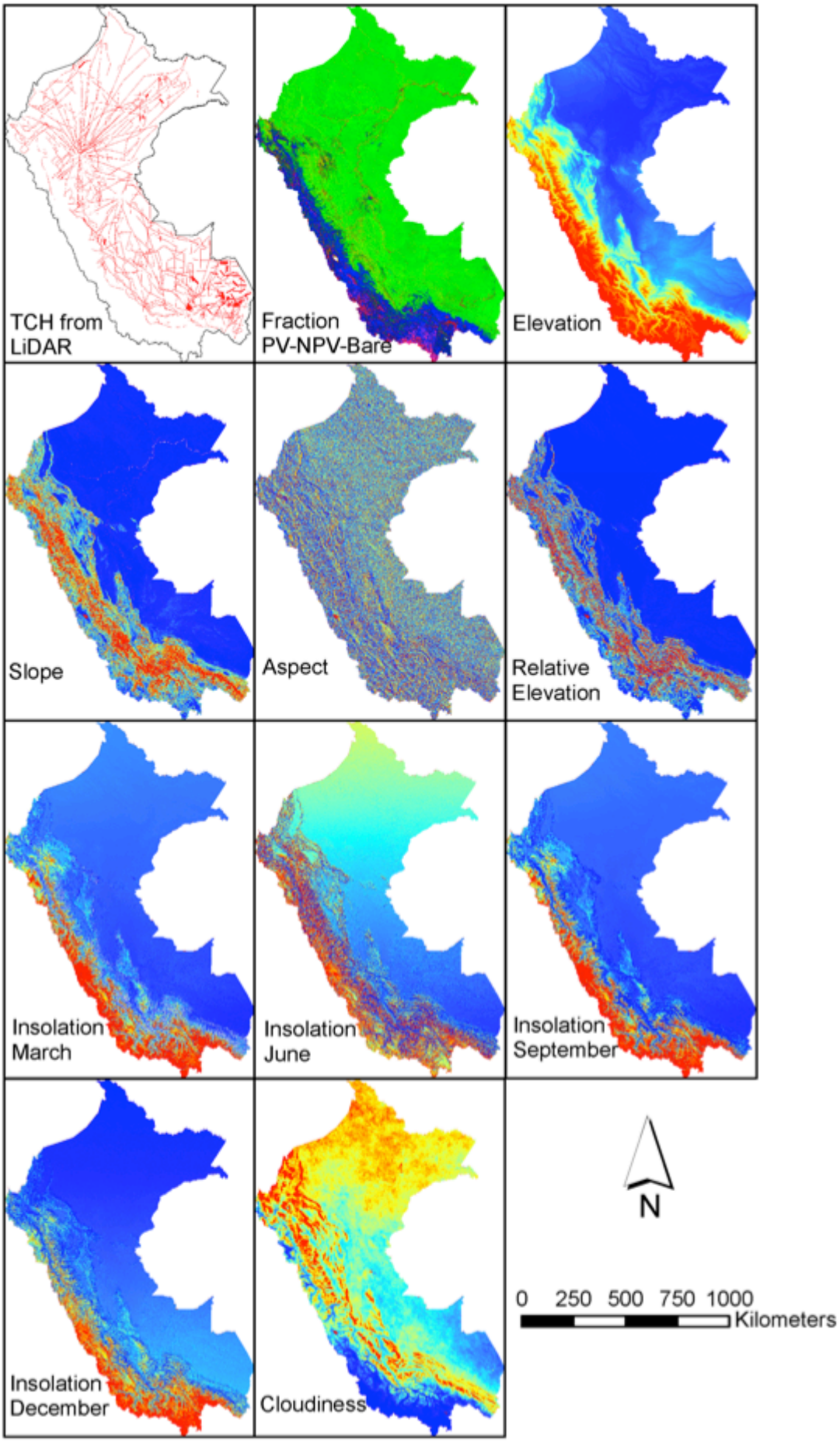
TCH from LiDAR
Fraction PV-NPV-Bare
Elevation
Slope
Aspect
Relative Elevation
Insolation March
Insolation June
Insolation September
Insolation December
Cloudiness
N
0 250 500 750 1000
Kilometers

Fig. S4

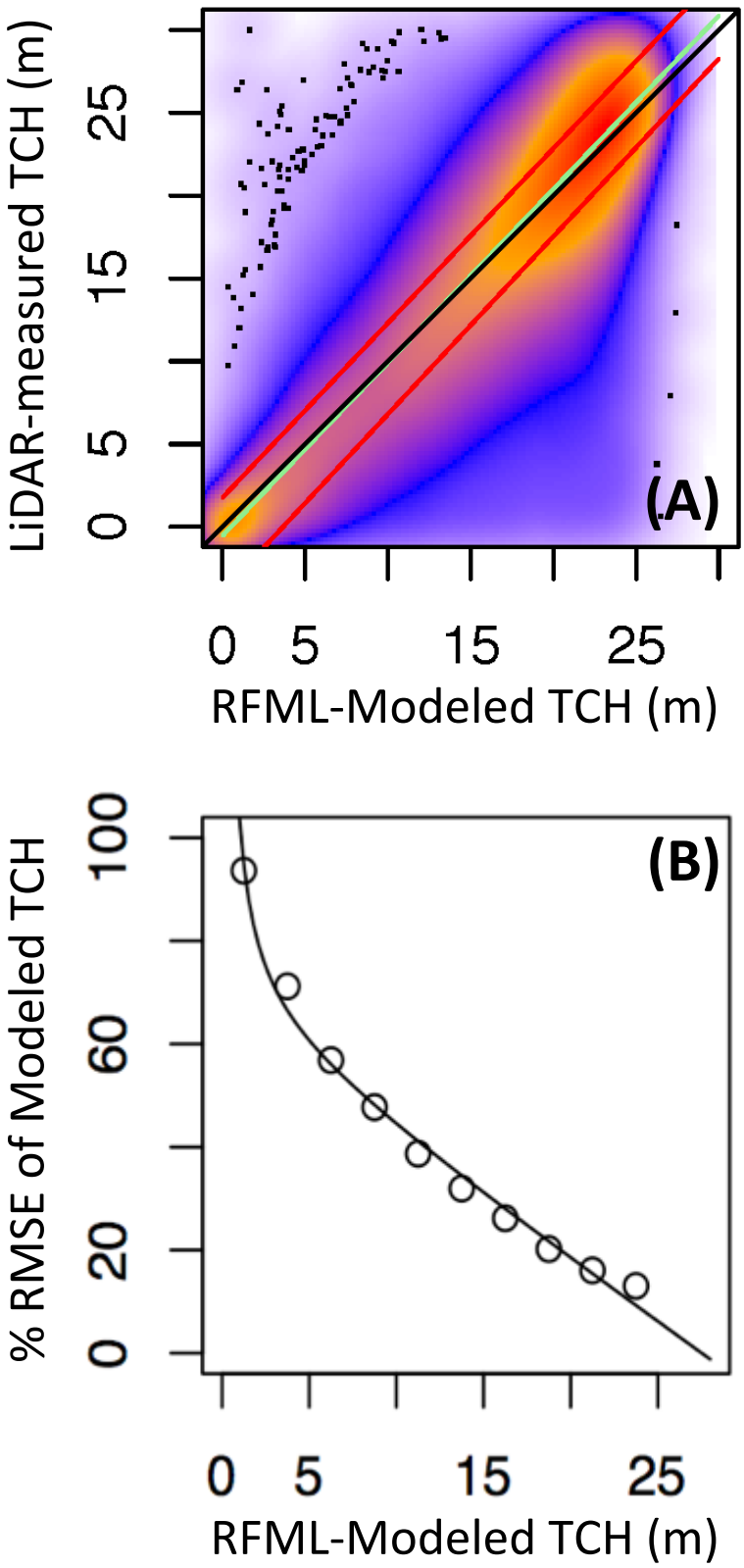
LiDAR-measured TCH (m)
0
5
15
25
(A)
0
5
15
25
RFML-Modeled TCH (m)
% RMSE of Modeled TCH
0
20
60
100
(B)
0
5
15
25
RFML-Modeled TCH (m)

Fig. S5

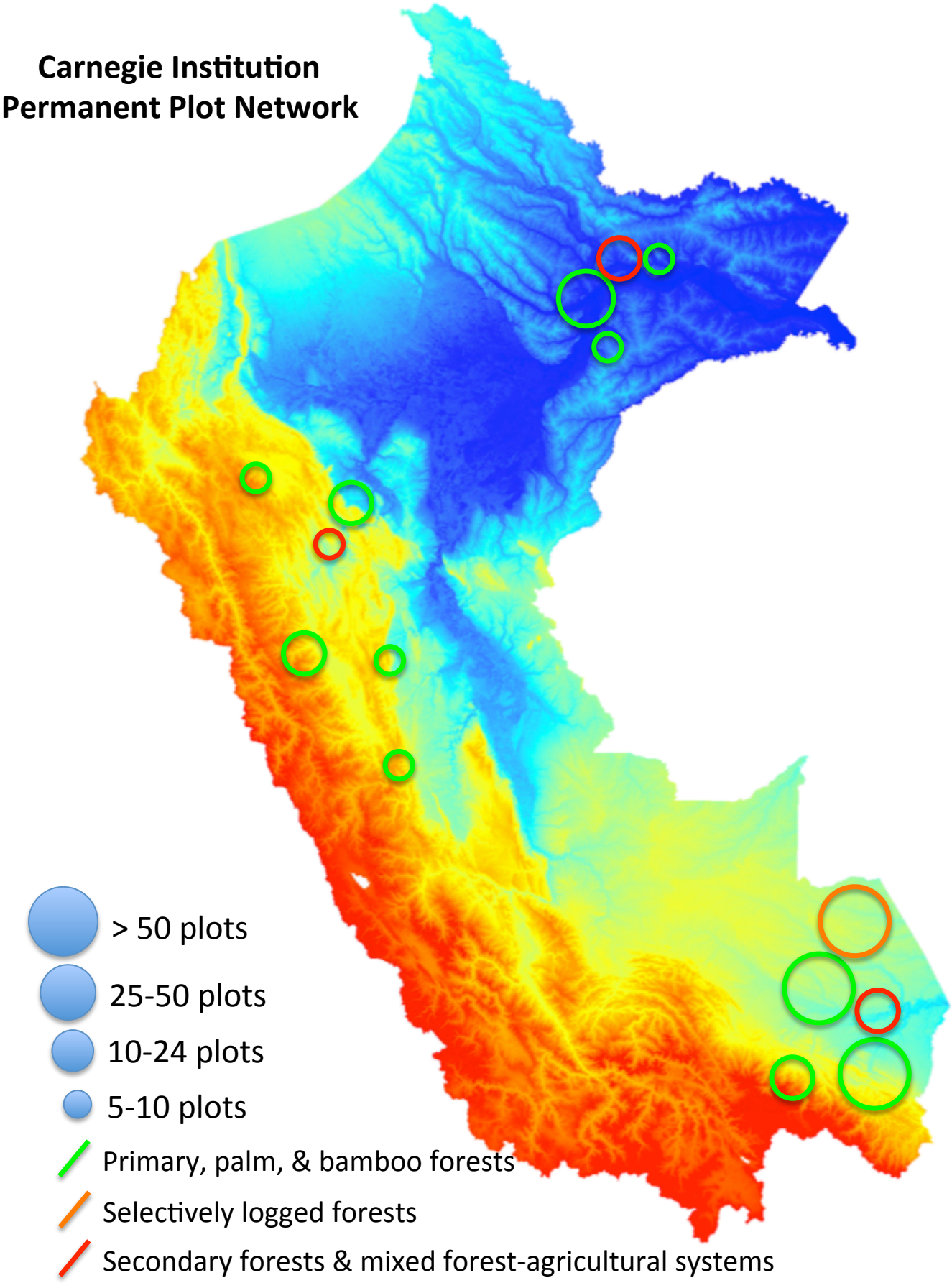
Carnegie Institution
Permanent Plot Network
> 50 plots
25-50 plots
10-24 plots
5-10 plots
Primary, palm, & bamboo forests
Selectively logged forests
Secondary forests & mixed forest-agricultural systems

Fig. S6

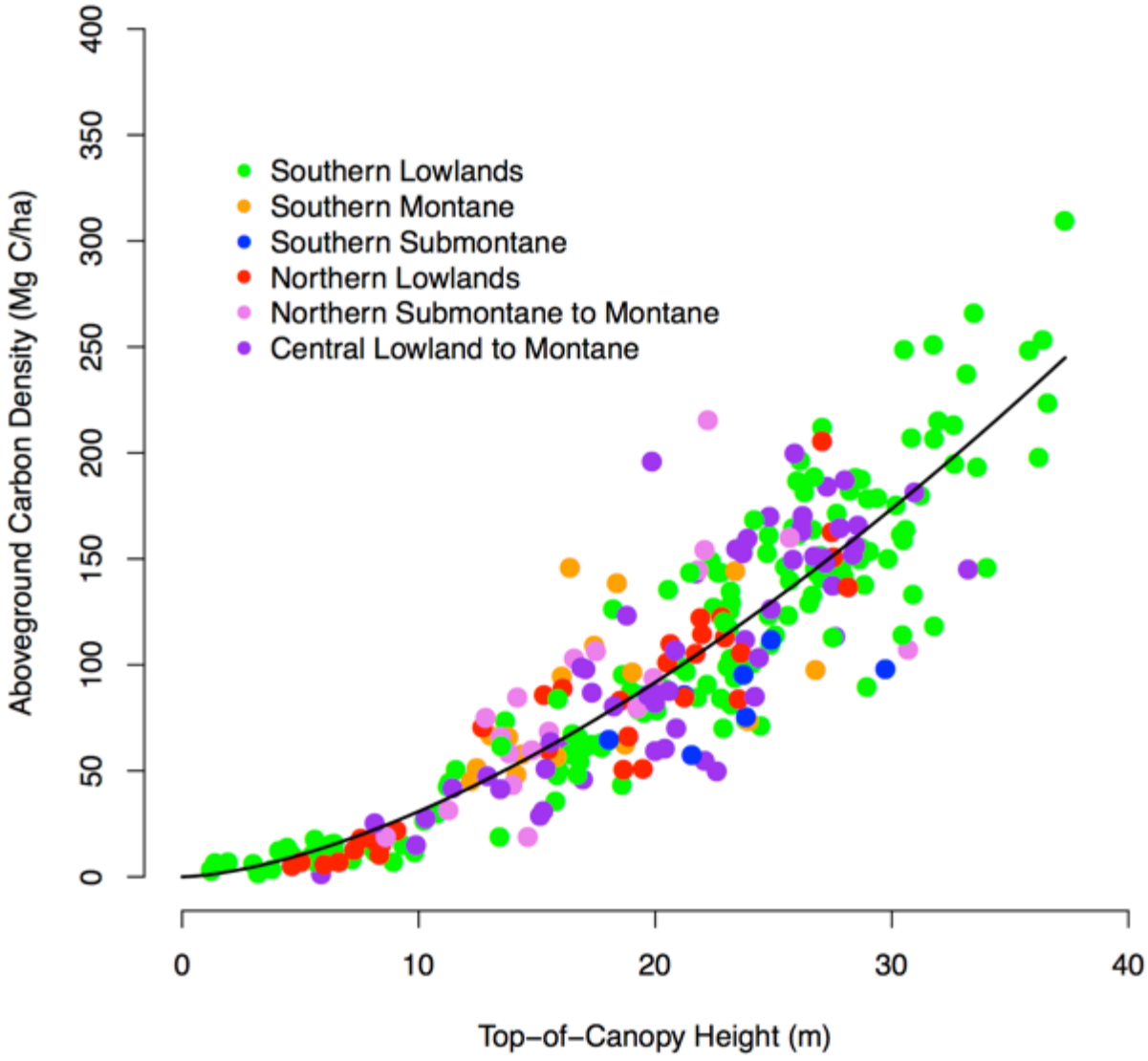
Aboveground Carbon Density (Mg C/ha)
0
50
100
150
200
250
300
350
400
Southern Lowlands
Southern Montane
Southern Submontane
Northern Lowlands
Northern Submontane to Montane
Central Lowland to Montane
0
10
20
30
40
Top−of−Canopy Height (m)

Fig. S7

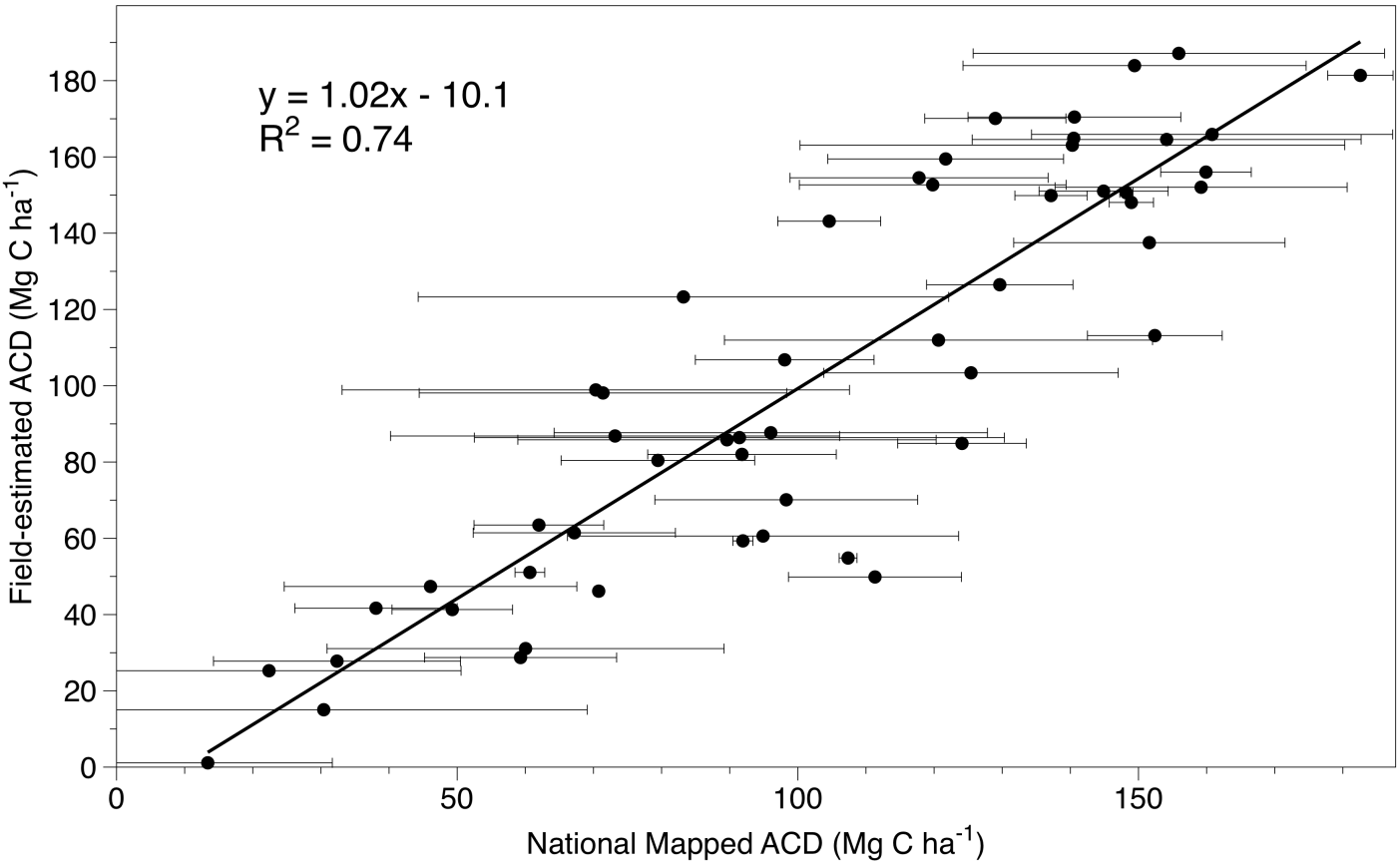
y = 1.02x - 10.1
R2 = 0.74
Field-estimated ACD (Mg C ha-1)
National Mapped ACD (Mg C ha-1)
0
20
40
60
80
100
120
140
160
180
0
50
100
150

Fig. S8

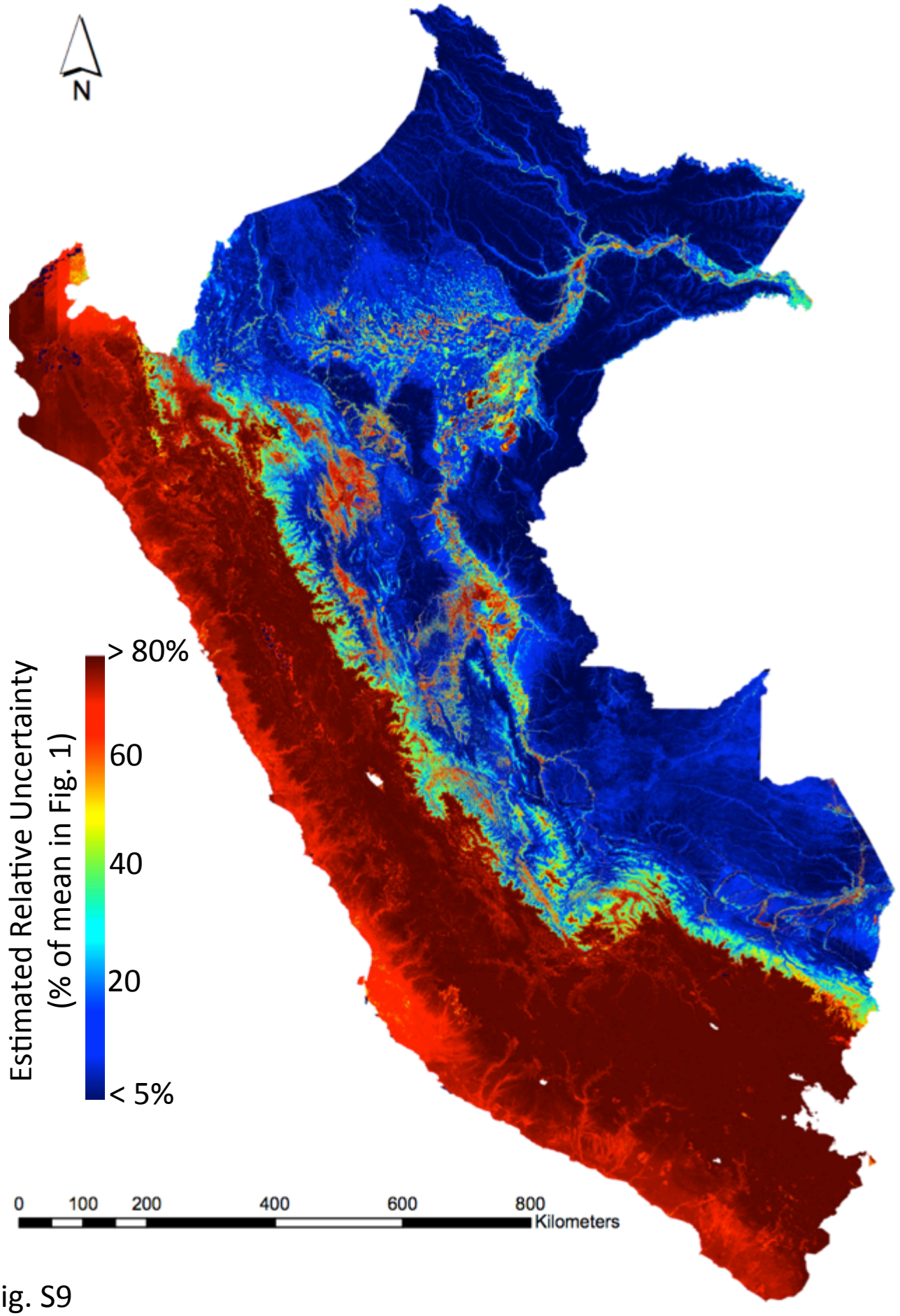
N
Estimated Relative Uncertainty
(% of mean in Fig. 1)
> 80%
60
40
20
< 5%
0
100
200
400
600
800
Kilometers

Fig. S9

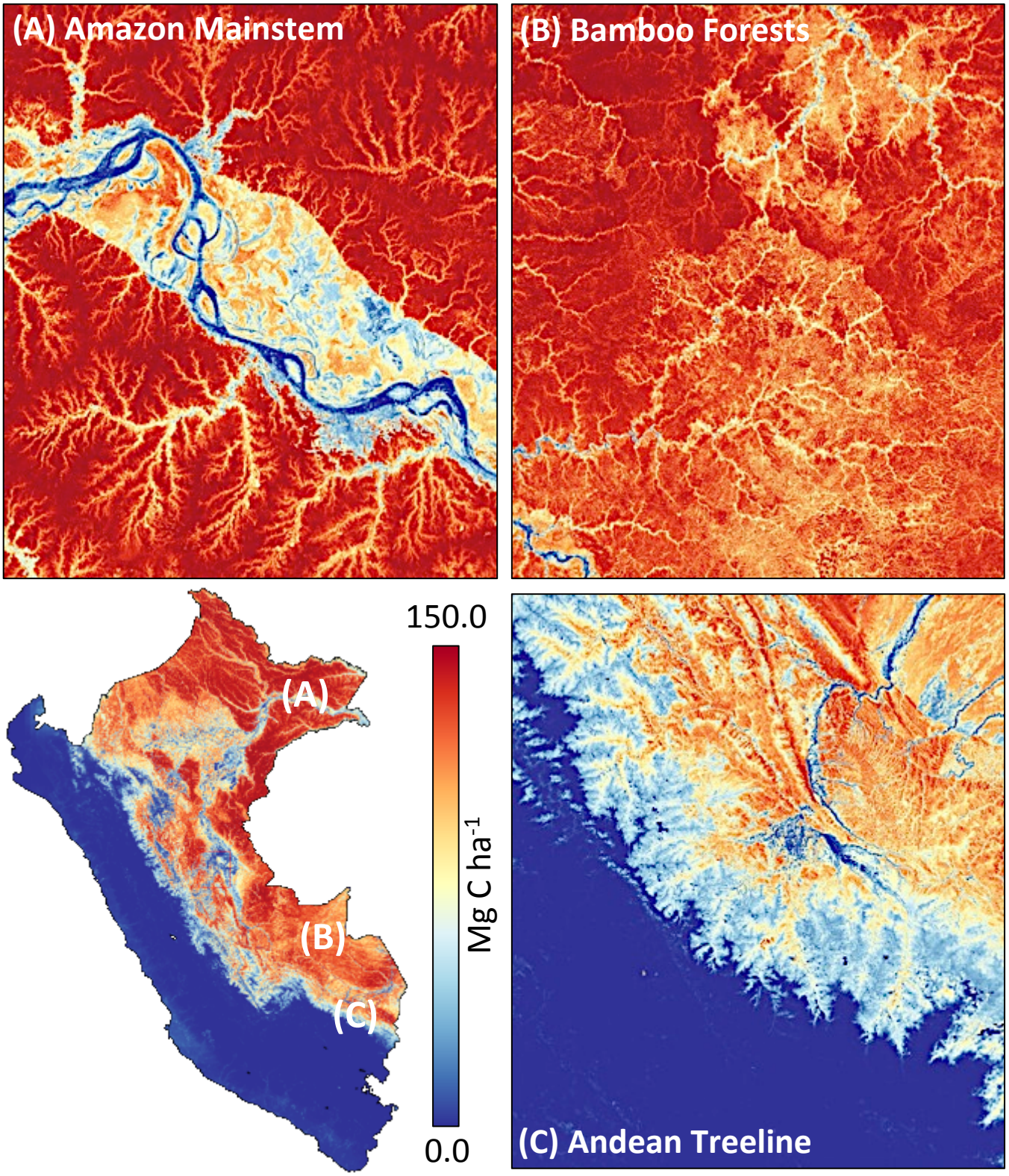
(A) Amazon Mainstem
(B) Bamboo Forests
150.0
(A)
(B)
(C)
Mg C ha-1
0.0
(C) Andean Treeline

Fig. S10

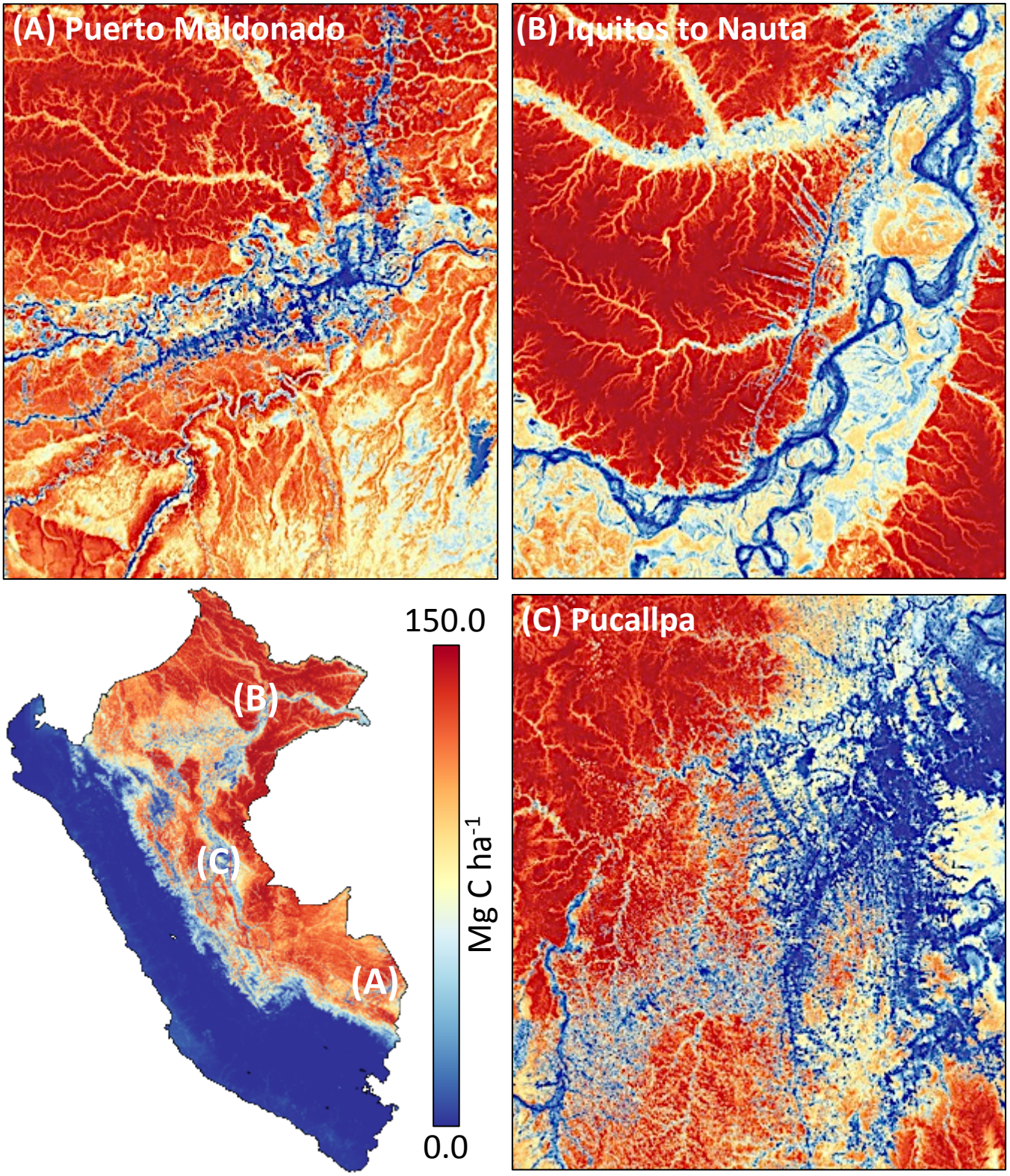
(A) Puerto Maldonado
(B) Iquitos to Nauta
(C) Pucallpa
(A)
(B)
(C)
150.0
0.0
Mg C ha-1

Fig. S11

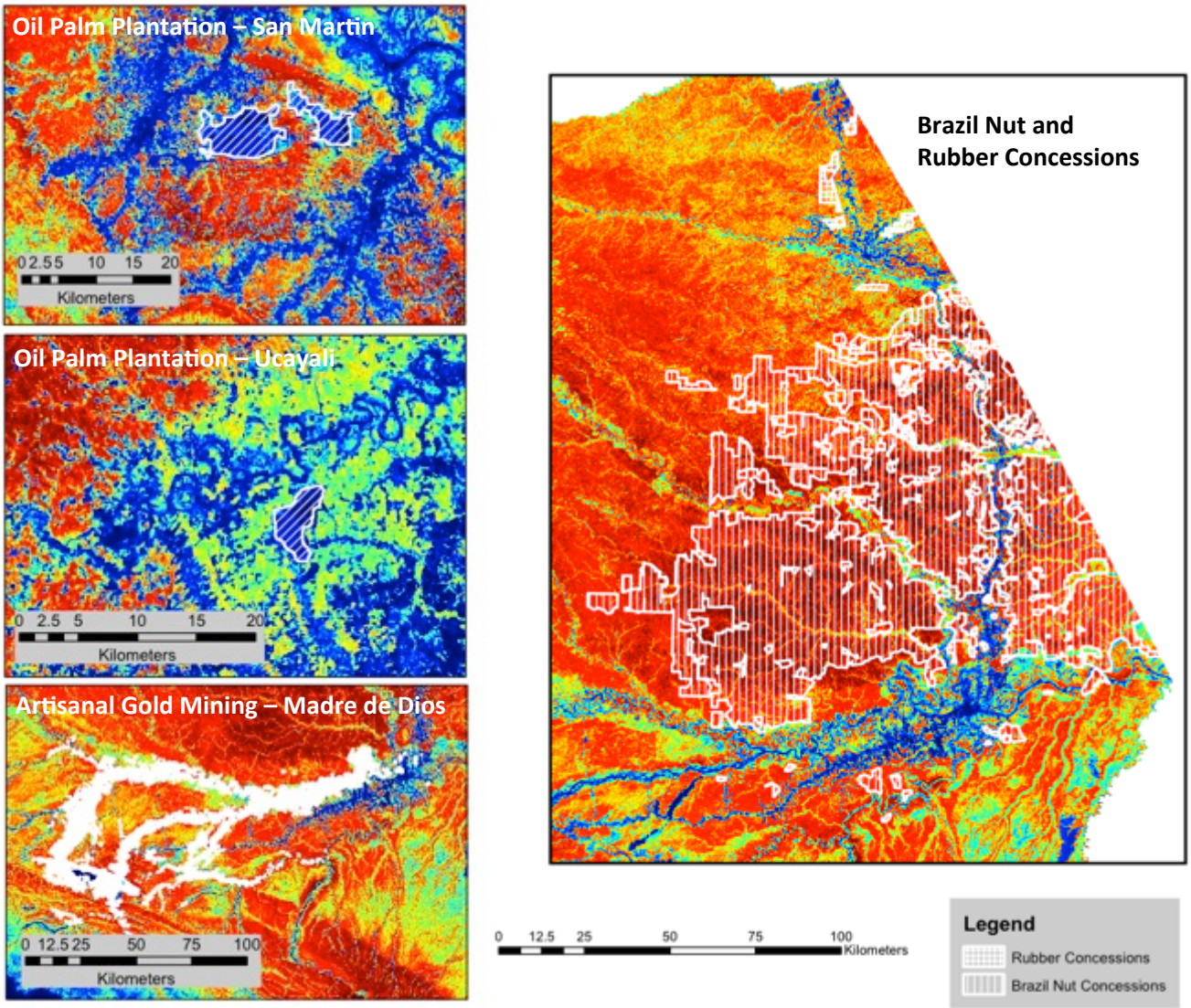
Oil Palm Plantation – San Martin
0 2.5 5 10 15 20
Kilometers
Oil Palm Plantation – Ucayali
0 2.5 5 10 15 20
Kilometers
Artisanal Gold Mining – Madre de Dios
0 12.5 25 50 75 100
Kilometers
Brazil Nut and
Rubber Concessions
0 12.5 25 50 75 100
Kilometers
Legend
Rubber Concessions
Brazil Nut Concessions

Fig. S12

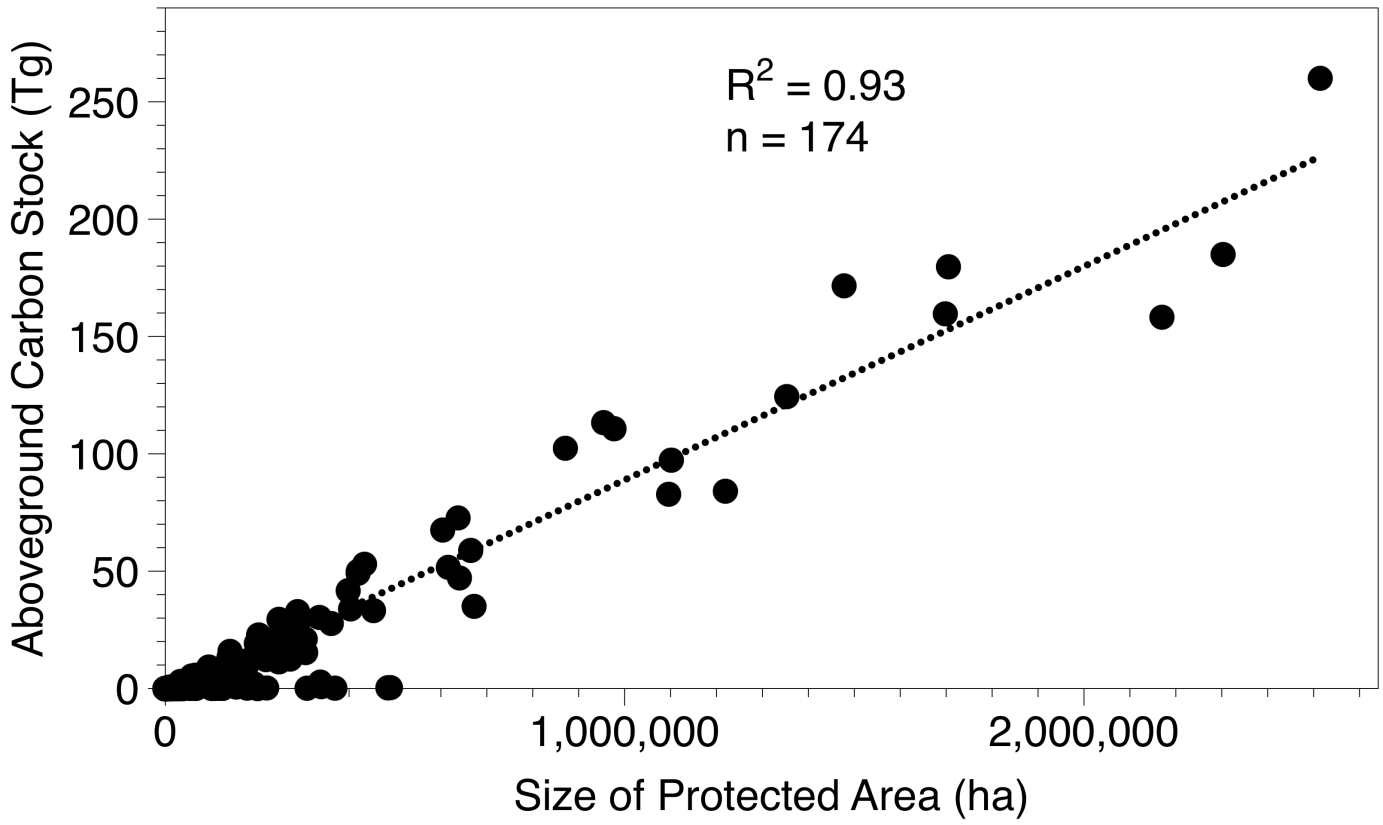
R^2 = 0.93
n = 174
Aboveground Carbon Stock (Tg)
250
200
150
100
50
0
0
1,000,000
2,000,000
Size of Protected Area (ha)

Fig. S13

Table S1. Mean and standard deviation of aboveground carbon density, and total aboveground carbon stock, for government and non-government administered protected areas in Perú. SD = standard deviation. Tg = Teragram = one million metric tons.

Name	Type	Area (ha)	Mean Carbon Density (Mg C ha^{-1})	SD of Carbon Density (Mg C ha^{-1})	Total Carbon Stock (Tg C)
A.B. del Canal Nuevo Imperial	4	17	13.7	3.64	<0.001
Abra Malaga	8	1032	18.54	16.54	0.019
Abra Malaga Thastayoc-Royal Cinclodes	8	74	0.76	0.75	<0.001
Abra Patricia-Alto Nieva	8	1423	56.98	8.35	0.081
Airo Pai	3	247884	119.29	15.22	29.547
Albufera de Medio Mundo	8	685	6.08	2.38	0.003
Allpahuayo Mishana	2	58084	93.38	25.33	5.424
Alto Mayo	4	177740	57.89	24.12	10.009
Alto Nanay-Pintuyacu Chambira	8	954646	118.75	11.57	113.361
Alto Purus	1	2514786	103.73	11.36	260.091
Amarakaeri	3	403828	84.18	20.1	33.975
Amazon Natural Park	8	64	81.96	25.34	0.005
Amazon Shelter	8	12	38	14.56	<0.001
Ampay	5	3847	4.48	5.56	0.017
Ampiyacu Apayacu	8	434182	122.15	10.59	53.037
Ancon	7	2186	11.26	5.65	0.000
Angostura-Faical	8	8868	16.13	2.81	0.143
Ashaninka	3	184462	66.6	27.26	12.271
Bahuaja	8	6	65.16	42.64	0.000
Bahuaja Sonene	1	1102039	88.39	25.55	97.372
Berlin	8	61	40.88	9.03	0.002
Boa Wadack Dari	8	23	76.53	14.48	0.002
Bosque Benjamin I	8	28	98.09	17.43	0.003
Bosque Benjamin II	8	29	107.96	14.14	0.003
Bosque Benjamin III	8	24	69.5	18.92	0.002
Bosque de Palmeras de la Comunidad Campe	8	5925	4.12	1.74	0.024
Bosque de Pomac	6	10919	31.7	17.35	0.346
Bosque de Puya Raymondi-Titankayocc	8	6265	0.64	1.01	0.004
Bosque de Zarate	7	546	3.01	1.56	0.002
Bosque Huacrupe-La Calera	8	7327	2.39	0.64	0.017
Bosque Moyan-Palacio	8	8527	2.46	1.17	0.021
Bosque Nublado	8	3372	48.59	14.1	0.164
Bosque Seco Amotape	8	125	4.54	0.45	0.001
Bosques de Neblina y Paramos de Samanga	8	2906	12.02	12.42	0.035
Bosques Nublados de Udima Sector Centro	8	73	3.37	2.17	0.000

Bosques Nublados de Udima Sector Norte	8	2273	2.36	1.16	0.005
Bosques Nublados de Udima Sector Sur	8	9889	10.15	7.87	0.100
Bosques Secos Salitral-Huarmaca Sector Norte	8	3703	2.35	1.33	0.009
Bosques Secos Salitral-Huarmaca Sector Sur	8	25319	1.92	0.56	0.049
Calipuy	2	4499	1.21	0.95	0.005
Calipuy	5	64099	1.76	1.56	0.112
Camino Verde Baltimore	8	20	109.92	13.23	0.002
Canoncillo	8	1506	4.59	1.3	0.007
Cerros de Amotape	1	152933	12.56	6.57	1.921
Chacamarca	6	2436	0.38	1.4	0.001
Chancaybanos	7	2659	4.33	2.13	0.012
Chaparri	8	40524	2.13	1.02	0.086
Chayu Nafn	3	23620	57.53	21.15	1.303
Checca	8	563	0.09	0.03	<0.001
Choquechaca	8	2071	1.81	2.55	0.004
Choquequirao	8	103803	7.7	10.94	0.789
Comunal Tamshiyacu Tahuayo	8	420071	117.01	17.67	49.153
Copallin	8	11566	31.98	16.68	0.370
Cordillera Azul	1	1353375	91.97	21.82	124.463
Cordillera de Colon	5	39232	53.66	21.57	2.105
Cordillera Escalera	8	150568	77.77	21.28	11.709
Cordillera Huayhuash	7	67570	2.93	2.46	0.197
Cutervo	1	8231	28.17	16.75	0.232
De la Pampa de Ayacucho	6	298	1.41	2.94	<0.001
El Angolo	8	65979	2.19	1.91	0.144
El Gato	8	44	76.27	16.26	0.003
El Sira	3	616380	83.88	29.03	51.700
Gneppf-Sekime	8	203676	112.44	15.11	22.874
Gotas de Agua I	8	3	2.29	0.32	<0.001
Gotas de Agua II	1	9	2.44	0.48	<0.001
Habana Rural Inn	8	29	55.99	15.11	0.002
Hatun Queuna - Quishuarani Ccollana	8	232	0.57	0.52	<0.001
Herman Dantas	8	49	112.55	17.93	0.006
Hierba Buena - Allpayacu	8	2282	34.9	14.21	0.080
Huamanmarca-Ochuro-Tumpullo	8	15680	0.29	0.35	0.005
Huascaran	1	339991	2.66	3.37	0.848
Huaylla Belen-Colcamar	8	6341	20.5	18.89	0.130
Huayllapa	8	21043	2.87	2.29	0.060
Huayllay	5	6737	0.38	0.42	0.003
Huaytapallana	8	22384	3	4.54	0.067
Huimeki	3	141258	112.48	16.45	15.888
Huiquilla	8	1139	23.1	15.73	0.026
Humedales de Puerto Viejo	7	276	5.8	2.19	0.002

Humedales de Ventanilla	8	283	7.51	3.38	0.002
Ichigkat Muja-Cordillera del Condor	1	88506	81.51	16.41	7.111
Illescas	7	37886	0.42	0.16	0.016
Imiria	8	135655	33.93	24.49	4.603
Inotawa-1	8	57	104.44	25.7	0.006
Inotawa-2	8	16	106.89	23.43	0.002
Japu-Bosque Ukumari Llaqta	8	18762	34.81	23.92	0.645
Jirishanca	8	12085	2.39	2.25	0.029
Junfn	2	52561	5.18	7.2	0.134
Juningue	8	37	38.37	16.69	0.001
La Huerta del Chaparri	8	50	1.31	0.82	<0.001
La Pampa del Burro	8	2781	53.82	10.97	0.150
Lachay	2	5131	6.98	2.21	0.036
Laguna de Huacachina	7	2457	10.25	0.95	0.025
Lagunas de Mejfa	5	726	10.17	5.15	0.007
Laquipampa	8	8371	2	1.48	0.017
Larga Vista I	8	20	58.19	15.18	0.001
Larga Vista II	8	25	52.36	19.67	0.001
Las Panguanas 2	8	1	122.49	0	<0.001
Las Panguanas 3	8	7	118.2	4.09	0.001
Las Panguanas 4	8	5	119.18	3.98	0.001
Llamac	8	6707	2.13	2.13	0.014
Lomas de Ancon	7	10959	4.76	1.6	0.052
Lomas de Atiquipa	8	19046	5.62	2.46	0.107
Los Chilchos	8	45987	46.64	18.01	2.141
Los Pantanos de Villa	8	256	9.21	3.66	0.002
Machiguenga	3	218926	80.3	26.59	17.549
Machupicchu	6	37300	10.66	13.04	0.396
Manglares de Tumbes	5	3004	14.09	4.32	0.041
Mantanay	8	361	2.53	3.42	0.001
Manu	1	1698526	94.06	26.14	159.718
Matses	2	420596	118.83	19.18	49.978
Megantoni	5	215854	60.76	27.69	13.116
Microcuenca de Paria	8	767	3.24	2.43	0.002
Milpuj-La Heredad	8	16	2.06	0.6	<0.001
Nor Yauyos-Cochas	8	221252	1.36	2.23	0.302
Nuevo Amanecer	8	30	116.75	20.77	0.004
Otishi	1	305979	50.75	22.89	15.391
Pacaya Samiria	2	2170219	72.94	29.17	158.286
Pacllon	8	14793	2.25	2.03	0.033
Pagaibamba	4	2038	11.5	7.15	0.023
Pampa Galeras Barbara DAchille	2	8008	0.21	0.08	0.002
Pampa Hermosa	5	11541	40.68	18.97	0.469

Pampacorral	8	764	0.43	0.99	<0.001
Panguana	8	132	82.93	21.19	0.011
Paracas	2	335432	12.47	3.47	1.389
Paraiso Natural Iwirati	8	101	93.75	13.71	0.009
Pillco Grande-Bosque de Pumataki	8	275	6.77	7.57	0.002
Pta Salinas-Isla Huampano-Isla Mazorca	2	13686	2.6	1.06	<0.001
Pucacuro	2	637916	114.09	11.17	72.758
Pucunucho	8	22	25.17	9.22	0.001
Pui Pui	4	54509	9.62	16.08	0.508
Punta Atico	2	3451	12.21	6.33	0.001
Punta Coles	2	3389	10.34	5.92	0.002
Punta Colorado	2	2190	6.44	0.43	<0.001
Punta Culebras	2	2932	4.71	1.32	<0.001
Punta Hornillos	2	2772	13.01	4.77	0.001
Punta La Chira	2	2448	8.45	3.13	<0.001
Punta La Litera	2	2043	8.77	0.84	0.001
Punta Lomas	2	2398	16.25	2.3	<0.001
Puquio Santa Rosa	4	68	8.09	2.96	0.001
Purus	3	202659	99.03	11.15	20.050
Qosqoccahuarina	8	1824	0.47	0.89	0.001
Refugio Kerenda Homet	8	35	51.54	15.62	0.002
Reserva Paisajistica Cerro Khapia	7	18487	0.29	0.25	0.005
Rio Abiseo	1	272428	46.66	33.46	12.640
Rio Nieva	7	36344	62.77	15.68	2.281
Sagrada Familia	8	126	67.64	20.32	0.009
Salinas y Aguada Blanca	2	369768	0.57	1.3	0.209
San Antonio	8	352	2.62	5.72	0.001
San Fernando	2	154718	6.43	2.58	0.713
San Juan Bautista	8	25	52.46	33.4	0.001
San Marcos	8	991	13.52	15.2	0.013
San Matias San Carlos	4	149321	88.26	27.89	13.180
Santiago Comaina	7	398488	104.75	15.35	41.720
Sele Tecse-Lares Ayllu	8	974	0.44	0.44	<0.001
Selva Botanica	8	171	115.1	22.41	0.020
Selva Virgen	8	25	80.36	19.07	0.002
Sierra del Divisor	7	1478180	116.18	15.53	171.671
Sub Cuenca del Cotahuasi	8	490550	0.92	1.46	0.450
Sunchubamba	8	61097	2.38	2.81	0.145
Tabaconas Namballe	5	32267	25.95	20.27	0.837
Tambo Ilusion	8	14	27.07	22.89	<0.001
Tambopata	2	280234	89.38	20.22	25.046
Taypipina	8	659	0.1	0.05	<0.001
Tilacancha	8	6804	3.8	7.04	0.026

Tingo Marfa	1	4776	75.02	20.61	0.358
Titicaca	2	36192	0.76	1.7	0.001
Tumbes	2	19422	20.72	5.15	0.402
Tuntanain	3	94994	97.49	16.32	9.261
Tutusima	8	5	35.27	8.24	<0.001
Uchumiri	8	10250	0.29	0.37	0.003
Vilacota Maure	8	125175	0.88	1.84	0.110
Yaguas	7	871383	117.57	14.79	102.448
Yanachaga-Chemillen	1	113611	57.55	27.03	6.359
Yanesha	3	33398	92.25	27.41	3.081
Non-Government Protected Areas					
Maria Yanet Macochoa Grifa	9	301	94.9	15.8	0.029
Roberto Mendoza Mayta	9	157	95.0	12.5	0.015
Geovana Lucia Sulla Lizaraso	9	195	103.4	12.8	0.020
Gustavo Luis Salgado Peralta	9	263	102.7	15.5	0.027
Helmer Gutierrez Preza	9	1017	98.9	14.3	0.101
Myriam Garcia Agapito	9	632	97.5	12.0	0.062
Usmilda Rosambite Araujo	9	143	88.5	13.0	0.013
Percy Pascualvaldez Sahuarico	9	584	107.7	10.7	0.063
Luis Alberto Garcia Agapito	9	185	101.7	12.0	0.019
Miriam Flores Silva	9	732	101.5	11.6	0.074
Concepcion Pablo Parillo Yerva	9	381	96.3	17.3	0.037
Rosa Trinidad Cachique Vela	9	511	109.0	19.7	0.048
Carmen Méndez Torres	9	1670	78.0	16.1	0.130
Jesús Augusto Preza Pisco	9	244	84.8	22.9	0.012
Alfredo Silverio Aguilar Gallegos	9	201	84.8	11.7	0.017
Aurelio Chuquitaipe Ayala	9	209	89.7	16.4	0.019
Jorge Raúl Chávez Masías	9	162	83.6	18.9	0.014
Eduardo López Huesembe	9	1197	93.1	20.8	0.111
Eduardo López Huesembe	9	4525	88.2	16.8	0.399
Eduardo López Huesembe	9	1091	72.3	25.8	0.079
Eduardo López Huesembe	9	1169	91.0	11.5	0.106
Roque Flores Tapuy	9	83	92.8	11.2	0.008
Elias Melendez Castro	9	558	94.6	16.9	0.053
Celso Robles Gutierrez	9	137	78.3	23.2	0.011
Lotty del Carmen Morey Amacifuen	10	38699	64.1	28.8	2.481
Asociacion El Paraiso De Yurilamas	10	6968	93.3	31.6	0.650
Conservacion Internaciona Rodal Tahuamanu	10	12875	95.1	10.0	1.225
Picaflor Research Center Tambopata Eirl	10	1343	106.4	8.8	0.143
Aprodes	10	1872	48.3	15.8	0.090
Estacion Ecologica Turistica Amaru Mayo S.A.	10	3602	66.6	24.9	0.239
Wildlife Conservation Society (Wcs-Peru)	10	9941	81.7	19.6	0.812

Universidad Alas Peruanas	10	12591	54.0	29.2	0.680
Antonio Fernandini Guerrero	10	487	64.0	20.7	0.031
Ccnn Queros	10	6984	58.1	16.1	0.406
Carlos Enrique Berninzon	10	7509	2.2	1.9	0.010
Asociacion Civil Aves Del Peru	10	515	8.0	2.1	0.004
Cuenca Del Rio Huayabamba	10	143829	20.6	22.5	2.965
Asoc. para la Conservación de la Cuenca Amazonica*	10	10154	107.9	11.5	1.095
Asoc. para la Conservación de la Cuenca Amazonica*	10	136402	105.7	13.0	14.416
ONG Aicon	10	30139	74.1	32.4	2.232
Lourdes Consuelo Fernandez Felipe-Morales	10	480	89.2	16.4	0.043
Javier Manuel Salazar Carbajal	10	224618	110.0	15.9	24.647
Ong Naturaleza Y Cultura Internacional	10	7981	1.2	0.4	0.009
Inversiones Manguare S.A.C	11	128	110.1	10.7	0.014
Ismael Cisneros Chunga (Lote A)	11	34	0.6	0.1	<0.001
Ismael Cisneros Chunga (Lote B)	11	41	1.3	0.2	<0.001
Jesus Ricardo Pissani Urdales	11	31	4.6	0.3	<0.001
Proyecto Agua Negra	11	285	58.1	23.3	0.017
Gilberto Vela Cardenas	11	989	89.9	22.7	0.089
Tambopata Expeditions S.A	11	4498	100.7	21.8	0.453
Reserva Ecologica Taricay	11	480	100.1	14.7	0.048
Complejoturistico Ayaymam	11	591	87.8	13.0	0.052
Reserva Natural Lagartococha	11	2545	76.9	30.7	0.196
Mader Sur Oriental Sosten-Madesos	11	3416	100.6	18.4	0.344
Amtuset	11	393	110.3	9.2	0.043
Inversiones Leniperu	11	10	4.5	0.2	<0.001
Jungle Odyssey Peru Eirl	11	1069	84.4	23.9	0.090
Justiniano Zuñiga Guzman	11	2081	73.8	23.0	0.154
Ccnn Infierno	11	1664	89.4	24.2	0.149
Amaitus	11	3793	66.3	35.4	0.252
Zafre S.Ac.	11	9725	101.3	14.8	0.985
Martin Alejo Condori Quispe	11	2004	87.3	15.2	0.175
Empresa Maveco Sand Tour	11	1436	10.4	1.3	0.015
Pantiacolla Tours Srltda	11	680	87.5	25.8	0.059
Inkaterra	11	7861	63.8	21.9	0.501
Ecoamazonia Lodge Srl	11	6316	77.5	29.9	0.490
Juan Carlos Hidalgo Mendoza	11	5347	76.4	18.4	0.409
Abraham Aguirre Apaza	11	1292	97.9	25.1	0.126
Rainforest Expeditions Sac	11	375	93.4	12.2	0.035
Ecoturismo Amazonico Y Andino Del Peru	11	245	58.6	13.6	0.014
Ecoturismo Perla Sac	11	3200	45.4	10.7	0.145
Jaime Perez Del Solar	11	299	35.3	13.2	0.011

Erasmo Sumalave	11	598	84.5	20.5	0.051
Asociacion De Productores De Ranas Venenosas Progr.	12	3859	58.6	29.5	0.226
Perufish Aquarium Eirl	12	729	113.0	10.9	0.082
Eber Moises Quispe Albergrin	13	580	41.3	10.2	0.024
Transfacao	13	171	37.7	9.5	0.006
Mario Puma Guillen	13	75	32.3	7.8	0.002
Suilberto Arias Leon	13	234	33.6	11.5	0.008
Maria Isabel Cavero Macedo	13	256	37.8	8.7	0.010
Luis Alberto Yalico Castañeda	13	33	37.9	15.4	0.001
Esther Bachmann Keller	13	833	37.8	10.9	0.031
Edmundo Frey Martinez	13	423	33.1	14.8	0.014
Kurt Antonio Verde Taquir	13	296	45.4	7.6	0.013
Teodosia Melgarejo Ponce	13	223	30.8	12.4	0.007
Piero Italo Costa Dall Orso	13	1033	38.4	9.7	0.040
Rolando Edmundo Piskulich Johnson	13	102	56.4	11.9	0.006
Guillermo Lopez Barbachan	13	72	58.4	12.7	0.004
Santiago Osorio Ortiz	13	284	41.3	9.5	0.012
Jose Manuel Abadia Duarte	13	20	32.7	13.9	< 0.001
Salbador Choque Quinto	13	49	41.8	8.7	0.002
Gregorio Garcia Ramirez	13	20	49.2	11.9	< 0.001
Paulino Garcia Gomez	13	14	43.8	10.8	< 0.001
Juana Herrera Luyo	13	16	49.5	7.2	< 0.001
Ana Lourdes Rios Egg	13	12	52.5	5.2	< 0.001
Jorge Antonio Chuqui Castillejo	13	50	39.8	8.6	0.002
Carlos Frey Martinez	13	206	38.9	12.0	0.008
Samuel Beto Villar Soto	13	93	34.9	17.9	0.003
Nery Pardave Soto	13	195	40.9	7.2	0.008
Felix Maximo Rivera Galarza	13	258	36.4	6.6	0.009
Juan Pomazongo Miranda	13	330	38.0	5.6	0.013
Felix Orbezo Adrian	13	23	40.6	8.3	0.001
Nora Eugenia Ratto Garcia	13	655	42.4	10.0	0.028
Esio Mario Arbocco Joann	13	676	47.0	9.4	0.032
Ruth Arbocco De Venegas	13	629	48.6	12.4	0.031
Armando Quispe Santos	13	564	39.6	8.0	0.022
Eligio Albengrin Gallo	13	1933	33.2	14.8	0.064
Guillermo Guido Beingolea Vingerhoets	13	702	37.3	8.1	0.026
Everardo Bao Richle	13	861	28.2	12.5	0.024
Maria Jesus Galindo Arriola	13	47	34.8	8.1	0.002
Ana Karina Estrada Santamaria	13	1389	1.2	0.3	0.002
Eduardo Palma Lama	13	10	2.4	0.3	< 0.001
Jean Carlo Freundt Suarez	13	1	3.4	0.0	< 0.001
Avelina Cumpa Chura	13	< 1	NA	NA	< 0.001

Cecilio Alarcon Espinoza	13	8	8.0	3.5	< 0.001
Hector Jaime Jaime	13	1	7.8	0.0	< 0.001
Asociacion de Junqueros de Playa Ci	13	87	7.7	3.2	< 0.001
Isabel Blanca Vilchez Ninahuanca	13	1019	39.4	11.1	0.040
Mercedes Guarnizo Coll de Pinedo	13	4620	40.0	14.7	0.185
Nelly Peña Herrera	13	1009	94.1	8.0	0.095
Cornelio Olivares Uchupe	13	770	92.9	8.5	0.072
Juana Quilca Lluscca	13	745	95.1	7.9	0.071
Margarita Fortunata Garcia Gutierre	13	901	92.1	7.5	0.083
Hipolito Melo Achata	13	786	93.0	6.2	0.073
Augusto Eli Moreno Trujillo	13	938	95.0	19.3	0.089
Elba Tatiana Espinosa Quiñones	13	924	79.2	21.9	0.073
Esteban Cansaya Quispe	13	350	83.0	9.9	0.029
Efrain Santos Quispe Cjuno	13	353	83.7	11.1	0.030
Beatriz Mio Villa	13	361	88.9	11.9	0.032
Antonieta Quispe Loaiza	13	352	91.1	12.6	0.032
Alfonso Mulisaca Pacori	13	356	101.4	9.2	0.036
Arturo Lazaro Chacon	13	350	106.9	3.3	0.037
Alejandro Mendez Huanca	13	265	60.0	34.2	0.016
Angel Damazo Salinas Tapia	13	265	61.1	32.5	0.016
Alejandro Chillihuani Condori	13	261	58.0	32.7	0.015
Edgar Barrios Zamata	13	266	83.6	17.6	0.022
Juan Apaza Quispe	13	261	85.3	15.8	0.022
Jesús Cascamayta Pari	13	266	74.1	30.6	0.020
Concepción Condori Leon	13	267	51.4	34.2	0.014
Isaac Contreras Pinares	13	149	73.5	24.0	0.011
Hilario Sevillano Santa Cruz	13	205	76.2	21.7	0.016
Jorge Minga Huayto	13	199	74.6	25.1	0.015
Celso Villavicencio Fernandez	13	199	69.5	24.3	0.014
Jorge Lopez Molina	13	210	65.9	25.3	0.014
Edmundo Vasquez Pinto	13	395	79.8	18.0	0.032
Edmundo Vasquez Vicente	13	396	81.8	16.4	0.032
Billy Javier Zea Gavilan	13	388	81.7	15.8	0.032
German Mario Fernández Hanco	13	396	80.9	16.4	0.032
Alberto Zúñiga Llanllay	13	187	80.8	30.2	0.015
Felipe Martín Luque Quispe	13	180	83.3	26.8	0.015
Benito Mendoza Bastidas	13	177	69.6	29.3	0.012
Humberto Vargas Fernández	13	186	67.9	27.3	0.013
Jesús Luque Llanllay	13	173	60.3	25.7	0.010
Juan Carlos Lara Rivas	13	186	77.3	17.7	0.014
Celestino Nicolás Lara Salon	13	190	74.4	21.3	0.014
Benito Huayllasi Valdivia	13	170	79.5	17.8	0.014
Alexander Huaña Tuya	13	181	78.4	23.1	0.014

Josefina Huaman Huillca	13	189	80.9	22.1	0.015
Alicia Vargas Llanllay	13	181	82.0	21.9	0.015
Gladys Georgina Llicahua Paccosoncco	13	419	71.0	22.0	0.030
Hilaria Ricarde Diaz	13	402	79.8	15.9	0.032
Asunción Fernández Champi	13	382	79.5	16.6	0.030
Augusta Paccosoncco Hualla	13	376	68.3	23.0	0.026
Juan Saravia Flores	13	76	97.7	10.6	0.007
Eulogio Capquique Vargas	13	208	85.1	16.0	0.018
Adriel Ttito Mamani	13	385	71.8	21.6	0.028
Abraham Pomari Lopez	13	1589	103.3	13.9	0.164
Orlando Campos Collantes	13	1012	112.6	12.3	0.114
Raúl Palomino Rojas	13	178	102.1	6.3	0.018
Roger Grimaldo Moscoso Mamani	13	348	84.5	11.5	0.029
Rufino Quispe Chicasaca	13	351	86.1	15.2	0.030
Leandro Quispe Mamani	13	361	87.5	13.3	0.032
Oswaldo Quispe Ramos	13	353	88.0	12.8	0.031
Luis Aguilar Loayza	13	363	93.6	12.8	0.034
Rosaura Quispe Ramos	13	359	105.3	5.5	0.038
Mauro Cansaya Aranibal	13	343	104.0	5.9	0.036
Raymundo Aguilar Simaraura	13	263	57.7	34.2	0.015
Juan Vara Surco	13	260	86.2	10.0	0.022
Nicomedes Quispe Puma	13	265	59.5	35.1	0.016
Ricardina Pillco De Nina	13	262	86.3	14.0	0.023
Valentina Lloclle Saire	13	269	81.5	20.2	0.022
Juana Quecaño Quispe	13	264	62.9	35.9	0.017
Teresa Chillihuani Layme	13	264	59.4	35.2	0.016
Mamerto Holgado Huilca	13	265	60.0	32.6	0.016
Luz Elizet Lopez Zurita	13	265	54.6	34.3	0.014
Mauricio Flores Huayta	13	267	53.4	32.5	0.014
Juan Carmen Palomino Ustua	13	203	83.9	17.2	0.017
Vicente Emiliano Cutire Pari	13	207	67.8	27.2	0.014
Victor Huaman Ccama	13	146	78.5	20.3	0.011
Sixto Luis Fernandez Barrientos	13	383	82.7	17.1	0.032
Saul Salvador Zea Gavilan	13	388	81.4	14.9	0.032
Leoncio David Mendoza Ticona	13	400	84.6	12.5	0.034
Pascual Mendoza Huarache	13	402	86.6	10.3	0.035
Juan Julio Fernandez Hanco	13	396	85.2	12.4	0.034
Luis Reynaldo Rodríguez Fernandez	13	385	80.5	18.4	0.031
Juan Pablo Gordillo Arias	13	189	89.4	24.8	0.017
Juvenal Chirinos Cusihuaman	13	182	79.9	27.8	0.015
Matilde Cadenas Quispe	13	180	78.9	31.3	0.014
Julián Paucar Gómez	13	185	74.3	24.4	0.014
Rosa Hermelinda Huaña Tuya	13	177	71.8	28.4	0.013

Vicente Mamani Mendoza	13	185	64.0	31.7	0.012
Mercedes Merma Guzman	13	190	63.2	23.8	0.012
Santos Dionisio Chirinos Zavala	13	190	71.1	21.3	0.014
Luis Ocsa Tacuri	13	174	80.4	20.2	0.014
Lucien Clare Quillahuaman Romero	13	161	61.7	27.2	0.010
Rufino Quispe Navarro	13	164	60.5	28.0	0.010
Camilo Lelis Enrique Supo Picha	13	154	60.4	29.3	0.009
Miguel Angel Ahuanari Manuyama	13	168	67.0	27.1	0.011
Henry Edmundo Gil Peña	13	156	60.2	29.5	0.009
Pablo Fernández Suaquita	13	437	82.2	13.6	0.036
Weaver Wilson Cari Mogrovejo	13	3051	109.5	13.0	0.334
Marlene Huillca Sutta	13	383	103.9	11.1	0.040
Alejandro Villanueva Mamani	13	189	52.8	29.6	0.010
Ricardo Quispe Puma	13	189	53.9	29.7	0.010
Lurdes Quispe Tueros	13	154	66.5	26.3	0.010
Jose Adrian Moscoso Delgado	13	192	58.2	31.6	0.011
Nestor Fuentes León	13	435	96.2	14.7	0.042
Jesusa Puma De Huamaní	13	447	87.0	17.0	0.039
Jenny Lexi Izquierdo Reategui	13	186	55.9	30.2	0.010
Hilario Chura Quispe	13	174	53.4	28.9	0.009
Jacinta Mollo Ticona	13	155	65.3	29.9	0.010
Gladys Roxana Fernández Guerreros	13	151	61.0	32.6	0.009
Gildo Quispe Gomez	13	160	62.4	27.7	0.010
Jimmy Ponce De Leon Andagua	13	70	57.3	25.7	0.004
Donato Yapura Huillca	13	185	55.4	28.3	0.010
Ciriaco Benito Mollo Ticona	13	150	61.5	31.9	0.009
Cuber Luis Sullca	13	1010	94.6	24.4	0.096
Mishari Rolando García Roca	13	912	91.2	17.8	0.083
Oscar Quispe Sotomayor	13	148	63.8	27.6	0.009
Elizabeth Tuero Carbajal	13	164	67.1	17.0	0.011
Celestina Navarro Huamani	13	134	86.2	10.4	0.012
Segundo Torres Sanchez	13	1250	114.1	10.0	0.143
Saulo Vasquez Irigoin	13	1075	112.8	10.9	0.121
Rosendo Horacio Vita Benito	13	100	101.7	13.6	0.010
Reynel Alfonso Rivas Corrales	13	107	105.9	8.8	0.011
Juvenal Moisés Rivas Corales	13	106	83.1	28.0	0.009
Juan Carlos Céspedes Flores	13	105	102.6	9.2	0.011
German Enrique Rivas Corrales	13	105	102.9	8.2	0.011
Elard Edison Rocha Huayllani	13	104	78.0	23.9	0.008
Froilan Quispe Mamani	13	109	106.8	9.4	0.012
Dalmecio Champi Cabrera	13	101	106.4	8.3	0.011
Ciriaco Ronal Flores Escalante	13	151	63.5	24.4	0.010
Rolando Gil Peña	13	165	64.7	26.6	0.011

Pablo Quispe Mátame	13	263	84.8	13.2	0.022
Juan Carlos Velásquez Molero	13	107	101.7	12.1	0.011
Willian Céspedes Huamani	13	108	104.9	9.8	0.011
Jaime Velásquez Molero	13	114	102.5	8.9	0.012
Emilio Huaman Apaza	13	110	103.3	7.3	0.011
Ebaristo Condori Machaca	13	114	106.9	5.8	0.012
Violeta Rivas Corrales	13	100	106.2	8.5	0.011
Teodoro Pantia Huaman	13	72	66.8	23.3	0.005
Victor Rojas Sabino	13	76	69.9	29.4	0.005
Gladys Sussy Shamaire Murayari	13	68	88.2	28.2	0.006
Roxana Mendoza Huaman	13	75	74.6	28.7	0.006
Yolanda Mendoza Huaman	13	80	96.6	25.4	0.008
Vicente Pacheco Flores	13	71	101.1	21.2	0.007
Miguel Chambi Ccallomamani	13	75	103.4	20.2	0.008
Evarista Huayllasi Valdivia	13	66	98.2	29.6	0.006
Esteban Vargas Tejada	13	78	85.7	23.3	0.007
Ernesto Huaman Flores	13	74	108.0	7.7	0.008
Ronal Rado Quispe	13	71	95.8	20.3	0.007
Eloy Orestes Chambi Chura	13	86	65.6	20.3	0.006
Asociacion De Comerciantes-Agrofocm	13	221	99.9	18.1	0.022
Asociacion De Comerciantes-Agrofocm	13	3176	71.6	30.4	0.228
Juan Perez Sanchez	13	281	106.6	11.2	0.030
Ciro Alagon Huamani	13	790	106.2	13.2	0.084
Alfredo Vrako Neuenschwander	13	2563	97.8	14.3	0.251
Julio Zea Valdivia	13	848	51.5	42.7	0.044
Juan Velasquez Cabrera	13	827	84.1	8.1	0.070
Guido Jesus Llicahua Pacosonco	13	781	88.5	15.0	0.069
Julio Gil Moscoso	13	1113	88.9	6.3	0.099
Serafin Moscoso Mamani	13	1008	74.5	40.0	0.075
Mario Alagon Huamani	13	407	97.0	26.0	0.039
Jesus Valverde Vargas	13	753	100.1	10.1	0.075
Francisca Sicos Vda De Cespedes	13	879	88.9	7.8	0.078
Fernando Mamani Cutipa	13	900	88.0	6.0	0.079
Alfredo Asto	13	871	102.0	6.8	0.089
Pedro Puma Champi	13	796	83.2	6.6	0.066
Domingo Llicahua Pecca	13	878	84.8	32.0	0.074
Cirilo Huaynapata Montesinos	13	862	79.5	32.2	0.069
Hugo Champiu Quispe	13	606	86.0	13.7	0.052
Ladislao Cespedes Sicus	13	663	95.1	7.7	0.063
Esteban Huamani Cayllahua	13	526	85.8	9.8	0.045
Valentin Quillahuaman Inquiltupa	13	900	86.2	7.0	0.078
Villanueva Rojas Martinez	13	957	92.4	9.1	0.088
Guido Lipa Gil	13	915	105.9	10.6	0.097

Susono Ninantay	13	984	96.5	8.3	0.095
Hilda Champi Ocampo	13	818	109.4	4.1	0.090
Areas para la Asociacion-Area N‖ 02	13	973	104.5	5.2	0.102
Candelaria Maldonado Cuadros	13	1004	96.9	13.6	0.097
Parcelas en Evaluacion de la Asocia	13	1966	75.1	42.9	0.148
Andres Huayllani Llerena	13	793	94.9	9.6	0.075
Alejandro Guillen Amao	13	1147	106.4	7.7	0.122
Carlos Barra Caller	13	791	107.6	7.1	0.085
Areas para la Asociacion-Area N‖ 01	13	1187	51.2	47.6	0.061
Guido Molina Valdez	13	908	104.1	10.1	0.095
Simeon Ernesto Centeno Castro	13	695	104.4	6.2	0.073
Grimaldo Augusto Inca Vilca	13	750	97.7	8.0	0.073
Daniel Condori Huayhua	13	769	94.5	6.7	0.073
Maribel Medina Valencia	13	753	98.7	7.3	0.074
Justina Arcos Pajuelo	13	968	100.3	6.9	0.097
Wilver Dionisio Quispe Guzman	13	907	101.8	7.5	0.092
Antonio Rodriguez Diaz	13	906	102.1	8.2	0.092
Marcial Reymundo Tellez Heredia	13	201	89.1	13.5	0.018
Emilio Sancama Chavez	13	209	84.2	14.9	0.018
Francisco Solano Ponce De Leon Merc	13	868	103.7	7.3	0.090
Eustaquio Eduardo Ccansaya Quispe	13	472	105.6	7.9	0.050
Juana Cahuana Huanaco	13	703	101.1	12.6	0.071
Candida Rodriguez Diaz	13	1005	106.4	8.4	0.107
Rebeca Mariela Chucuya Alfaro	13	969	102.2	8.9	0.099
Lucia Ttito Quispe	13	950	104.5	8.2	0.099
Ubaldina Vargas Aroni	13	814	101.9	8.8	0.083
Miguel Grimaldo Moscoso Delgado	13	603	104.3	8.2	0.063
Rosendo Antonio Castillo Cahuana	13	758	99.2	8.2	0.075
Antonio Apaza Choqueluque	13	761	98.3	6.5	0.075
Juliana Quispe Vda De Champi	13	710	90.5	6.9	0.064
Jardy Hugo Nina Iquiapaza	13	158	97.3	7.8	0.015
Valentina Lopez Nina	13	190	87.8	17.0	0.017
Emilio Palomino Ccoa	13	152	92.7	8.8	0.014
Raymundo Huaynasi Lopez	13	391	104.2	9.0	0.041
Gladys Guerrero Rumaldo	13	777	104.4	8.6	0.081
Onofre Basilebez Guerreros Rumaldo	13	737	100.0	9.3	0.074
Mamerto Rodriguez Huaman	13	584	100.9	10.2	0.059
Carmen Rosa Diaz Hancco	13	720	98.7	11.9	0.071
Domingo Jose Fernandez Urdanivia	13	701	99.4	7.3	0.070
Daniel Andia Monzon	13	506	96.6	9.4	0.049
Basilio Yana Vaga	13	460	99.3	8.4	0.046
Vicente Escobar Huarcaya	13	123	104.8	6.9	0.013
Agripina Nicolasa Andia Espinosa	13	121	99.3	8.3	0.012

Monica Gonzales Rodriguez	13	121	100.4	10.8	0.012
Alejandrina Condori Vargas	13	78	104.0	6.2	0.008
Liz Mayra Quispe Rodriguez	13	568	105.1	7.7	0.060
Juana Fernandez Champi	13	658	103.2	11.6	0.068
Roman Ttito Quispe	13	688	98.9	8.1	0.068
Prudencia Tuero Soel	13	990	102.7	10.0	0.102
Adriel Champi Quispe	13	706	90.0	14.8	0.064
Odilon Sinti Condori	13	797	84.4	8.6	0.067
Ana Lucia Hurtado Abad	13	101	99.3	4.5	0.010
Haydee Giovana Alarcon Pillco	13	88	94.7	13.2	0.008
Wilbert Villegas Alvarez	13	105	97.2	5.0	0.010
Gregoria Castro Chalco	13	88	91.7	9.5	0.008
Miguel Angel Puclla Gutierrez	13	103	85.4	15.5	0.009
Pedro Huaman Apaza	13	96	88.4	11.0	0.008
Elmer Velasquez Valdivieso	13	91	89.8	12.2	0.008
Carlos Mendoza Huaman	13	88	89.5	9.7	0.008
Pastora Condori Torres	13	96	90.3	5.8	0.009
Escolastico Zely Paye Condori	13	95	89.3	5.4	0.008
Vicente Flore Cruz	13	94	90.3	6.5	0.008
Alfredo Palomino Lopez	13	91	99.4	7.2	0.009
Celestono Mendoza Llanos	13	96	104.3	5.3	0.010
Jose Luis Lara Rivas	13	90	102.8	8.4	0.009
Edwin Donato Cayo Yapura	13	90	99.6	9.8	0.009
Celso Ortiz Maqque	13	260	103.1	11.9	0.027
Lucio Velasques Ttito	13	762	102.3	8.6	0.078
Aurelio Yana Taipe	13	339	104.3	8.6	0.035
Tadeo Quispe Gomez	13	707	104.2	10.9	0.074
Fortunato Adrian Centeno Checalla	13	415	102.0	17.8	0.042
Lius Clodoveo Perez Sanchez	13	511	110.4	5.5	0.056
Josefina Yeny Lipa Gil	13	1187	106.2	10.4	0.126
Saturdino Demetrio Pacheco Estaca	13	838	110.1	5.2	0.092
Javier Palomino Rojas	13	912	108.1	8.7	0.099
Jesus Camacho Acasaba	13	505	99.2	8.9	0.050
Antonio Jaime Lopez Nieto	13	3297	44.5	21.1	0.147
Remberto Reategui Paredes	13	5	58.4	4.0	< 0.001
Mercedes Villarreal De Galindo	13	5	6.8	0.9	< 0.001
Felix Cesar Calderon Urtecho	13	4	6.1	1.2	< 0.001
Antonio Fernandini Guerrero	13	1711	90.2	21.5	0.154
Maximo Julio Ventura Monasterio	14	307	115.0	15.1	0.035
Maximo Cahuana Rivera	14	720	112.0	17.6	0.081
Juan Saavedra Meza	14	1272	112.7	15.5	0.143
Antonio Valdez Simons	14	629	103.5	27.0	0.065
Manuel Vargas Cucho	14	2762	107.1	19.6	0.296

Miguel Farfan Gomez	14	2475	101.1	23.1	0.250
Guillermo Chota Leon	14	655	90.2	34.4	0.059
Maria Jesus Grandiller Olivera	14	98	112.9	16.1	0.011
Armando Valdes Simons	14	1137	119.6	11.2	0.136
Marcelino Sayago Ortega	14	312	116.8	10.5	0.036
Julio Chambi Cahuana	14	735	103.7	12.2	0.076
Juan Gualberto Chota Leon	14	61	118.8	3.7	0.007
Ursula Ursina Pizango Navi	14	1977	103.8	8.8	0.205
Neri Alcida Diaz De Agapito	14	232	97.1	21.4	0.023
Angel Augusto Cespedes Tapia	14	691	117.4	9.8	0.081
Ismael Solorzano Huanuire	14	416	111.3	12.7	0.046
Alberto Alfredo Palla Panduro	14	950	118.1	12.4	0.112
Sixto Carazas Quispe	14	1053	117.8	16.7	0.124
Victor Eusebio Diaz Moreno	14	719	117.9	11.6	0.085
Nelson Arnaldo Morey Silva	14	795	118.4	9.5	0.094
Justino Collante Guzman	14	173	76.9	43.1	0.013
Eduardo Palomino Melo	14	399	117.1	9.9	0.046
Victor Macochoa Machoa	14	301	119.3	11.2	0.036
Zenobio Grandiller Olivera	14	263	119.2	18.7	0.031
Pedro Marchena Mendieta	14	204	101.3	32.8	0.021
Encarnación Mamani Larico	14	1120	118.6	13.9	0.133
Justino Palla Dea	14	1139	105.9	16.7	0.121
Felicitas Troncoso Huayta	14	798	114.4	16.3	0.091
Nemesio Mamani Machacca	14	1044	118.2	14.9	0.123
Adolfina Yalta Gonzales	14	137	113.5	20.1	0.016
Braulio Valencia Valencia	14	1054	120.5	8.0	0.127
Julia Saca Alvarez	14	999	122.2	11.9	0.122
Francisco Tapia Mamani	14	1358	108.7	26.4	0.148
Santiago Castellanos Laynes	14	2010	111.0	13.1	0.223
Santiago Taipe Chuima	14	763	112.4	9.8	0.086
Guillermo Calderon Ramirez	14	1050	114.8	11.8	0.121
Diguer Mario Villafuerte Cornejo	14	998	109.0	8.0	0.109
Adis Aurora Villafuerte Cornejo	14	688	107.8	9.6	0.074
Inmer Camargo Chavez	14	938	88.1	19.2	0.083
Francisco Quispe Chani	14	2012	107.8	9.4	0.217
Jeronimo Emiliano Taipe Chuima	14	652	112.3	10.7	0.073
Mohasi Vasquez Rolin	14	991	116.0	8.5	0.115
Alicia Fatima Noa Grifa	14	1211	108.1	14.9	0.131
Carlos Antonio Valdivia Sanchez	14	564	112.5	8.1	0.063
Emilio Macochoa Noa	14	918	113.4	10.7	0.104
Armando Mejia Lopez	14	789	105.1	18.5	0.083
Enrique Tije Arasaire	14	560	123.9	7.8	0.069
Rosa Tapia De Ramirez	14	262	110.9	14.4	0.029

Fidel Yupanqui Dueñas	14	593	120.2	11.8	0.071
Pedro Quispe Kana	14	1261	114.3	13.0	0.144
Julio Alejandro Espinoza Loayza	14	1592	101.1	27.6	0.161
Claudio Augusto Tacoma Pontisil	14	716	111.8	18.5	0.080
Martin Laura Herrera	14	758	111.5	21.7	0.085
Dario Ccoica Medoza	14	1389	116.4	13.1	0.162
Dolly Magdalena Simplicio Arias	14	1049	99.9	16.3	0.105
Celinda Gonzales Carrillo	14	213	123.6	4.9	0.026
Cancio Huaman Hurtado	14	632	113.6	17.7	0.072
Jacinto Parillo Quispe	14	534	111.9	12.1	0.060
Alberto Garcia Rojas	14	293	121.6	13.5	0.036
Blanca Victoria Sahuarico De Aradivi	14	268	111.2	27.1	0.030
Ernesto Mendoza Huancacuri	14	1676	101.2	25.5	0.170
Amancio Dimas Ibañez Tapuy	14	400	117.5	8.7	0.047
Macario Dionicio Cuadros Quispe	14	609	115.4	13.8	0.070
Jose de la Cruz Carrasco	14	646	110.0	23.0	0.071
Luz Marina Grandiller Olivera	14	88	124.3	3.7	0.011
Maria Adela Moreno Tapuy	14	205	97.1	12.0	0.020
Vidal Diaz Vargas	14	520	112.3	16.1	0.058
Manuel Auquipata Santa Cruz	14	123	110.0	18.2	0.014
Yordi Ronald Arimuya Rodriguez	14	679	118.8	10.7	0.081
Rodolfo Herrera Inuma	14	497	110.2	27.1	0.055
Laura Palla Panduro	14	635	112.4	14.1	0.071
Clemente Ccolque Champi	14	746	118.7	12.9	0.089
Juan Sanchez Montes	14	62	80.5	39.2	0.005
Juan Crisostomo Prada Bravo	14	231	103.2	27.3	0.023
Gregorio Torres Melendez	14	400	109.8	30.5	0.044
Franklin Torres Caller	14	213	122.1	4.5	0.025
Favio Celestino Palacios Mejia	14	707	114.4	17.4	0.081
Adelma Alicia Palla Dea	14	660	120.6	10.9	0.080
Aurelio Garcia Caceres	14	561	121.2	3.2	0.068
Rigoberto Paredes Martinez	14	474	109.2	10.3	0.052
Alejandrina Huesembe De Marchena	14	554	114.2	13.4	0.063
Mariano Cahuantico Huaman	14	237	113.5	23.8	0.027
Sergio Flores Lloza	14	531	118.7	11.6	0.063
Mirian Marice Herbozo Reategui	14	1854	107.4	19.7	0.199
Gregoria Cahuantico Lizaraso	14	662	120.2	11.8	0.080
Mauro Flores Trigoso	14	1365	104.0	12.5	0.142
Luis Enrique del Aguila Sinuire	14	1911	105.4	11.3	0.201
Jorge Choquehuanca Mamani	14	1182	112.0	10.6	0.132
Wilfredo Condori Obando	14	831	109.7	12.3	0.091
Julio Ramirez Montes	14	511	112.8	19.9	0.058
Wilfredo De La Peña Gonzales	14	1020	116.0	13.9	0.118

David Rodriguez Grifa	14	955	110.9	20.6	0.106
Regina Palla De Calle	14	645	107.5	23.2	0.069
Cesar Macochoa Noa	14	666	113.8	11.1	0.076
Nicanor Vasquez Huisa	14	378	118.2	10.5	0.045
Ignacio Macochoa Noa	14	606	106.6	23.3	0.065
David Rodriguez Tenoy	14	942	113.4	14.1	0.107
Eduardo Macochoa Noa	14	237	121.7	9.2	0.029
Mariano Barbaro Jacinto Irco	14	1193	111.1	25.5	0.133
Melchor Huaracha Yauri	14	727	111.6	9.5	0.081
Suplicio Herrera Anayanqui	14	247	88.8	33.2	0.022
Cipriano Tito Quispe	14	927	117.8	14.5	0.109
Vilma Sueros Ramirez	14	434	92.1	32.4	0.040
Alfredo Zambrano Tapia	14	513	116.6	13.6	0.060
Oscar Sahuarico Begazo	14	1366	99.5	35.8	0.136
Cesar Delgado Andia	14	1105	97.5	19.6	0.108
Juan Jose Alberto Salazar Valencia	14	103	102.9	33.9	0.011
Edwin Espinoza Nina	14	112	69.6	35.6	0.008
Alejandro Vilca Mamani	14	843	112.5	8.9	0.095
Miguel Antonio Grandiller Olivera	14	356	122.2	6.9	0.044
Gumercindo Panduro Linares	14	498	116.5	23.1	0.058
Agustin Diaz Aparicio	14	24	105.9	24.2	0.003
Luz Eva Valdivia Sanchez	14	816	113.2	15.5	0.092
Jorge Lipa Menacho	14	235	112.6	27.3	0.026
Juliana Parillo Quispe	14	803	104.8	8.3	0.084
Nancy Rosmeri Macochoa Tapia	14	464	111.9	10.1	0.052
Maria Zaida Rodriguez Tapuy	14	519	104.1	16.1	0.054
Luis Collque Quispe	14	1023	113.3	10.9	0.116
Berlinda Arias De Simplicio	14	1761	110.6	12.8	0.195
Hilario Grifa Palla	14	1053	114.7	16.2	0.121
Lina Sahuarico Begazo	14	850	115.7	12.8	0.098
Andres Cutipa Gonzales	14	260	99.8	29.8	0.025
Francisca Consuelo Cahuana Saravia	14	276	120.4	25.0	0.033
Madeley Tapuy Palla	14	578	109.9	9.7	0.064
Carlos Gongora Cabaña	14	643	109.7	21.4	0.071
Javier Roman Mejia Flores	14	1544	109.3	8.2	0.169
Yobana Melendez Tamachiro	14	1020	109.6	11.9	0.112
Delfin Hugo Mejia Rivera	14	528	103.3	29.4	0.055
Eufrasia Parillo Quispe	14	443	111.6	9.5	0.049
Edgar Collado Delgado	14	2929	98.4	11.1	0.288
Miguel Silva Pereira	14	571	92.5	22.4	0.053
Ignacio Noa Grifa	14	563	96.3	14.0	0.054
Wilfredo Valdez Macochoa	14	843	105.5	14.4	0.089
Hipolito Cesar Condori Limpe	14	625	112.3	11.3	0.070

Aurelio Armando Mamani Mamani	14	1173	114.3	11.7	0.134
Francisco Almanza Diaz	14	240	86.1	29.7	0.021
Saturnino Demetrio Parillo Quispe	14	1628	107.2	7.6	0.174
Maria Elvira Cahuana Tapuy	14	1215	111.2	13.9	0.135
Juan Gutierrez Inuma	14	697	105.8	28.2	0.074
Fermin Cruz Rodriguez	14	240	100.6	28.6	0.024
Eustaquio Paro Cayo	14	1024	117.0	11.3	0.120
Marcelino Cruz Apaza	14	725	113.3	16.6	0.082
Felix Alvarez Gonzales	14	1033	114.0	13.2	0.118
Marcial Pacco Espinoza	14	503	102.2	9.6	0.051
Lener Vilchez Vasquez	14	527	104.2	12.5	0.055
Edwin Mamani Suri	14	1162	109.2	8.5	0.127
Luis Alberto Ingaruca Báez	14	503	94.0	9.2	0.047
Iris Tije Dea	14	509	104.2	8.7	0.053
Jose Luis Huayllani Huamani	14	1595	103.9	11.8	0.166
Edwin Yoel Puma Tapuy	14	970	99.2	8.5	0.096
Elena Paredes Espinoza	14	998	106.2	9.5	0.106
Manuel Huanuire Econema	14	887	106.6	9.6	0.095
Edwin Tineo Villafuerte	14	1171	104.8	9.0	0.123
Telésforo Vásquez Zavaleta	14	1083	99.8	9.3	0.108
Juana Contreras Suclli	14	1065	96.2	9.2	0.102
Olger Jacinto Mochcco Muñoz	14	1417	99.2	8.5	0.141
Carmen Rosa Olivera Gutierrez	14	943	99.5	8.2	0.094
Gabriela Rossana Parillo Quispe	14	603	105.2	10.2	0.063
Claudia Rosa Gutierrez Cruz	14	951	94.0	13.7	0.089
Hilaria Gina Lipa Gil	14	1157	104.8	8.9	0.121
Alipio Arnolio Poma Checalla	14	998	107.8	9.4	0.108
Olga Gutierrez Cruz	14	909	103.2	8.7	0.094
Laly Delcy Sahuarico Tuesta	14	745	101.1	11.0	0.075
Jose Carmen Saavedra Damian	14	818	93.7	13.0	0.077
Elar Parillo Quispe	14	1223	103.6	10.1	0.127
Hubert Daniel Padilla Flores	14	754	93.5	14.4	0.071
Silvestre Núñez Vásquez	14	647	101.2	11.5	0.065
Sonia Blanco Yupanqui	14	779	103.8	16.9	0.081
Nathi Jesica Sánchez Vera	14	1558	99.3	10.8	0.155
Eusebio Lima Laura	14	778	101.6	7.7	0.079
Diana Natalia Tohalino Rios	14	662	105.1	9.3	0.070
Jose Luis Quispe Condori	14	950	101.0	12.6	0.096
Telly Lisbeth Mendoza Vera	14	519	90.4	12.4	0.047
Javier Luis Limpias Howard	14	760	100.1	8.8	0.076
Rosa Gonzáles Cruz	14	1504	98.8	12.2	0.149
Georgina Lezama López	14	1193	103.7	10.1	0.124
Agustina Zavala Mamani	14	503	91.3	15.7	0.046

Elkjaer Albert Farfán Noa	14	768	82.4	17.1	0.063
Isabel Vizcarra Yatto	14	1127	94.0	10.5	0.106
Lebana Olivia Quispe Sueros	14	205	107.0	26.3	0.022
José Cahuana Saravia	14	861	95.1	15.1	0.082
Emma Tije Dea	14	1282	93.9	16.6	0.120
Roger Tije Dea	14	723	103.0	9.6	0.074
Urias Valdéz Tapuy	14	643	101.6	12.5	0.065
Víctor Macochoa Noa	14	43	113.1	27.8	0.005
Víctor Elmer Sahuarico Begazo	14	362	92.1	14.2	0.033
Martín Noel Quispe Vicente	14	1166	104.3	11.9	0.122
Rocío Luz Mamani Ancco	14	689	84.6	19.3	0.058
Lina Adneyda Valdéz Sahuarico	14	982	98.2	17.9	0.096
Pascual Flores Castillejos	14	1009	102.8	9.7	0.104
Nelson Herrin Noa Grifa	14	483	90.7	30.7	0.044
Lucidio Acosta Juvino	14	1384	101.0	9.0	0.140
María Mory Cumary	14	721	85.5	16.3	0.062
Estanislao Rodríguez Ramos	14	499	106.4	8.5	0.053
Raul Poviz Rojas	14	588	96.9	11.5	0.057
Ulises Arimuya Grifa	14	835	117.1	10.1	0.098
Teresa Pizango Navi	14	681	107.3	12.7	0.073
Martina Sabina Mamani Cahuana	14	319	108.8	13.7	0.035
José Mario Noa Grifa	14	1093	121.0	8.2	0.132
Juan Navarrete Huamán	14	471	110.2	9.2	0.052
Hilda Dea Rodríguez	14	444	114.4	9.8	0.051
Héctor Ernesto Pizango Navi	14	911	117.7	10.1	0.107
Factor Calatayud Curo	14	1403	105.6	24.5	0.148
Edilberto Dea Rodríguez	14	526	118.8	9.3	0.062
Daniel Mamani Jaramillo	14	861	115.9	11.9	0.100
Carlos Dea Campo	14	920	117.5	14.2	0.108
Asunta Olivia Díaz Moreno	14	845	119.0	11.1	0.101
Gerónimo Quispe Quispe	14	1046	116.6	23.0	0.122
Sebastian Tapuy Panduro	14	1057	118.0	11.9	0.125
Valentín Parrillo Yerba	14	988	112.5	9.4	0.111
Lucio Andrés Pizango Navi	14	2432	116.8	9.9	0.284
Augusto Arimuya Quispe	14	500	115.6	9.9	0.058
Ángel Torres Racua	14	735	109.0	21.3	0.080
Alejandroloboasayag	14	458	106.0	13.1	0.049
Manuelriverodíaz	14	1538	93.9	10.3	0.144
María Vilmarojaspari	14	727	98.4	15.2	0.072
Rony Cardicel Perez	14	791	114.5	12.1	0.091
Teodoro Mamani Mamani	14	317	87.9	27.9	0.028
Carlos Alejandro Balarezo Panduro	14	197	87.3	22.4	0.017
Edgar Belluma Huanuire	14	1057	120.4	8.2	0.127

Noemi Quiroz Diaz	14	924	114.1	13.4	0.105
Fredy Aliaga Condori	14	2029	114.5	12.6	0.232
Agustin Huamani Anco	14	85	102.4	12.2	0.009
Jose Javier Huinga Maceda	14	433	105.5	11.2	0.046
Carmelo Moreno Huanuire	14	599	114.6	6.5	0.069
Maria Encarnacion Perdiz Guzman	14	545	116.1	8.5	0.063
Gabriel Eduardo Tejada Aguirre	14	818	115.0	9.3	0.094
Gloria Gonzales Guzman	14	518	113.9	13.1	0.059
Benancio Huani Inuma	14	3529	109.1	9.1	0.385
Oscar Vega Navi	14	174	89.9	19.3	0.016
Luis Racua Salazar	14	519	110.2	20.4	0.057
Leonardo Quispe Quispe	14	322	102.1	14.5	0.033
Maria Rosa Vargas Racua	14	617	108.2	23.1	0.067
Esteban Halanocca Quispe	14	238	108.8	14.8	0.026
Maria Del Carmen Cristina Perdiz Valera	14	1800	110.7	19.9	0.199
Nely Quispe Miranda	14	1566	106.9	8.2	0.167
Teobaldo Reategui Rodriguez	14	662	115.1	8.9	0.076
Santos Agapito Cruz	14	148	89.5	31.1	0.013
Roy Mario Dueñas Taricuarima	14	1752	115.6	8.8	0.203
Pascual Huaman Fuentes	14	224	117.2	7.8	0.026
Odilia Tehuay Sanda	14	658	98.5	13.2	0.065
Nicolas Argandoña Piña	14	104	115.6	14.8	0.012
Maximo Loayza Benites	14	347	108.9	32.2	0.038
Martin Enriquez Valencia	14	775	108.0	11.3	0.084
Maria Paccosoncco Castillo	14	630	121.9	12.7	0.077
Maria Estela Perdiz Valera	14	1164	117.2	17.6	0.136
Maria Argandoña Piña	14	51	114.8	7.9	0.006
Marcelina Flores Rengifo	14	795	118.6	7.3	0.094
Leonidas Morales Zegarra	14	2706	119.2	7.4	0.323
Julia Yumbo Canelos	14	1381	119.7	7.3	0.165
Juan Tito Condori Suyo	14	242	118.1	17.1	0.029
Jorge W. Galindo Tineo	14	395	109.9	11.7	0.043
Jesus Racua Rodriguez	14	62	106.5	25.4	0.007
Jesus Chavez Vargas	14	190	98.7	28.4	0.019
Jessica Sharmey Cordova Narvaez	14	586	119.8	8.7	0.070
Ignacio Condori Flores	14	326	113.9	24.2	0.037
Hugo Alvarez Belzon	14	584	115.8	10.7	0.068
Hermelinda Pacco Molina	14	484	105.7	24.2	0.051
Hermelinda Argandoña Piña	14	82	113.6	14.9	0.009
Guillermo Miguel Racua Caya	14	216	91.1	31.8	0.020
Edwinson Edgar Torres Gonzales	14	316	105.3	29.4	0.033
Edinson Eloy Gongora Martinez	14	521	96.3	25.9	0.050
Cristobal Sullca Huaman	14	892	107.2	12.4	0.096

Cirilo Condori Atamari	14	2585	115.8	15.3	0.299
Braulio Serrano Valenzuela	14	659	120.1	7.8	0.079
Benito Escalante Quispe	14	554	111.9	10.5	0.062
Asunta Amasifuen De Llamas	14	1369	120.3	10.2	0.165
Anselmo Racua Mariche	14	131	98.0	42.9	0.013
Alfredo Zeballos Mozombite	14	363	126.3	4.6	0.046
Alfredo Alberto Collazos Caycho	14	51	110.0	29.2	0.006
Adan Baltazar Pacherrez Salazar	14	515	114.4	10.0	0.059
Abigail Sanz Salinas	14	896	112.6	12.9	0.101
Jorge Vargas Quiroz	14	1358	109.9	18.2	0.149
Flora Yatto Flores	14	990	103.8	13.1	0.103
Miguel Jorge Zevallos Narvaes	14	736	111.8	19.2	0.082
Rene Toribio Coral Reategui	14	1905	106.5	8.3	0.203
Juan Becerra Gallegos	14	1067	117.6	10.1	0.125
Juan Diaz Huesembe	14	1704	118.8	6.2	0.202
Gueisa Gonzales De Rodriguez	14	442	108.8	21.1	0.048
Elia Del Aguila Chavez	14	676	107.4	26.9	0.073
Patricia Jilapa De Flores	14	1262	112.3	11.4	0.142
Juan Araujo Sangama	14	1459	108.8	14.4	0.159
Eulogia Cutipa Ayma	14	353	107.8	11.0	0.038
Celso Flores Sanipico	14	1442	113.3	11.8	0.163
Cesar Agusto Reyna Durand	14	172	100.9	17.6	0.017
Melquiades Farfan Blanco	14	489	101.7	31.6	0.050
Serapio Velasquez Limpi	14	1144	118.8	6.6	0.136
Nilda Mendoza Arguedas	14	1324	106.1	19.4	0.140
Felipe Borda Flores	14	438	104.9	23.7	0.046
Santos Saul Moreno Econema	14	795	116.5	10.5	0.093
Leopoldo Flores Rodriguez	14	1016	117.1	20.1	0.119
Andres Guerra Irarica	14	428	110.2	19.3	0.047
Milqueades Hanco Sulla	14	1250	94.3	19.2	0.118
Julian Condori Atamari	14	992	116.7	11.3	0.116
Maria Belma Bemuya Gongora	14	1095	119.0	8.3	0.130
Matilde Giersch Dumay	14	916	100.7	15.9	0.092
Nazreth Mayta Chirinos	14	568	113.7	10.8	0.065
Victor Quispe Flores	14	1475	110.6	11.9	0.163
Ines Pastor Gongora	14	569	105.8	16.1	0.060
Enrique Moreno Aguirre	14	1377	115.3	11.1	0.159
Luz M Menacho Sanchez	14	992	112.3	12.6	0.111
Wilber Jacinto Pierola Huasco	14	400	110.6	6.7	0.044
Manuel Caituiro Barriales	14	295	113.1	16.1	0.033
Delia Howard De Limpias	14	273	38.8	40.1	0.011
Julio Saldaña Grandes	14	1058	116.6	7.3	0.123
Evangelino Leguia Palacios	14	486	101.0	18.0	0.049

Omar Maileva Vargas	14	687	97.1	13.9	0.067
Lola Ibañez Flores	14	1096	116.8	11.0	0.128
Hector Pautre Miashiro	14	1354	119.5	10.3	0.162
Alejandrina Troncoso Valdivia	14	1558	114.8	10.8	0.179
Andrea Ramos Papa	14	1082	115.5	11.4	0.125
Norma Sanchez Irarica	14	452	122.1	6.0	0.055
Enrique Paucar Valdivia	14	2640	118.5	7.1	0.313
Rafael Pedraza Ariza	14	1929	101.6	23.5	0.196
Luis Pautre Perez	14	1540	106.9	15.7	0.165
Bernabe Ccarita Florez	14	972	90.0	24.6	0.087
Julian Laura Duran	14	691	104.7	9.9	0.072
Sabino Huaman Ccopa	14	770	105.9	15.2	0.082
Mario Huaman Ccopa	14	575	121.1	4.2	0.070
Eugenio Carrasco Durand	14	649	114.6	11.5	0.074
Zenia Luna Centeno	14	1137	116.6	8.4	0.133
Facundo Cahuantico Cahuantico	14	856	114.8	13.3	0.098
Enrique Montesinos Tinta	14	1225	103.3	10.5	0.127
Segundina Quispe Vera	14	1804	119.4	9.2	0.215
Andres Avelino Rojas Aguirre	14	828	115.8	11.6	0.096
Bradimiro Grifa Noa	14	384	117.9	9.2	0.045
Hortensia Canelos Macochoa	14	1767	116.7	10.9	0.206
Juan Lucio Palomino Choque	14	886	105.0	8.0	0.093
Salome Lesmes Chavez Cardenas	14	1310	101.3	13.0	0.133
Laurentis Huamani Valdez	14	1022	117.7	15.4	0.120
Lucia Taricuarima De Dueñas	14	845	118.4	6.6	0.100
Juan Melendres Perez	14	1536	109.2	16.4	0.168
Gavino Huayhua Vilca	14	1529	115.0	9.6	0.176
Jesus Torres Vasquez	14	1120	108.1	13.5	0.121
Elvira Yatto Tibubay	14	1195	110.1	13.7	0.132
Fidelia Quiros Grifa	14	1159	105.8	17.2	0.123
Alejandro Aranibar Ochoa	14	204	116.7	9.1	0.024
Felipa Huamani Anco	14	1336	101.6	15.5	0.136
Elda Luz Vera Gonzales	14	612	101.6	10.7	0.062
Jorge Sota Santos	14	862	105.3	15.2	0.091
Juan Manuel Huamani Anco	14	622	97.2	19.2	0.060
Justa Castro Quispe	14	615	104.8	32.0	0.064
Raymundo Jaen Salva	14	764	106.9	17.4	0.082
Segundo Chavez Giersch	14	684	101.2	15.6	0.069
Leonarda Otorongo Quispe	14	839	105.2	21.1	0.088
Doralisa Muchari Viuda de Soto	14	2959	115.0	8.3	0.340
Lizardo Rodriguez Sanchez	14	647	120.5	8.7	0.078
Maria Domiciana Vela Medina	14	622	116.3	9.8	0.072
Isabel Canales Flores	14	1895	115.1	11.5	0.218

Andres Martin Lazo Pizango	14	1667	120.9	6.4	0.202
Fidelia Mamani Pari	14	620	117.6	18.6	0.073
Florentino Cañari Turpo	14	789	117.7	8.0	0.093
Maria Lopez Vera	14	1554	115.9	12.0	0.180
Angel Bustamante Huallpayunca	14	269	115.7	8.8	0.031
Domingo Carpio Claros	14	904	115.5	19.7	0.104
Julio Izquierdo Sangama	14	1083	108.1	14.8	0.117
Luis Reynaldo Canelos Grifa	14	746	113.9	15.6	0.085
Alida Arias Pizango	14	467	112.0	12.9	0.052
Vicencio Yaricahua Nieto	14	1235	103.8	14.2	0.128
Albino Gonzales Erpillo	14	1013	95.0	22.8	0.096
Anselmo Leonidas Estrada Yepez	14	591	94.6	14.4	0.056
Enrique Escompani Viñas	14	1011	122.5	4.1	0.124
Francisco Chavez Chura	14	176	111.0	24.3	0.020
German Revilla Gonzales	14	539	103.4	26.7	0.056
Hernan Bermudez Aparicio	14	2009	119.4	7.4	0.240
Isabel Enrequez De Vela	14	1366	117.3	9.7	0.160
Leonor Quispe Huaman	14	2075	104.7	9.2	0.217
Liberata Luna Yupanqui	14	1100	112.9	10.1	0.124
Madeleyne Valdivia Vela	14	1873	117.3	8.1	0.220
Mario Valencia Ccoñislla	14	1892	94.3	15.9	0.178
Nelson Belluma Huanuyre	14	191	85.3	31.3	0.016
Wily Alfredo Torrejon Machaca	14	3320	114.0	10.6	0.378
Alejandro Sajami Sinti	14	1159	118.1	9.3	0.137
Juan Moreno Aguirre	14	981	112.6	13.2	0.110
Juana Julia Gongora Cabana	14	493	111.1	14.6	0.055
Erasmo Cardicel Tananta	14	793	116.1	9.3	0.092
Gavino Rojas Montalvo	14	500	110.3	19.6	0.055
Mirta Carreño Guevara	14	3393	117.9	8.4	0.400
Ines Siani Beyuma	14	660	119.5	7.1	0.079
Saturnina Maileva Chavez	14	1136	118.8	12.7	0.135
Rosa Julia Huanca Tintaya	14	1041	120.7	5.1	0.126
Tiburcio Mescco Segundo	14	1048	104.1	13.8	0.109
Tomasa Huaman Oblitas	14	231	117.8	5.1	0.027
Luis Hernan Lopez Torres	14	1250	106.6	22.8	0.133
Bertha Olivera Palomino	14	576	102.9	17.0	0.059
Luisa Ochoa Puma	14	950	108.9	14.8	0.103
Alfredo Moreno Fuller	14	1026	120.0	10.7	0.123
Alcides Bocangel Estrada	14	1359	120.6	8.1	0.164
Angel Fuentes Torres	14	1172	106.2	12.2	0.125
Dominga Mayta Salcedo	14	1215	100.1	17.3	0.122
Helberth Merma Ancco	14	889	102.8	16.4	0.091
Julian Vera Papa	14	722	104.9	23.5	0.076

Margarita Venilda Rodriguez Benites	14	726	109.4	15.7	0.079
Romulo Condori Condori	14	418	109.1	7.5	0.045
Reynaldo Kuno Cumpa	14	621	117.0	12.2	0.073
Ruben Uartiaga Murrieta	14	440	121.1	9.9	0.053
Sabina Condori de Chura	14	41	96.5	30.1	0.004
Teofilo Pedraza Ariza	14	806	117.9	11.2	0.095
Margarita Azucena Morales Zegarra	14	888	108.7	15.3	0.096
Matias Huamani Flores	14	604	100.9	16.7	0.061
Ana Aimituma Huanca	14	1426	103.1	20.3	0.146
Leonardo Sanchez Pinedo	14	654	118.7	11.6	0.078
Pedro Quispe Quispe	14	648	106.9	26.9	0.069
Mateo Vargas Dueñas	14	639	112.7	11.8	0.072
Andres Igidio Gamarra Ayma	14	1012	102.5	17.1	0.104
Samuel Huamani Aranguri	14	371	111.2	16.3	0.041
Alcides Ccuno Chahuara	14	1187	106.1	9.8	0.126
Robustiano Lima Quispe	14	579	114.3	17.5	0.066
Felix Mamani Yucra	14	1546	113.2	8.1	0.175
Domingo Guzman Borda Flores	14	1172	109.6	11.6	0.128
Rene Florencio Vargas Pineda	14	293	107.2	14.6	0.031
Benilde Pacherres Salazar	14	1192	117.2	8.6	0.140
Damaso Irco Mamani	14	877	106.3	10.7	0.093
Marta Condori Quispe	14	978	103.6	14.3	0.101
Raymundo Caballero Gonzales	14	166	112.9	19.8	0.019
Adrian Miranda Martinez	14	1153	114.9	12.6	0.132
Humberto Mayta Aguirre	14	444	106.7	17.8	0.047
Antonio Pinedo Ramirez	14	843	107.1	11.5	0.090
Hernan Jimenes Llanos	14	119	100.8	28.6	0.012
Julissa Roxana Herrera Alpiri	14	527	106.9	9.3	0.056
Blanca Luz Vargas Pashanaste	14	849	118.0	13.5	0.100
Pedro Crisologo Moreno Huanuyre	14	1057	115.8	16.9	0.122
Juan Enrique Pereyra Guerra	14	1362	122.0	12.8	0.166
Julian Mora Huaman	14	723	117.5	10.0	0.085
Guillermo Velarde Castro	14	1004	100.2	10.8	0.101
Guillermo Flores Cama	14	1084	102.6	27.4	0.111
Regina Mamani De Ramirez	14	954	99.5	18.0	0.095
Luis Anarco Mamani Balarezo	14	908	107.4	14.6	0.098
Julio Cesar Moreno Aguirre	14	385	114.8	18.1	0.044
Alipio Olivera Estrada	14	874	93.2	21.6	0.081
Evangelina Molina Huallpa	14	1126	98.3	15.0	0.111
Juan Mario Gonzales Rodriguez	14	1216	112.6	9.9	0.137
Miguel Huaman Salas	14	1021	112.0	8.6	0.114
Rolando Samuel Toalino Perez	14	624	102.1	19.2	0.064
Saturnino Solis Muñoz	14	1071	117.6	9.6	0.126

Leoncio Pacheco Ayala	14	336	120.1	8.3	0.040
Pacifico Ferro Capa	14	1020	104.3	13.2	0.106
Juan Arnolfo Camargo Nakaganeku	14	981	117.6	9.2	0.115
Matilde Rodriguez Guevara	14	850	118.4	7.3	0.101
Vilma Torres Quispe	14	832	107.8	11.9	0.090
Manuel Machaca Chambi	14	276	116.2	8.5	0.032
Esther Armas Diaz	14	955	117.9	11.5	0.113
Silverio Quispe Ttupa	14	402	109.2	25.8	0.044
Guilma Guevara Macahuache	14	1135	100.0	14.9	0.114
Adolfo Vela Hidalgo	14	2222	102.6	16.8	0.228
Rosas Condori Condori	14	1419	90.2	32.7	0.128
Miguel Angel Maceda Guerra	14	327	107.1	4.9	0.035
Juan Bautista Uscamayta Huillca	14	710	113.1	24.3	0.080
Emilio Mercado Roque	14	1357	105.2	25.1	0.143
Gerardo Cesar Guzman Quispe	14	956	104.9	26.3	0.100
Marcos Olgado Quispe	14	244	100.2	24.0	0.024
Delfin Rodriguez Flores	14	1336	110.6	10.7	0.148
Valentin Huaman Amachi	14	1100	109.6	19.2	0.121
Ubaldo Fernandez Choquehuanca	14	1241	99.1	13.2	0.123
Luis Zamalloa Bolivar	14	847	99.2	24.4	0.084
Cesario Claudio Espinoza Lenes	14	844	102.4	14.4	0.086
Fermin Barriga Villamar	14	1128	119.9	7.1	0.135
Inely Mestanza Villaroel	14	1253	117.1	8.9	0.147
Julian Onecimo Mercado Palomino	14	1270	110.8	17.6	0.141
Julio Mercado Sanchez	14	400	109.9	18.5	0.044
Grimanesa Magdalena Gonzales Huatanabe	14	1117	105.2	16.5	0.118
Jackeline E. Ugarte Guerra	14	1403	101.9	14.7	0.143
Jose Audon Auquilla Condori	14	1072	114.3	13.0	0.123
Hernan Hidalgo Guevara	14	1848	114.9	10.8	0.212
Silveria Mamani Choque	14	377	101.8	15.8	0.038
Elva Nieves Moreno Econema	14	797	92.5	18.0	0.074
Martin Ascue Sallo	14	406	111.2	10.5	0.045
Silvia Mendoza Bermudes	14	448	112.9	8.5	0.051
Eddie Lizardo Jimenez Gonzales	14	1328	119.1	7.9	0.158
Catherine Melendez Vargas	14	271	107.6	28.0	0.029
Luciano Mamani Perez	14	420	103.1	31.2	0.043
Mario Pablo Mamani Chura	14	644	115.4	10.4	0.074
Teofila Oscalla Espinoza	14	376	106.1	11.9	0.040
Jose Mamani Choque	14	867	108.6	10.6	0.094
Rosita Marisol Trigoso Vargas	14	666	113.3	10.6	0.075
Romulo Nemesio Perez Mercado	14	782	113.7	15.6	0.089
Manuel Gamarra. Fuentas	14	1070	109.5	17.3	0.117
Olimpia Adela Balbin Castañeda	14	1155	116.2	10.1	0.134

Pedro Surco Achahuanca	14	803	108.0	21.2	0.087
Armando Taricuarima Mozombite	14	675	109.1	18.5	0.074
Matilde Vicentina Idme Idme	14	95	107.5	20.3	0.010
Segundo Salas Pizango	14	561	104.6	13.8	0.059
Pedro Nina Huamantica	14	467	106.7	21.4	0.050
Enrique Huaman Quispe	14	1220	106.0	21.0	0.129
Pedro Torres Racua	14	892	112.7	13.8	0.101
Fransisco Diaz Vargas	14	425	112.0	13.2	0.048
Martha Sandoval Laurente	14	682	116.9	9.4	0.080
Victor Huamani Ccamo	14	1176	117.5	10.6	0.138
Hermancia Rodriguez Flores	14	561	114.5	16.1	0.064
Daniel Idme Guetierrez	14	24	103.5	31.7	0.002
Manuel Escalante Huaman	14	1328	108.8	19.8	0.145
Carlos Gutierrez Villamar	14	370	114.4	16.4	0.042
Isaac Gutierrez Orconi	14	422	114.8	7.1	0.048
Adrian Ttito Arenas	14	1024	112.2	18.4	0.115
Jose Ayerbes Andaluz	14	927	101.2	23.6	0.094
Patricio Leon Mayta Mendoza	14	270	78.7	29.1	0.021
Segundino Torres Huaman	14	1427	111.4	9.2	0.159
Juan Gualberto Condori Sullo	14	395	113.5	27.4	0.045
Celestino Romero Peña	14	469	114.4	13.9	0.054
Francisco Mamani Condori	14	549	103.5	11.6	0.057
Lucinda Novoa De Romero	14	440	112.3	20.1	0.049
Hilda Giersch De Kojagura	14	719	91.6	19.8	0.066
Agripino Quispe Tinta	14	667	103.2	13.3	0.069
Hector Cardicel Perez	14	880	112.9	9.6	0.099
Sofia del Carpio Chair	14	678	93.8	16.7	0.064
Antolin Tupac Choque	14	855	115.9	10.7	0.099
Lucas Gallegos Mejia	14	926	106.8	18.4	0.099
Sotero Gonzales Pacco	14	1045	117.4	9.2	0.123
Alfredo Gonzales Romero	14	744	112.6	15.8	0.084
Jose Flores Pereyra	14	410	115.0	12.4	0.047
Celso Julio Zegarra Paiva	14	1182	98.8	20.5	0.117
Juan Mayta Choque	14	582	102.8	17.0	0.060
Nila Delia Peña Mamani	14	1113	121.4	7.7	0.135
Honorio Huesembe Chota	14	737	100.8	13.3	0.074
Eloy Bernabe Cassanca Rosombite	14	865	104.7	9.4	0.091
Genaro Concho Gutierrez	14	669	102.6	17.7	0.069
Jesus Ramos Huaman	14	1016	110.2	8.3	0.112
Alvino Lima Cconchoy	14	734	111.0	8.5	0.082
Ana Gonzales De Rodriguez	14	358	114.7	11.2	0.041
Alejandra Celiana Villagaray Gutierrez	14	1355	112.7	11.8	0.153
Leoncio Jasmani Huaraca Jaquehua	14	277	121.3	7.6	0.034

Alfredo Quispe Ramos	14	242	110.7	11.8	0.027
Moises Rodriguez Loaiza	14	613	104.6	12.0	0.064
Wilmer Alvaro Mamani Balarezo	14	2045	115.4	10.0	0.236
Richard Apaza Mamani	14	471	113.5	11.6	0.053
Santos Gutierrez Cahuantico	14	173	91.7	19.4	0.016
Pedro Pipa Maucaylla	14	357	93.2	24.7	0.033
Felicitas Ramirez Surco	14	297	109.1	27.0	0.032
Julia Rita Peña Mamani	14	2158	107.2	14.7	0.231
Raimundo Idme Tihuallanca	14	481	115.3	14.6	0.055
Serapio Condori Flores	14	1734	94.7	17.9	0.164
Ynocencio Bacilio Huaman	14	154	112.6	22.8	0.017
Cirilo Ayma Puma	14	932	102.0	33.1	0.095
Rosas Condori Condori	14	553	111.0	11.0	0.061
Lucio Mendoza Quispe	14	687	101.2	14.2	0.070
Sergio Mendoza Quispe	14	660	107.7	12.0	0.071
Leonidas Sollace Carpio	14	507	97.5	19.5	0.049
Delio Mendiguri Mendoza	14	417	108.3	25.5	0.045
Segundo Torres Sanchez	14	3547	108.5	11.3	0.385
Juan Carlos Zuñiga Mejia	14	1017	117.6	10.1	0.120
Exaltacion Carrion Telsi	14	1851	94.6	17.7	0.175
Georgina Sangama Huesembe	14	995	114.7	17.1	0.114
Teodocio Ancalle Llamoca	14	849	93.2	22.9	0.078
Marcelina Gamarra Carrillo	14	766	115.9	10.7	0.089
Oscar Duran Quispe	14	2928	93.3	18.4	0.273
Luis Alberto Huesembe Huesembe	14	529	102.3	13.5	0.054
Abel Galindo Izquierdo	14	1597	119.5	6.3	0.191
Empresa Eko Hotel S.A.C	14	1457	98.0	18.2	0.143
Rosa Ayma Condori	14	468	113.0	10.6	0.053
Rafael Lorenzo Jara Quispe	14	278	108.6	12.8	0.030
Felipe Mayo Yapura	14	1130	122.2	10.8	0.138
Nelida Cortez Zegarra	14	2078	116.0	9.6	0.241
Jorge Huamani Chacondori	14	446	118.4	5.5	0.053
Georgina Pereira Lima	14	591	113.4	14.3	0.067
Florentino Navi Guevara	14	653	115.9	17.1	0.076
Fidel Caballero Sajami	14	467	110.7	22.5	0.052
Ceferina Bautista Ferro	14	111	106.4	20.3	0.012
Avelino Ricardo Tuesta Guevara	14	95	120.2	5.3	0.011
Agustina Quispe Condo	14	872	92.8	23.7	0.081
Sergio Papa Manuyama	14	753	112.7	22.0	0.085
Marcos Mestanza Villaroel	14	3432	121.9	9.4	0.418
Oswaldo Ponpilla Rosas	14	597	103.9	19.2	0.062
Carlos Caviñas Balarezo	14	1841	102.9	13.8	0.189
Sergio Cusi Huaman	14	71	91.9	36.1	0.007

Victoria Ortega Flores	14	689	105.9	11.3	0.073
Juan De Mata Jara Juarez	14	1167	114.7	14.9	0.134
Alberto Arroyo Merma	14	409	114.3	6.6	0.047
Sonia Victoria Santibanez Caceres	14	607	120.3	6.9	0.073
Esteban Rene Lopez Torres	14	482	114.3	16.6	0.055
Martina Arenas Callañaupa	14	1328	120.7	7.9	0.160
Alberto Arroyo Merma	14	124	109.2	5.0	0.014
Hipolito Muñoz Sarmiento	14	394	110.4	19.8	0.043
Nieves Vergas Canamari	14	548	105.1	18.2	0.058
Rene Gualberto Mejia David	14	397	106.5	25.7	0.042
Pablo Callo Condori	14	564	109.1	26.4	0.062
Hernando Vega Alpiri	14	586	94.5	26.1	0.055
Dionisia Ccorahua De Zapana	14	624	113.6	22.2	0.071
Juan Tito Meza Huayta	14	406	99.6	33.7	0.040
Teresa Argandoño Piña	14	544	100.4	19.1	0.055
Javier Ernesto Vera Guevara	14	1086	107.8	22.4	0.117
Juan Vicente Sanchez Pinedo	14	2369	112.8	10.8	0.267
Casiano Cahuana Arque	14	348	115.4	14.6	0.040
Felipe Mosqueira Trujillo	14	525	106.8	11.5	0.056
Eulalia Gongora Vera	14	827	116.0	11.5	0.096
Juan Gualberto Aguirre Perez	14	564	114.6	14.5	0.065
Felicitas Macochoa Grifa	14	277	119.5	7.4	0.033
Victor Collazos Sanchez	14	810	111.4	11.0	0.090
Bethy Maria Antas Vasquez	14	716	111.8	11.8	0.080
Empresa Sol De Selva Rep Tacano Junkich	14	1508	104.6	21.4	0.158
Rodolfo Mamani Yari	14	1112	108.4	26.8	0.121
Emperatriz Barra Paucar	14	114	82.5	28.2	0.009
Jacinto Moscoso Ramirez	14	563	113.6	10.8	0.064
Jose Victor Flores Rodriguez	14	649	115.3	16.6	0.075
Isabel Tejada Aguirre	14	926	116.8	10.2	0.108
Edgar Mendoza Rodriguez	14	304	94.8	33.6	0.029
Segundo Juan Izuiza Papa	14	259	103.8	7.8	0.027
Mauricio Cassa Champi	14	200	110.0	27.9	0.022
Jorge David Trigoso Reategui	14	491	115.3	9.9	0.057
Sonia Flores Dancuar	14	2266	95.0	23.2	0.215
Jose Chavez Chambi	14	1489	117.0	7.5	0.174
Rafael Mariche Econema	14	758	115.3	10.6	0.087
Juan Cansio Chalco Irarica	14	1500	104.3	8.7	0.156
Carmen Lucy Leon Amasifuen	14	808	114.3	9.7	0.092
Angelica Amasifuen Palomeque	14	894	112.1	11.1	0.100
Alfredo Aguirre Rolin	14	614	116.0	9.9	0.071
Alfonsa Moreno Aguirre	14	989	103.6	18.1	0.102
Grimaldo Sanz Palza	14	1169	107.3	11.5	0.125

Arturo Odon Vela Moreno	14	508	115.7	9.4	0.059
Antonio Ayma Aranzabal	14	170	109.2	27.2	0.019
Cecilio Quighua Melo	14	783	98.3	25.5	0.077
Froilan Quispe Ttupa	14	1046	100.7	31.8	0.105
Eugenia Ramos Salcedo	14	965	111.8	12.8	0.108
Liliana Octavia Huamani Pillaca	14	1061	117.3	10.0	0.124
Villanueva Huamani Suarez	14	963	120.4	9.0	0.116
Wilson Guzman Ramirez	14	1876	120.0	9.2	0.225
Javier Marcelino Huaman Quinto	14	915	120.4	7.9	0.110
Emiliano Flores Merma	14	46	96.3	25.6	0.004
Juan Toribio Panduro Pizango	14	276	108.6	18.8	0.030
Roberto Vega Barroso	14	1305	121.6	7.7	0.159
Aldo Aguirre Rolin	14	1040	104.7	18.4	0.109
Juan De La Cruz Cusihuaman Condori	14	381	111.6	12.9	0.043
Maria Francizca Barros Guerra	14	562	112.9	9.9	0.063
Inocencio Caceres Saloma	14	768	102.9	31.7	0.079
Cecilia Cacuna Racua	14	2148	106.6	22.8	0.229
Maria Salome Mendivil Medina	14	1206	111.4	18.0	0.134
Mateo Tejeira Huillca	14	596	107.2	26.1	0.064
Cristina Pariguana De Mamani	14	695	112.3	17.7	0.078
Leonidas Cuno Solis	14	770	119.4	9.1	0.092
Ambrosio Ayala Huaman	14	367	98.0	30.3	0.036
Consuelo Arevalo Martinez	14	719	106.1	20.7	0.076
Pascual Reategui Roque	14	990	116.8	12.3	0.116
Cecilio Reategui Aguirre	14	846	119.8	10.6	0.101
Luis Tuesta Guevara	14	1375	122.2	6.0	0.168
Alfredo Vera Burga	14	731	98.6	12.0	0.072
Juaquin Perez Rengifo	14	970	108.0	20.6	0.105
Mercedes Soria Olgado	14	544	113.9	12.9	0.062
Angel Fuentes Yupanqui	14	1453	106.6	15.1	0.155
Luisa Cruz de Viza	14	825	103.4	14.4	0.085
Jacinta Huaman Apaza	14	220	109.5	18.3	0.024
Moises Gutierrez Galicia	14	991	122.4	13.5	0.121
Jaime Llamas Martinez	14	1390	107.0	19.6	0.149
Angelica Carrasco De Rocca	14	1784	101.2	24.1	0.181
Cecilia Adriana Tamashiro Cato	14	1850	98.6	23.8	0.182
Vicente Oroche Condori	14	826	106.1	17.2	0.088
Federico Barrientos Martinez	14	1129	121.6	5.7	0.137
Zoila Berta Vela Vera	14	1178	117.6	9.6	0.139
Wilfredo Ahuanari Patiño	14	560	112.6	16.1	0.063
Constantino Huaman Casas	14	688	112.6	14.6	0.077
Marcelino Huaman Llacma	14	936	96.8	19.0	0.091
Octavio Montesinos Quispe	14	814	98.6	12.9	0.080

Gumercinda Colque Quispe	14	1174	100.8	9.3	0.118
Celestino Silva Mamani	14	1271	118.0	8.7	0.150
Gregorio Garsez Auccapiña	14	572	97.7	23.9	0.056
Martha Huaman Quispe	14	738	107.0	24.1	0.079
Jose Moasi Acosta Jovino	14	958	117.5	9.6	0.113
Aura Dueñas Quispitupa	14	676	117.3	8.9	0.079
Saturnino Condori Cahuantico	14	578	120.9	9.8	0.070
Faustino Mamani Huayta	14	874	120.7	9.7	0.106
Mirian Hanco Bernal	14	440	123.1	3.9	0.054
Jessica Mesias Lopez	14	1038	104.9	16.5	0.109
Pascual Huamani Anco	14	914	96.3	12.9	0.088
Justo Montaño Avila	14	432	102.6	15.9	0.044
Marilin Luz Bautista Barros	14	546	120.4	5.5	0.066
Serapio Chilca Huaman	14	1272	111.1	17.6	0.141
Domingo Quispe Pinedo	14	495	117.6	8.5	0.058
Tito Alfredo Mercado Sanchez	14	846	109.8	19.7	0.093
Pablo Bolivar Alvarez	14	298	123.2	5.4	0.037
Juan Onesimo Ayerbes Ohuichi	14	343	109.1	19.2	0.037
Wilder Reategui Camargo	14	1012	120.1	7.1	0.122
Nimia Medina Bate	14	1998	119.9	8.6	0.240
Juana Mendoza De Escobar	14	471	106.6	21.3	0.050
Maria Bertha Sangama De Benites	14	1597	106.6	20.9	0.170
Cosme Dueñas Merma	14	1562	113.8	15.2	0.178
Dionicio Quispe Betancur	14	1672	117.9	10.9	0.197
Maximo Eleuterio Tapia Santos	14	1363	111.6	13.7	0.152
Ladio Bolivar Huamani	14	801	114.7	13.4	0.092
Fernando Grifa Palla	14	1608	118.7	8.3	0.191
Elvis Rodriguez Aguirre	14	1156	120.3	8.1	0.139
Norma Lute Moreno De Noriega	14	2446	120.0	8.1	0.293
Jorge Carlos Gonzales Irarica	14	217	100.4	17.7	0.022
Carlos Aguilar Huaman	14	244	98.5	31.0	0.024
David Palomino Turpo	14	151	111.4	15.0	0.017
Marcelo Choque Ramos	14	191	111.9	16.0	0.021
Esther Sanchez Silva	14	891	114.6	5.9	0.102
Edith Glady Herboso Reategui	14	1201	120.2	10.6	0.144
Zaida Huillca Herboso	14	620	111.9	11.4	0.069
Abed Mancilla Munchari	14	591	98.5	15.6	0.058
Aureliano Francisco Donaires Orosco	14	2415	104.5	14.1	0.252
Teodocia Victoria Huaraca Maquehua	14	1126	121.1	12.0	0.136
Joyse Magdalena Moreno Inuma	14	593	114.8	8.3	0.068
Honorato Pacamia Guerra	14	795	114.1	13.1	0.091
León Kkano Umalla	14	633	112.9	18.3	0.071
Adolfo Morey Tuesta	14	1205	96.5	13.4	0.116

Paulino Quispe Ramirez	14	1456	121.8	10.0	0.177
Carlos Narciso Moreno Fuller	14	693	110.4	14.5	0.077
Gregoria Roca Guerra	14	704	107.8	28.6	0.076
Julio Saloma Perez	14	600	109.5	27.6	0.066
Victoria Cahuana Arque	14	1180	112.4	15.8	0.133
Saturnino Villafuerte Blanco	14	218	109.9	18.4	0.024
Washinton Maceda Irarica	14	1845	122.1	7.5	0.225
Leandro Flores Huillca	14	3201	103.8	15.3	0.332
Siles Flores Rengifo	14	1030	116.7	10.0	0.120
Nelson Lopez Aguirre	14	1358	112.2	14.8	0.152
Lucia Nelida Baca De Beltran	14	541	117.1	7.7	0.063
Julia Sahuarico Ovalle	14	926	113.2	5.7	0.105
Lita Reategui Huesembe	14	1135	115.5	6.7	0.131
Fernando Gonzales Garcia	14	328	117.0	7.4	0.038
Mariacarmen Abarca Choque	14	1045	119.0	8.8	0.124
Nora Esperanza Belluma Huanuire	14	1104	119.4	6.3	0.132
Hermelinda Caller Rodriguez	14	1338	116.0	9.9	0.155
Rolando Espinoza Barrientos	14	1229	116.0	10.2	0.143
Agustin Paco Mendoza	14	768	114.6	10.4	0.088
Irenea Cose Apaza	14	1176	103.8	9.5	0.122
Jose Vizcarra Sanchez	14	743	120.0	9.7	0.089
Nora Albina Grifa Horiuchi	14	1094	121.9	8.8	0.133
Elvira Jaqueline Vizcarra Yatto	14	883	120.4	6.8	0.106
Lidaura Flores Mondragon	14	994	119.7	8.3	0.119
Irma Tito Cortez	14	733	119.0	6.1	0.087
Aprovechamiento y Proyectos en Recursos	14	3030	114.7	10.9	0.348
Alicia Huamani Perez	14	442	111.6	8.0	0.049
Luciano Arias Choque	14	473	95.4	11.9	0.045
Enrique Navio Arias	14	813	109.8	18.6	0.089
Emer Edinson Arimuya Perez	14	308	116.5	7.7	0.036
Saul Abuid Vargas	14	918	108.5	18.6	0.100
Segundo Rodolfo Aguirre Pizango	14	466	123.9	4.6	0.058
Juan Flores Machaca	14	1107	101.3	31.2	0.112
Agapito Pacco Barrientos	14	408	116.7	10.3	0.048
Hober Luis Del Aguila Izquierdo	14	1267	115.7	11.3	0.147
Blanca Rosa Ruiz Cardenas	14	495	95.9	13.5	0.047
Silveria Cruz Montalvo	14	1508	114.5	11.6	0.173
Cancio Quispe Nina	14	300	117.8	7.8	0.035
Normando Huinga Chapiama	14	782	115.2	6.7	0.090
Rafael Torres Cacuna	14	1501	110.4	20.4	0.166
Salustio Ccopa Auccailla	14	1517	119.6	7.9	0.181
Florentina Huaman Quispe	14	1335	116.4	10.4	0.155
Marco Antonio Gonzales Irarica	14	611	108.5	10.4	0.066

Juan Condori Jihullanca	14	1175	107.6	13.6	0.126
Julio Cacuna Racua	14	1269	108.6	22.0	0.138
Aidina Dea Huesembe	14	453	101.1	11.8	0.046
Bladimira Cevallos Cachique	14	1587	110.6	16.9	0.176
Emerson Manuel Vera Guevara	14	1440	120.1	8.9	0.173
Adrian Canelos Quiroz	14	1961	118.4	9.5	0.232
Cecilio Econema Jipa	14	1008	108.9	16.0	0.110
Paulina Aguirre Olarte	14	655	112.3	8.0	0.074
Paula A. Guerra Flores	14	454	110.0	17.1	0.050
Jorge Grifa Noa	14	1176	106.6	17.2	0.125
Paulino Roca Guerra	14	359	109.6	21.0	0.039
Rufino Condori Cahuata	14	886	119.9	11.2	0.106
Benjamin Romulo Moreno Guerra	14	415	115.5	10.4	0.048
Ciro Juan Morales Bellido	14	3301	113.0	7.9	0.373
Edmundo Contreras Pumacayo	14	3787	112.2	11.3	0.425
Pilar Mandujano Baca	14	1891	115.0	8.6	0.217
Consuelo Vela Areque	14	1334	114.9	11.0	0.153
Juan Ernesto Rivera Lazo	14	3971	118.4	11.0	0.470
Orfelinda Ochoa Pizango	14	852	119.6	7.4	0.102
Dolores Chavez Yumacal	14	645	110.9	9.2	0.072
Virgilio Sapa Pineda	14	1128	114.4	9.5	0.129
Milciades Gerardo Daniel Alcazar Villeg	14	1814	111.9	7.3	0.203
Carlos Esven Hidalgo Canales	14	436	122.4	5.5	0.053
Jesus Econema Cacuna	14	401	103.9	23.2	0.042
Eduardo Cumari Papa	14	497	102.8	24.8	0.051
Raymundo Canelos Yumbo	14	674	116.5	7.8	0.079
Abril Natividad Hancco Olivera	14	747	106.7	27.5	0.080
Nora Beltran Baca	14	1319	112.8	12.2	0.149
Hipolito Quiñones Quispe	14	1089	118.5	6.6	0.129
Luis Andia Sahuarico	14	371	68.8	32.1	0.026
Anselmo Vargas Mamani	14	723	122.7	4.2	0.089
Benigno Irco Mamani	14	874	107.7	12.1	0.094
Laura Baca Econema	14	852	117.4	14.0	0.100
Teodoro Becerra Gallegos	14	1841	116.4	12.9	0.214
Yolanda Apaza Yapura	14	287	91.4	9.0	0.026
Casimira Huaman De Mishisaka	14	730	112.4	15.6	0.082
Nicomedes Ayte Vargas	14	836	111.7	15.8	0.093
Nicolai Minaya Cardenas	14	1007	110.1	9.3	0.111
Valentin Villena Hinojosa	14	1897	114.7	7.1	0.218
Susana Margot Pastor Fernandez	14	1521	110.6	8.1	0.168
Justino Colque Lazaro	14	137	102.3	32.2	0.014
Heber Callata Supo	14	73	93.9	36.8	0.007
Gustavo Alejandro Rios Hermoza	14	826	125.1	4.2	0.103

Wilber Balladares Ramirez	14	1023	116.1	6.4	0.119
Eleuterio Jurado Frisancho	14	726	105.7	9.8	0.077
Hilaria Pacco Molina	14	596	116.5	9.5	0.069
Agapito Delgado Cruz	14	919	121.1	8.8	0.111
Julian Barragan Haytara	14	854	106.7	23.7	0.091
Wilbert Mesco Zevallos	14	781	112.1	13.6	0.088
Wilfredo Mendiguri Mendoza	14	542	112.9	19.8	0.061
Gregorio Chacon Fernandez	14	2971	118.4	10.3	0.352
Miguel Torres Cuevas	14	675	108.1	19.3	0.073
Anelia Valencia Condori	14	648	99.0	17.1	0.064
Esteban Peña Camaza	14	991	105.9	18.3	0.105
German Guerra Irarica	14	247	100.5	18.3	0.025
Alejandro Vela Hidalgo	14	1194	115.4	9.7	0.138
Jose Raul Lobaton Sequeiros	14	104	75.7	44.2	0.008
Julio Hurtado Garay	14	219	91.7	31.3	0.020
Jorge Humberto Tafur Valderrama	14	409	97.5	24.4	0.040
Segundo Moreno Huanuyre	14	593	111.7	22.4	0.066
Ulises Moreno Huanuire	14	950	118.3	18.6	0.112
Felipe Quispe Fernandez	14	511	101.5	29.8	0.052
Avelino Bolivar Zamalloa	14	1608	107.7	16.7	0.173
Gabriel Ponce Auccaylla	14	684	115.7	11.4	0.079
Edelmira Flores De Vela	14	98	98.2	27.8	0.010
Pedro Liberato Amau Gallegos	14	585	100.7	19.4	0.059
Luis Rojas Quispe	14	731	95.6	36.5	0.070
Percy Humberto Espirilla Condo	14	476	110.9	23.2	0.053
Flora Dorila Torres Ahuanari	14	1473	106.8	10.3	0.157
Rosa Ofelia Fernandez Guerra	14	1016	119.9	8.2	0.122
Sara Hurtado Orosco	14	1220	113.5	12.6	0.138
Guillermo Rios Pickman	14	1584	119.0	9.5	0.188
Julian Mamani Chino	14	943	114.1	20.0	0.108
Juan Huanuire Econema	14	663	115.7	11.9	0.077
Cornelio Bolívar Vizarreta	14	155	100.1	30.1	0.016
Alfonso Vicente Quispe Quiñones	14	158	114.4	9.9	0.018
Juan Emilio Barriga Vissa	14	1415	120.5	6.7	0.170
Manuel Quispe Gutiérrez	14	241	106.5	22.7	0.026
Felix Armando Arimuya Inuma	14	953	110.2	17.9	0.105
Alfonso Valera Perez	14	280	104.7	8.3	0.029
Milba Bartra Perez	14	945	115.1	10.8	0.109
Rosa Graciela Sanchez Arquino	14	1481	117.0	7.4	0.173
Soledad Ruiz Torres	14	543	118.2	7.7	0.064
Marcos Barriga Villamar	14	699	100.2	16.6	0.070
Irma Cruz Gutierrez	14	789	105.0	10.2	0.083
Bonifacio Rocca Ttito	14	205	101.6	17.8	0.021

Francisco Vargas Puma	14	1074	115.9	16.0	0.124
Ysela Aida Bolivar Barriga	14	438	121.5	9.2	0.053
Pablo Alegre Usca	14	556	112.9	11.5	0.063
Igidio Mamani Ccorimanya	14	189	118.3	3.7	0.022
Jose Quispe Condori	14	1228	115.2	8.4	0.141
Julian Flores Condori	14	637	95.9	17.0	0.061
Felix Antonio Huaman Gutierrez	14	1389	123.2	5.8	0.171
Juan Roberto Delgado Mendoza	14	324	112.4	10.9	0.036
Fabio Huaman Chavez	14	1621	121.4	5.4	0.197
Santos Fernandez Alva Zavallos	14	397	115.2	9.0	0.046
Faustino Chalco Paucar	14	403	109.9	11.6	0.044
Antonio Mamani Conto	14	1163	103.6	8.9	0.120
Oscar Angel Alvarez Belson	14	2358	122.9	5.6	0.290
Teresa Acevedo Alvarado	14	1245	103.4	9.6	0.129
Rosa Albina Canelos Grifa	14	818	120.0	5.9	0.098
Hugo Mamani Chavez	14	205	105.9	14.5	0.022
Franklin Quispe Gomez	14	130	123.8	3.4	0.016
Melina Hidalgo Pisco	14	1575	118.4	8.8	0.187
Bernardo Flores Pereira	14	928	112.8	9.0	0.105
Aide H. Mejia Ramirez	14	179	102.8	29.3	0.018
Exilda Shuña Canales	14	113	92.3	40.3	0.010
Raul Vargas Racua	14	433	104.7	26.0	0.045
Ruth Marjorie Flores Saenz	14	960	113.9	8.6	0.109
Hugo Cesar Huaman Ccopa	14	776	115.7	11.3	0.090
Gino Castro Molina	14	940	109.5	9.6	0.103
Rolando Alberto Molina Bocangel	14	934	105.3	10.6	0.098
Carmelo Moreno Cachique	14	664	121.7	8.3	0.081
Nemesio Zavala Perez	14	340	110.6	19.5	0.038
Nelida Canelos Quiroz	14	1609	123.2	5.7	0.198
Eulogio Puma Checcori	14	624	110.5	20.1	0.069
Victor Econema Pacaya	14	1666	117.4	8.6	0.196
Diana Bouroncle Troncoso	14	743	122.4	6.1	0.091
Luz Marina Irarica Sanchez	14	1479	115.1	8.2	0.170
Jesus Francisco Murayari Fasabi	14	795	120.5	6.6	0.096
Eulogio Amao Romero Rodriguez	14	1167	93.3	13.7	0.109
Cayetano Pizarrro Amao	14	1540	102.8	8.3	0.158
Francisco Solano Auquilla Condori	14	950	119.9	7.4	0.114
Eulogia Suni Uturunco	14	913	116.2	8.5	0.106
Antonio Cose Apaza	14	455	108.1	9.8	0.049
Eduardo Alejandro Gutierrez Carpio	14	1458	110.9	6.7	0.162
Aydee Flores De Canales	14	446	94.9	26.5	0.042
Aladino Racua Cacuna	14	539	110.6	16.3	0.060
Javier Romeo Chullo Espinoza	14	1069	93.3	19.4	0.100

Esteban Chullo Llanos	14	921	105.6	14.4	0.097
Pilar Soto Condori	14	134	115.3	12.7	0.015
Maria Cristina Loayza Valeriano	14	781	102.0	11.8	0.080
Felix Condori Taina	14	707	106.2	27.8	0.075
Harold Terrazas Flores	14	848	118.1	6.9	0.100
Libio Guzman Tapia	14	459	112.5	12.1	0.052
Marly Villavicencio Mamani	14	2622	109.6	7.3	0.287
Dyahana Zegarra Ruiz	14	1007	106.4	13.7	0.107
Fany Violeta Mostacero Mayo	14	1014	112.6	11.2	0.114
Julio Lopez Callo	14	380	119.4	5.5	0.045
Jesus Carlos Aranzabal Carpio	14	967	109.0	12.4	0.105
Walter Anselmo Chavez Sanchez	14	1147	114.0	11.0	0.131
Jose Manuel Corahua Quispe	14	603	114.2	11.0	0.069
Rocio Miluska Durand Chavez	14	718	116.7	9.0	0.084
Wilmer Palomino Cordova	14	262	106.6	10.6	0.028
Luis Alberto Farfan Pezo	14	901	118.7	7.5	0.107
Janet Encarnacion Capa Panduro	14	1021	113.6	10.8	0.116
Madison Pilor Aquise Paco	14	581	110.3	10.9	0.064
Erasmo Condori Flores	14	1189	106.4	11.5	0.127
Victor Rene Diaz Paredes	14	1344	104.3	15.8	0.140
Francisco Callo Parhuayo	14	415	101.2	33.7	0.042
Carlos Revilla Gonzales	14	1083	116.5	13.1	0.126
Sofia Rosa Paredes Dueñas	14	1393	100.6	14.1	0.140
Felipe Mauricio Limachi Paucar	14	571	94.2	12.2	0.054
David Asturima Huamantica	14	671	106.8	8.2	0.072
Samuel Huamani Vilca	14	1828	112.8	5.8	0.206
Guillermo Federico Del Aguila Zuñiga	14	980	112.8	7.2	0.111
Celia Fpuro Taiña	14	229	97.6	18.1	0.022
Dagui Marilu Ynuma Beyuma	14	719	115.1	7.2	0.083
Dennys Pizarro Alarcon	14	813	105.1	8.2	0.085
Elmer Perez Piño	14	124	113.6	15.6	0.014
Jacqueline Solis Vera	14	660	107.0	8.3	0.071
Karen Elizabeth Frisancho Taborga	14	1462	111.9	10.7	0.164
Luis A Collazos Sanchez	14	943	118.4	8.3	0.112
Martin Ricardo Miranda Rivera	14	147	72.0	36.0	0.011
Matilde Pacherres De Guerra	14	292	110.9	5.6	0.032
Miguel Ulises Odagawa Sanchez	14	292	117.1	7.1	0.034
Rita Moreno Jipa	14	1637	111.9	10.7	0.183
Guillermina Carpio Ramos	14	1034	112.9	15.1	0.117
Fredy Quispe Aguilar	14	1490	105.9	11.5	0.158
Faustina Quispe Carrasco	14	864	96.1	17.1	0.083
Daniel Suclli Laura	14	901	114.6	13.1	0.103
Paola Dulanto Chapiama	14	1546	122.1	5.8	0.189

Luz Angelica Roca Guerra	14	431	105.1	30.2	0.045
Rofina Quispe Barreto	14	912	101.7	8.4	0.093
Dalila Nuñez Fernandez	14	1051	111.2	6.8	0.117
Rony Asipali Lopez	14	524	119.7	8.6	0.063
Juan Huallpa Quispe	14	1434	115.0	10.3	0.165
Gumercindo Blanco Vargas	14	762	118.4	6.8	0.090
Jackelina Morales Troncoso	14	1859	116.0	6.0	0.216
Edgar Tipula Mullisaca	14	1547	113.6	9.1	0.176
Francisco Rodrigue Seiko	14	768	118.1	9.4	0.091
Justo Ticona Colquehuanca	14	4415	107.5	10.0	0.475
Herver Flores Saavedra	14	640	113.7	10.6	0.073
Liliana Solis Chalco	14	1206	113.4	9.9	0.137
Andres Ernesto Cachique Chapiama	14	609	113.8	9.8	0.069
Ismenia Mariño Gonzales	14	859	101.8	10.0	0.087
Yvan Quispe Duran	14	1127	112.4	9.6	0.127
Apolinario Carlos Vasquez	14	1066	115.4	12.7	0.123
Maria Jesus Vargas Ramirez	14	826	112.4	8.4	0.093
Clara Dorotea Moroco Cartagena	14	742	100.6	20.6	0.075
Janet Sonia Paucar Muriel	14	1117	114.3	11.1	0.128
Nelson Wiltembug Gutierrez Carpio	14	672	79.9	16.7	0.054
Alcibiades Canelos Yumbo	14	842	114.2	17.2	0.096
Faustina Vicente Pauccar	14	809	110.4	14.4	0.089
Santiago Edelyn Sierra Tito	14	1111	111.2	8.8	0.124
Aida Evita Gosalvez Campos	14	1034	111.6	9.4	0.115
Froilan Jaime Aliaga Condori	14	497	102.2	7.7	0.051
Bacilia Mamani Sucasaire	14	185	108.5	26.4	0.020
Eleuterio Martinez Arimuya	14	246	96.8	22.4	0.024
Maria Salome Mendivil Medina	14	635	116.6	14.8	0.074
Silvia Apaza Hidalgo	14	855	116.5	8.1	0.100
Dionisio Lima Armuto	14	877	114.7	11.5	0.101
Jose Cotaluque Maihua	14	1059	119.1	12.1	0.126
Gregorio Huillcca Gallegos	14	1420	121.5	13.1	0.173
Justino Palomino Mercado	14	2503	120.2	6.1	0.301
Rudencinda Gutierrez Garcia	14	147	105.4	11.9	0.015
Richard Antonio Fernandez Narvaez	14	628	110.9	9.8	0.070
Lidaura Flores Mondagron	14	1059	122.2	8.4	0.129
Hilda Chavez Jipa	14	522	113.1	12.7	0.059
Cirilo Torres Ttito	14	377	112.2	16.5	0.042
Florinda Flora Yupanqui Quispe	14	2184	117.0	9.1	0.256
Oswaldo Saavedra Gongora	14	719	118.4	7.3	0.085
Marcos Maximiliano Gonzales Gamarra	14	924	119.4	8.2	0.110
Zoila Norma Racua Guerra	14	1748	104.4	21.9	0.182
Humberto Ovalle Arana	14	733	109.3	6.4	0.080

Hidelita Josefa Quispe Jacobo	14	932	57.6	17.9	0.054
Yuri Lima Laura	14	706	100.8	7.4	0.071
Agueda Pacherres Salazar	14	140	114.2	19.9	0.016
Florencio Guerra Irarica	14	724	103.8	22.5	0.075
Luis Nina Pacheco	14	605	117.7	8.4	0.071
Daniel Grifa Noa	14	579	119.0	6.7	0.069
Salomon Correa Terrones	14	635	103.7	18.8	0.066
Estanislao Lopez Vera	14	737	117.4	8.0	0.086
Asunta Machaca Amanqui	14	522	100.6	24.0	0.053
Edgar Huaman Palomino	14	452	115.7	8.1	0.052
Zoila Nelida Yaricahua Arimuya	14	1122	91.9	20.8	0.103
Vicente Guido Achapuri Alanquia	14	791	107.9	7.4	0.085
Patricia Quispe Vega	14	657	68.9	28.7	0.045
Juvenal Torres Cereceda	14	1	120.7	0.0	< 0.001
Miriam Laura Quispe	14	814	103.1	8.0	0.084
Nicanor Cjuno Peña	14	101	104.8	27.7	0.011
Anastacio Challco Visa	14	1319	101.1	12.7	0.133
Beatriz Valencia Ayma	14	1569	99.8	11.3	0.157
Elvis Ivan Barriga Guevara	14	661	104.5	11.4	0.069
Cirilo Zenon Cari Collanqui	14	828	107.9	18.9	0.089
Jesusa Cussi Mirano	14	815	108.7	10.5	0.089
Bernardino Villafuerte Mamani	14	2634	108.0	16.0	0.284
Daniel Sanchez Rengifo	14	584	94.9	19.0	0.055
Eulogio Quispe Chani	14	575	114.6	21.9	0.066
Donato Machaca Cruz	14	2128	107.9	16.9	0.230
Piero Mirko Trigoso Torres	14	840	108.2	21.1	0.091
Leni Cacuna Rodriguez	14	261	116.7	11.6	0.030
Lidia Rosa Torres Canelos	14	1260	122.2	7.6	0.154
Teobaldo Aristides Reategui Trigoso	14	444	118.2	12.5	0.052
Eritxon Aldo Aguirre Peralta	14	867	110.6	11.8	0.096
Maribel Yeni Aparicio Carpio	14	828	111.0	10.7	0.092
Benedicto Baca Rosado	14	770	71.2	32.7	0.055

***Protected area type:**

1. National Park
2. National Reserve
3. Communal Reserve
4. Protected Forest
5. National Sanctuary
6. Historical Sanctuary
7. Reserve Zone
8. Other
9. Rubber Concession
10. Conservation Concession
11. Ecotourism Concession
12. Wildlife Management Concession
13. Reforestation Concession
14. Brazil Nut Concession